April 2019

Firefighting Remote Exploration Device

Eva Marie Barinelli
Worcester Polytechnic Institute

Gavin Keith MacNeal
Worcester Polytechnic Institute

Jacob Louis Berman-Jolton
Worcester Polytechnic Institute

Karina R. Naras
Worcester Polytechnic Institute

Yil Alberto Verdeja
Worcester Polytechnic Institute

Firefighting Remote Exploration Device

A Major Qualifying Project Report

Submitted by:
EVA BARINELLI | JACOB BERMAN-JOLTON | GAVIN MACNEAL | KARINA NARAS | YIL VERDEJA

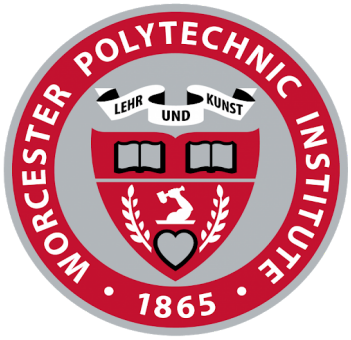

WORCESTER POLYTECHNIC INSTITUTE

A report submitted in partial fulfillment
of the requirements for the degree of
BACHELOR OF SCIENCE

Advisors:
Professor Carlo Pinciroli
Professor Sarah Wodin-Schwartz
Professor William Michalson

Submitted on: April 25, 2019

Abstract

Fire environments are dangerous and constantly changing. The goal of this project was to design and build a robot to provide firefighters with additional information about a fire environment to help them make more informed decisions when fighting a fire. We have built a prototype robot that is compact and quick to deploy, with a heat, water, and impact-resistant chassis designed to function in unpredictable firegrounds. The remote-controlled robot returns a real-time video feed and a heat map of a designated area in a building.

Acknowledgements

We would like to thank everyone who has provided input, feedback, and support throughout this project. First and foremost, we would like to thank our advisors, Professor Pinciroli, Professor Wodin-Schwartz, and Professor Michalson, for their guidance, patience, and valuable feedback throughout the past four terms. They have been with us every step of the way through this project, and FRED would not exist without them.

Thank you to our graduate advisors, Dominic Cupo and Josh Bloom, for their feedback on our project and their insights about firefighting. A special thanks to Dominic for letting us use his 3D printer, without which we would have no whegs.

We would also like to thank Deputy Chief Martin Dyer of the Worcester Fire Department for providing insight into modern firefighting hazards and answering all our questions about firefighting procedures.

We would like to thank the Washburn Shops lab staff for their assistance in machining our unusual collection of chassis materials. Thank you to Ray Ranellone, Fritz Brokaw, and the other members of the WPI Fire Protection Engineering Department who helped us conduct our thermal testing safely.

Thank you to Michael Tasellari and Yuchang Zhang for their assistance with our background research. Thank you to Ben Mart for sharing your machining expertise and mechanical know-how to help us fix our never-ending stream of mechanical issues. Thank you to the SCREAM MQP team, FRC Team 190, the WPI CollabLab, and the WPI NEST Lab for sharing tools, hardware, and lab space.

Table of Contents

List of Figures

List of Tables

Chapter 1. Introduction

The twenty-first century is being called an Internet Industrial Revolution due to the rapid rise of technological systems. The advancing technologies of this modern industrial revolution are increasing preventability and recovery from destruction caused by both natural and human-made disasters. Emergency response teams are now using technologies including drones, satellite imagery, social media, and robotics to aid their response to unfolding disasters while modern buildings are now outfitted with advanced fire and smoke detectors [1]. Additionally, firefighters are equipped with durable protective equipment and go through comprehensive training to increase their success while fighting a fire. Despite these improvements, firefighting remains one of the deadliest jobs in the world [2].

The area in which firefighters carry out their operations, known as a *fireground*, is a dangerous and constantly changing environment. Currently, operational decisions at a fireground are made by an Incident Commander (IC). The IC is typically a senior member of the crew that makes decisions about tactics and resource management primarily based on their past experiences and instinct. Decision making on the fireground is limited by the collection of available data. Real-time data about the building, fire, and firefighters would help ICs make better-informed decisions. A strategy to improve the IC's decision making would be to increase the available information by collecting and integrating information from a wide range of databases and sensor networks, both within and beyond the fireground. According to the National Institute of Standards and Technology (NIST), the addition of "Smart" technologies to firefighting would "enable [considerably] better situational awareness, predictive models and decision making." [1]

There is a clear need for a "Smart" system to facilitate and improve the way fire situations are currently addressed. In Worcester, Massachusetts, firefighters have a particular need for technologies when working in converted manufacturing buildings. Worcester is no longer a primarily industrial city; therefore, many of its factory buildings have been repurposed as restaurants, stores, and office spaces. These renovations have made large buildings compartmentalized, which makes interior navigation more complicated for firefighters.

Challenges in Firefighting

Firefighting is one of the most dangerous professions due to its unsafe and constantly changing environment. Firefighters may be required to operate under conditions with a high level of uncertainty and must make time-critical decisions using insufficient information [5].

Despite thorough preparation, firefighters continue to face challenges while operating in structural fires. These challenges are the result of uncertainties of structural integrity, unpredictability of fatal events such as flashovers and backdrafts, and getting disoriented or lost when entering buildings with unknown layouts.

Flashover and Backdraft

Flashovers and backdrafts are two dangerous events that can occur during a fire. Both situations can occur without adequate warning, and this unpredictability poses a danger to the lives of firefighters.

A *flashover* is a rapid transition of fire from the *growth* stage into the *fully developed* stage in which the temperature rises exponentially as shown in Figure 1 [16]. It is the physical event in which the temperature of the room has reached a critical point (approximately 500 ºC) causing objects in the room to dry out and emit flammable gases. When this occurs, everything in the room will instantaneously burst into flames causing a rapid increase of temperature. Flashovers are typically contained in one room. Currently, firefighters attempt to anticipate the occurrence of flashover by looking at the smoke above them. If the smoke is ignited, it means a flashover is about to occur and they need to evacuate the room immediately.

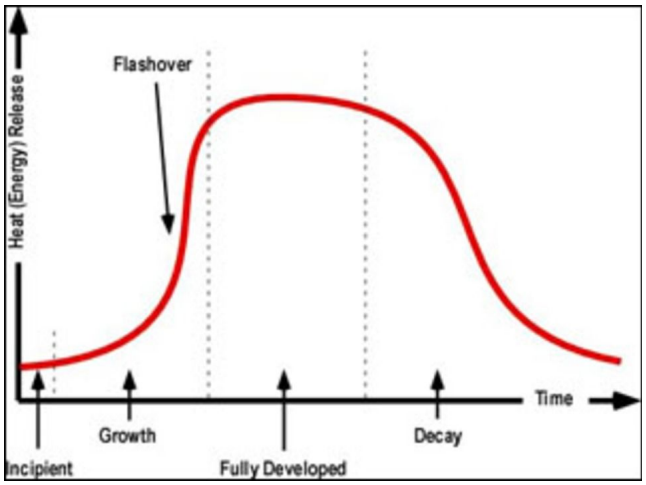

Figure 1. Stages of a fire in an enclosed structure [17]

A *backdraft* is an explosion that occurs when a large quantity of additional oxygen is introduced to a smoldering flame with a temperature great enough to ignite the added oxygen. Additional oxygen can be introduced into the system by a crack in the structure's exterior, or by an opened window or door. A backdraft also involves the deflagration, or rapid combustion, of flammable products upon mixing with air. Backdrafts are more difficult to predict than flashovers because they happen quickly. Firefighters are trained to anticipate backdrafts by watching smoke patterns. If the smoke is being sucked into a room rather than flowing out, that means there is

low pressure in the room and a backdraft may occur. Unlike a flashover, a backdraft can affect an entire floor of a building and even cause the building to collapse [18]. Figure 2 shows the point at which backdrafts are likely to occur in relation to the heat release in the room.

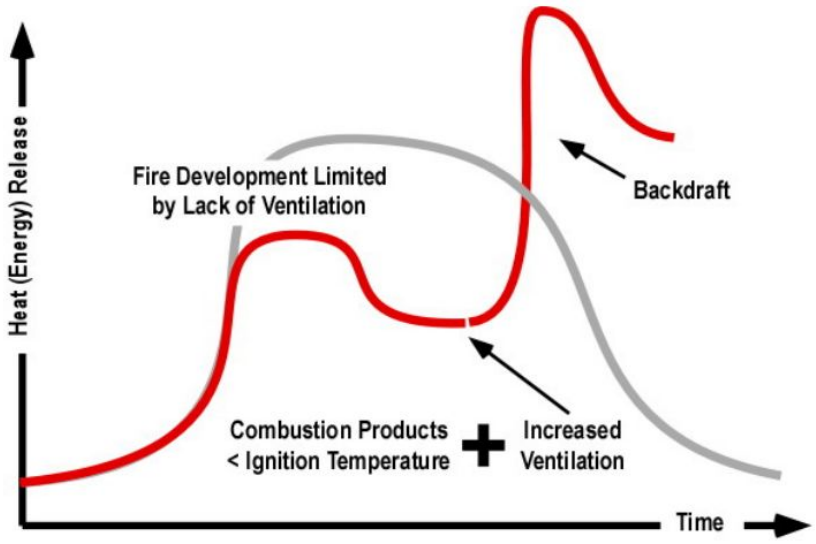

Figure 2. Occurrence of backdraft [18]

Disorientation

One of the largest threats to firefighter safety is getting lost in a hostile environment. Firefighters typically do not know the layout of a building before they enter it, which can lead to confusion and disorientation. William R. Mora wrote an article in "Understanding and Solving Firefighter Disorientation" about a study he conducted between 1999 and 2001 [10]. Mora found that, in general, firefighters who become lost or disoriented in a fire tended to follow a disorientation sequence which led to fatalities or serious injuries. The sequence involves the following steps:

1. Fire in an enclosed structure with smoke showing
2. An aggressive interior attack[1]
3. Deteriorating conditions such as Prolonged Zero Visibility Conditions (PZVC)[2], flashover, backdraft, or structural collapse
4. Handline[3] separation
5. Disorientation
6. Serious Injury or Firefighter Fatality

[1] An aggressive interior attack is also known as an *offensive attack* where firefighters enter the building and fight the fire from inside.
[2] PZVC is defined as 15 or more minutes of zero visibility after heavy smoke fills the environment. This was a big problem during the Cold Storage fire in Worcester, MA.
[3] A handline is a hose. Firefighters are trained to hold onto the hose so they can follow the hose out of the building should they get disoriented [31].

Problem Statement

Fire environments are dangerous and constantly changing. Firefighters can become disoriented or lost when engaging in interior attacks on structural fires in compartmentalized buildings which can lead to risk of injury or death. Robots can be used to provide real-time data and a map of a building's complex, unpredictable layout. The goal of this project is to design and build a robot that will provide firefighters with additional information about a fire environment to help them make more informed decisions when fighting a fire. The robot must be compact and quick to deploy with a heat, water, and impact resistant chassis to function in unpredictable firegrounds. The remote-controlled robot will return a real-time video feed and a heat map from inside the building.

Contributions

In this project, we created a Firefighting Remote Exploration Device (FRED) to assist firefighters by gaining more information about fireground conditions. The team researched fireground hazards and designed a compact remote-controlled robot that can be deployed in a fireground to sense temperature and wirelessly transmit thermal data to a member of the firefighting crew. The robot is robust and human-portable for ease of deployment and is designed with heat-resistant, water-resistant, and impact-resistant features to face the hazards of a fireground. Material decisions were made with the goal of keeping the robot inexpensive in order to be affordable for fire departments. The robot also does not require a tether, to avoid getting in the way of firefighters. FRED is equipped with a camera, thermal arrays, and distance sensors; it is able to gather and send real-time thermal information and live video feed of the environment back to its operator. FRED also has a unique drivetrain specifically for unpredictable fireground terrain; it is driven by two passive transformable whegs that provide the smooth drive of standard wheels but the obstacle scaling capabilities of whegs.

Chapter 2. Related Work

Fire Safety Research

The challenges faced by firefighters vary based on the environment and circumstances of the fireground. These are directly related to the fire department's location and available resources. This section explores some of the issues that are faced in modern structural fire environments.

Structure Characteristics

Structural fires have become more dangerous even though fire prevention technology has advanced. As shown in Figure 3, the number of home structure fires reported over the last 40 years has decreased by more than 50%, which indicates that fires are becoming more preventable.

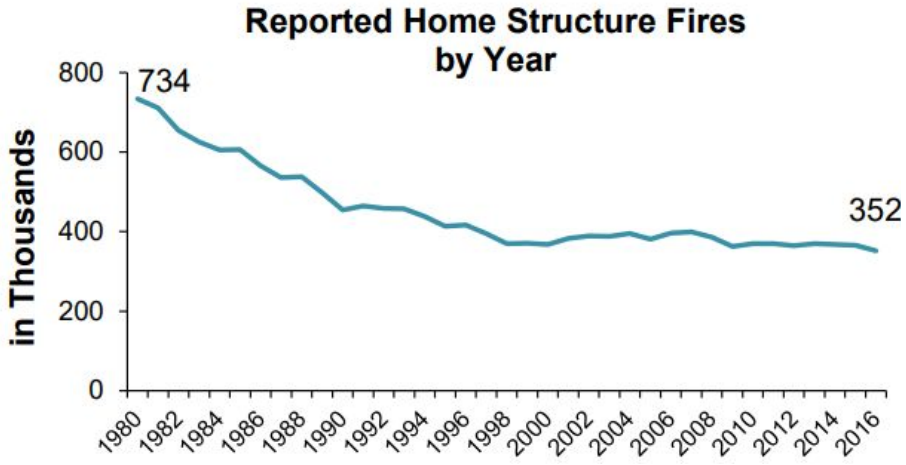

Figure 3. NFPA, Reported Home Structure Fires by Year [6]

This decrease is the result of cities enforcing stricter fire safety codes and other building regulations to minimize risks and prevent fires. Additionally, modern homes and businesses are equipped with advanced fire and smoke detectors. Despite the reduced occurrence of fire, Figure 4 shows that the number of deaths per thousand fires has stayed roughly the same since 1980.

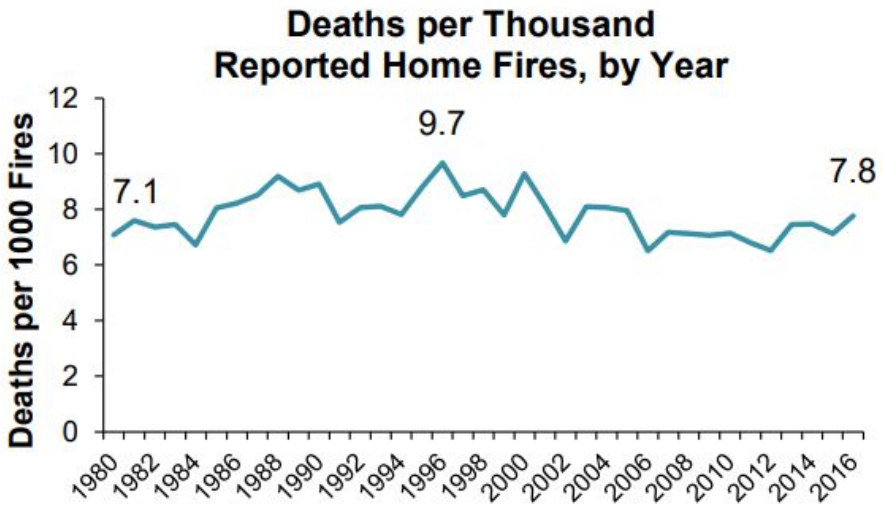

Figure 4. NFPA, Deaths per Thousand Reported Home Fires by Year [6]

Due to the use of new materials for construction and furniture, modern residential fires are more difficult to escape and more likely to result in flashovers (see Section 2.1.1). Unlike properties in the 20th century, modern buildings have replaced natural materials (e.g. cotton and wood) with lightweight synthetic materials (e.g. polyester and plastic), which burn more quickly and emit gases that are more hazardous [7]. Although synthetic materials pose greater risks when burned, they are still commonly used because they are less expensive and more durable than natural materials. The same applies to wall linings (e.g. drywall), which are thinner today and, therefore, easier for fires to penetrate [8].

NIST collaborated with Underwriters Laboratories (UL) to create a video [9] that compares the flashover rates (see Section 2.1.1 for more details about flashover) between a modern room furnished with synthetic materials and a "legacy" room furnished with natural materials. In less than ten minutes, a small fire in the modern room became a flashover whereas the legacy room completely ignited in triple that time. The additional danger caused by synthetic materials cannot be prevented by firefighters, so efforts must be made to improve firefighting to match the growing danger.

Enclosed Structures

An enclosed structure is an environment with very few windows or doors that cannot provide for immediate ventilation and emergency evacuation. In 2005, William R. Mora's Firefighter Disorientation Study found enclosed structures to be one of the most common sources of firefighter disorientation, and subsequently firefighter fatalities [10]. Basements and high-rise buildings are both enclosed-structure environments that often present challenges for firefighters when extinguishing a fire.

Basement Fires

Basement fires are not only considered to be one of the most challenging operations to encounter, but they are also known to result in property loss and fatalities. Firstly, they are difficult to identify because the fire may appear to be coming from the ground floor[4]. Secondly, basements are difficult to access as smoke and heat builds up immense pressure that forces firefighters away. Because many basements have no walls or doors and the contents of a basement are often highly flammable, fires can develop rapidly and egress routes are limited. Lastly, basement fires can be very dangerous as basement ceilings are susceptible to collapse during a fire bringing risks to both firefighters on the ground floor as well as the basement [11].

High-rise Building (HRB) Fires

High-rise building (HRB) fires pose two types of challenges for firefighters both in and outside the building. The main challenge presented to firefighters is the height of the building. For active firefighting outside the building, equipment does not always reach the top floors. There is an upper limit on the amount of water pressure that can be applied by fire engine hoses which means water cannot reach the upper floors of HRBs. Additionally, firefighters inside HRBs have to carry heavy equipment up many flights of stairs while simultaneously evacuating any remaining occupants [12]. Once a firefighting unit is at the source of the fire, the second challenge is to fight it. Fires in high-rise hallways are problematic because they are defined as enclosed spaces (i.e., they are long and narrow, and they lack windows and open doors). According to Mora's 2005 study, survivors of high-rise fires have described flashovers as "blowtorch-like" due to the winds blowing into the fire from an open hallway door [10].

Warehouses and Large Compartmentalized Buildings

Another type of environment that is difficult for firefighters is warehouses and large compartmentalized buildings. Deputy Chief Martin Dyer of the Worcester, MA Fire Department (WFD) identified that the WFD struggles with large compartmentalized buildings because of their unpredictable layout. Although compartmentalization hinders a firefighter's ability to combat a fire, the design is adopted in modern buildings as a passive firefighting technique [13]. Subdividing buildings into a number of compartments prevents the rapid spread of fire, reduces the chances of fires growing, and limits the damage done to a building [14].

In Worcester, these large compartmentalized buildings are often old manufacturing buildings that have been renovated into new spaces for a variety of different businesses. The building layout firefighters may expect based on records in their databases may be drastically different than the

[4] The ground floor is considered to be the floor above the basement. It is generally the level of entry.

current layout of the building. Deputy Chief Dyer described the building layout as a maze where some firefighters can become so lost and disoriented that they cannot find their way out. This description is consistent with the Worcester Cold Storage and Co. fire on December 3, 1999. This fire resulted in the deaths of six firefighters. These firefighters got disoriented and lost on the upper floors of the building. According to the NFPA records, this structural fire was the first to claim six firefighters where neither building collapse nor explosion were the main cause of the fatalities [15]. Although there has not been a warehouse fire as fatal as this one, the WFD continues to struggle with fires in large compartmentalized buildings.

Temperature and Location

In a fireground, fire and smoke can have a direct impact depending on where a person is located. When a room catches fire, the flame will burn upwards towards the ceiling which, in turn, creates a very unevenly distributed heat flux in the room. Below, Figure 5 shows a typical example of a residential fire inside a living room just a moment before the occurrence of a flashover. As shown in the bottom left corner of the heat map, the source of fire located in a corner of the room creates a flame that burns upwards causing the ceiling to accumulate heat. Generally, before a flashover occurs, the floor has a temperature below 140ºC, while the ceiling has a much higher temperature which can go up to 500ºC [19].

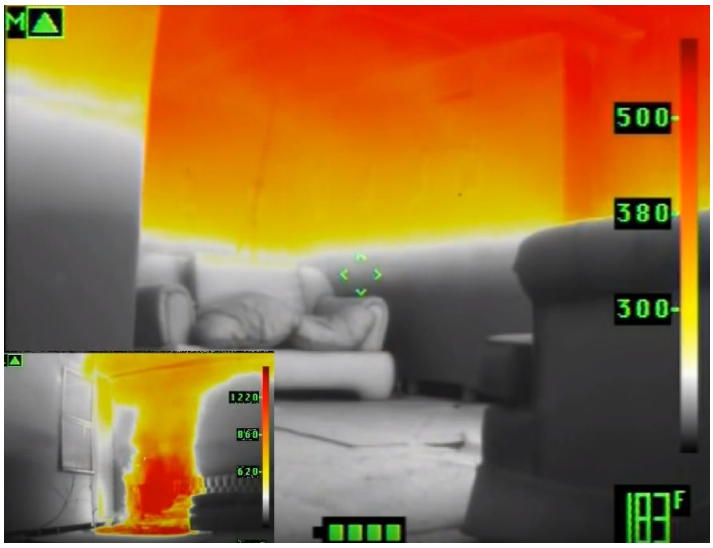

Figure 5. Heat Flux Distribution in Degrees Fahrenheit of a Burning Room [20]

Disaster Robotics

Currently, many robotic solutions exist that can aid workers in public safety jobs. Robots are machines that are commonly used to replace humans in labor-intensive, repetitive, or dangerous tasks [21]. Without prior information on the building layout during a structural fire and without real-time information on the current state of firefighters and the environment, firefighters put

their lives at risk when entering a fireground. While robotics can mitigate the risks posed to firefighters and the victims of a fire, most robotic solutions are large and heavy which can make it difficult to navigate a fireground. The following disaster relief robots have been developed to assist in the fireground.

Hoya Firefighting Robot

In 2009, the South Korean Hoya Robot Company designed a compact firefighting *spy* robot (Figure 6) that could be thrown and withstand a fall impact of 15 meters high, as well as withstand temperatures up to 160ºC for a 30-minute duration. The robot can be easily held by hand as the chassis has a height of 12.5 centimeters (cm) and weighs approximately two kilograms (kg). By using sensors to monitor the environment (measuring temperature, oxygen, and carbon dioxide concentrations) and having the ability to recognize voices, this remote-controlled device is an efficient means of exploring an unknown layout and providing significant information to firefighters to plan their actions accordingly [22][23]. Additionally, both the *tmdwl* [24] and *hoyarobot* [25] YouTube channels have videos to showcase the robot's functionality and demonstrate the device operating side-by-side with actual firefighters [26].

Figure 6. Hoya Firefighting Robot Chassis [22]

Although this device has promising functionality, there is no information regarding progress on this product after 2010. Nonetheless, the development and testing of this device demonstrates that this is a demand in the public safety sector.

ArchiBot-M & ArchiBot-S

DTB Fatec, a Korean robotics company focused in developing technology for field robots in the area of firefighting, has engineered the ArchiBot-M and ArchiBot-S series of robots[27]. ArchiBot-M, shown in Figure 7, is designed to be sent into inaccessible fire sites such as large buildings, tunnels, or storage facilities to check for explosives or combustibles, and guide firefighters to sources of fire. This robot has a suspension system that allows it to ascend and descend stairs. The robot is also waterproof and is able to withstand high temperatures. It weighs 45 kg, and it has an operating time of two hours. The maximum velocity is 20 km/hr.

Figure 7. ArchiBot-M [27]

ArchiBot-S, shown in Figure 8, is designed to be sent into inaccessible and dangerous places involving underground areas. It is designed to inform firefighters of geographical information, locations of trapped people, and burning sites. This robot is designed to be capable of rotating around in a narrow space, including ascending and descending stairs. This version also supports operation in high temperatures and has waterproof capabilities. It weighs 40 kg and provides one hour of operation [27].

Figure 8. ArchiBot-S [27]

Firo-S

IZ Holding is a manufacturing company in Singapore which has a security division focused primarily on robotics and surveillance systems. Among other products, IZ Holding has developed Firo-S [28], a firefighting robot that aims to operate in burning sites to obtain geographical information, detect humans, and track fire sources. The design includes a cooling system that allows the robot to operate at 500ºC for up to one hour. It has a built-in thermal image camera for search and rescue (S&R) operations and fire source detection. The robot, shown in Figure 9, is remotely controlled from a laptop that is equipped with a supporting software for operation. It weighs 40 kg and it can operate for up to four hours.

Figure 9. Firo-S and its GUI [28]

While the robots presented have their advantages, there is no currently available robotic solution that is human-portable (less than 40 pounds) and can survive a fireground.

Chapter 3. Approach

Problem Formulation

Given the robotic solutions currently available, there is no solution that is human-portable and can survive the harsh environment of a fireground. Therefore, this project was created to develop a small, human-portable mobile sensing platform that can operate in a fireground to assist firefighters. This section goes through the customer requirements and lists the requirement metrics used to develop the robot.

Customer Requirements

Based on the research conducted and the interview with Deputy Chief Martin Dyer of the Worcester Fire Department (WFD), the operational environment and details of a robot to assist the needs of the WFD were defined. The environment in which the assistance of a robot may be useful is converted manufacturing buildings because of their unpredictable layouts. The customer's requirements for the robot are:

- Quickly deployable
- Affordable
- Operate in the building ahead of firefighters
- The ability to survive the environment
- Evaluate and map the interior of the building
- Collect accurate environmental data
- Send data back to the Incident Commander (IC) via a simple, intuitive user interface
- Remotely controlled and easy to operate
- Long range communication
- Low power consumption
- The ability to transmit large amounts of data

The robot must be easy to deploy (i.e., take the shortest amount of time and effort possible) so that firefighters can focus on combating the fire rather than setting up the robot. Firefighters already have specific tasks they must complete in a time-limited scenario, so the deployment of the robot must be an insignificant task to add to their workload. It must also work ahead of the firefighters in order to not obstruct their normal tasks. To increase the adoption of the robot by more fire departments in the future, the robot should be affordable. Fire departments are government funded and typically have a very limited budget. The robot must also be able to survive the fire environment so that it remains useful. If the robot becomes damaged beyond use,

it will no longer be providing data to improve the fighting of fires. The robot must also be able to be used for multiple fires because it will likely be too expensive to be disposable.

Advanced technology is not widely used in firefighting. At the WFD, for example, each dispatch vehicle is equipped with one iPad that displays data from the dispatcher such as the address of the alarm and the locations of nearby hydrants, but beyond this only non-electronic systems like whiteboards and clipboards are used. Deputy Chief Dyer recognized that beyond personal smartphones, many firefighters do not interact deeply with technology. Therefore, in order to be useful to fire departments, robot-gathered data must be analyzed by the system itself and presented in a manner that is simple, concise, and relates easily to technologies that firefighters are already familiar with. The robot will be teleoperated and easy to use so that firefighters will have control of the robot at all times and will need minimal training to use it. As discussed before, the robot must have little to no interference with how fire crews normally function. Making it remote-controlled will ensure that the activities of the robot do not conflict with the activities of the firefighters at any time.

Because the robot is designed for use in large, compartmentalized buildings, it will need to communicate information to the IC outside the building. The robot will be collecting and analyzing large amounts of data, so it will need to have the capability to send that data back to the IC. Additionally, the robot should be energy-efficient so that the onboard battery will last long enough to map multiple rooms.

Requirement Metrics

From the customer requirements and background information, a set of metrics were created for each requirement. The *Metric* column is the goal, while the *Reach Metric* column are goals that would optimize the performance of the robot but were not required to be met.

Table 1. Firefighting Robot Requirement Metrics

Requirement	Metric	Reach Metric
Quickly Deployable	The robot should boot and pair within 30 seconds of firefighters exiting the truck to a fireground.	Optimize the robot to a boot and pair at a time of 10 seconds.
Affordable	A single unit should cost no more than $2000.	
Operate in the building ahead of firefighters	The robot should have a max speed of 0.5m/s (~19.7in/s) on a flat, unobstructed surface	
The ability to survive the environment		
Fire Resistant	The robot should survive at 150°C (300°F) for 15 minutes.	The robot should survive at 500°F (260°C) for 3 minutes.
	The internal temperature of the robot should stay below the maximum operating temperature of the electronic circuit components (60°C)	Should stay within a range 20 °C < temp < 45 °C
Water Resistant	The robot can withstand 5 gallons of water poured at the top of its chassis.	The robot can survive being submerged in water for 5 seconds
Impact Resistant	The robot can survive up to 2kg objects being dropped on it from 1 meter.	The robot can survive a drop of 1.5 meters
Collect accurate environmental data	The sensors on the robot should have an accuracy of <5%	Optimize the sensors to have an accuracy of <2%
Low power consumption	At room temperature, the robot battery should last 15 minutes in a 150°C (300°F) environment.	
Remotely Controlled and easy to operate	Remote control of robot is functional by qualitative assessment.	
Send data back to IC via user interface	Sustain a video feed of at least 10 frames per second.	Sustain a video feed of at least 24 frames per second.
Long range communication	Video feed and teleoperation is maintained through a single wall.	Video feed and teleoperation is maintained from X meters away through at least 1 wall.

Some of these metrics were tested to verify whether the requirements for this project were met, and the test setup and results are in the Experimental Evaluation chapter.

Design Overview

The team's approach to robot development is based on division into "subteams" to focus on the three main systems of the robot: mechanical, electrical, and software. Each subteam had the following responsibilities:

1. Mechanical subteam tasks:
    a. Robot wheels design
    b. Overall chassis shape design
    c. Material layering system design
2. Electrical subteam tasks:
    a. Sensor integration
    b. Power distribution design
    c. Motor controls design
3. Software subteam tasks:
    a. Data processing
    b. Wireless communication
    c. User interface

Robot Chassis

The decision to have the robot operate on the floor was made prior to designing the chassis. Heat rises, so operation on the ground will generally expose the robot to the coolest possible temperatures. Drones were ruled out as an option because air currents in a thermally dynamic environment like a fire make flying extremely difficult. Figure 10 shows a SolidWorks model of the final chassis design.

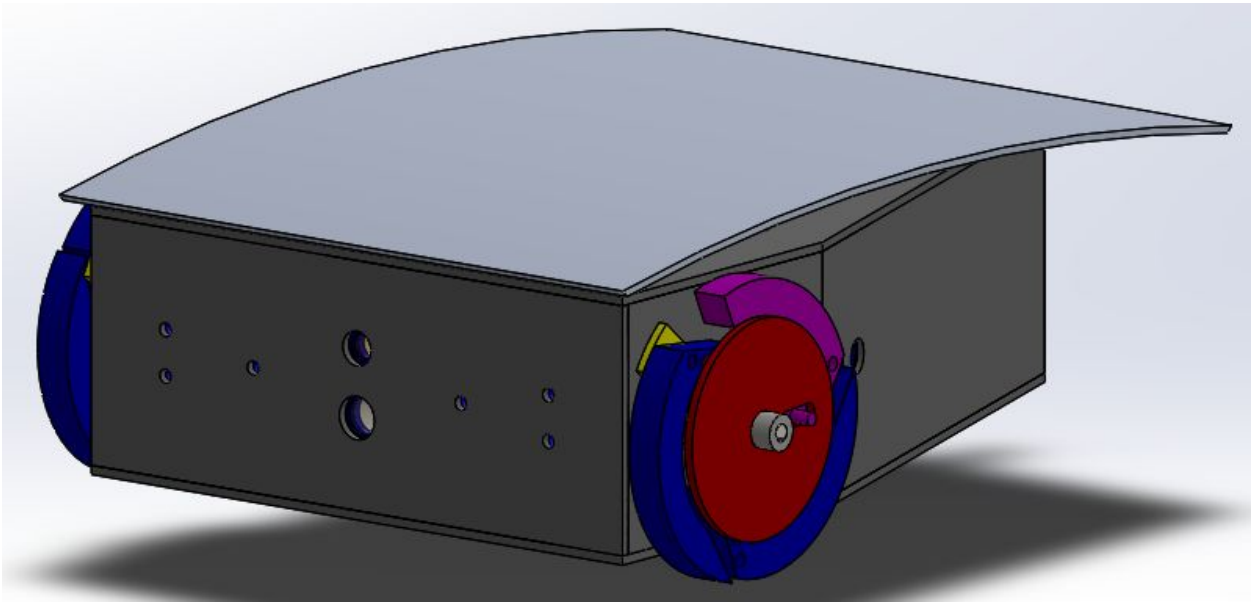

Figure 10. Final chassis design

The robot chassis was designed in three different parts: wheel design, overall shape, and insulation. Different wheel designs were compared using a set of criteria to optimize the robot's mobility and meet the project requirements. Once the wheel design was finalized, the overall shape of the robot was modeled. A layered structure of insulating materials was developed to increase the operation time of the robot in a high-heat environment. Each layer of material was thoroughly researched in order to optimize the operation time of the robot in a fireground.

Wheel Design

Multiple wheel designs were considered for the robot. These wheel designs included whegs, treads, wheels, transformable wheel, and wheels in a tread formation. A Pugh chart was created to compare each of these wheel designs. The requirements chosen for the wheel design were determined to optimize the functionality of the robot. The Pugh chart weights were used to rank the requirements in terms of importance. Ultimately, the Pugh chart was used to narrow down the wheel designs to the optimal wheel design choice for the robot.

Requirements

Given the complex and unpredictable nature of a fireground, it is of critical importance that the robot's drive system is robust but also flexible. The following criteria were defined to maximize drivetrain efficiency. The robot must be able to navigate over small obstacles, such as bits of fallen ceiling debris or raised door thresholds. Additionally, the robot's drivetrain must be able to withstand impacts of being dropped or deployed roughly. The robot must be able to drive quickly enough to stay ahead and out of the way of firefighters but also be able to drive and turn smoothly so that the sensors receive consistent data. For example, a robot that bounces or

wobbles excessively would return a very shaky camera feed. A lightweight drivetrain with a minimal number of motors is optimal because one of the project requirements is that the robot be needs to be human-portable. Along with the rest of the robot, the drivetrain must be easy to maintain once built; a system that requires frequent fixing or maintenance will complicate the jobs of firefighters. The final factor considered was ease of implementation. A system with many customizations or actuated parts would be less efficient than common, off-the-shelf parts.

In summary, the requirements of the drive system are:

- Obstacle navigation
- Impact Resistant or Springy
- Drive quickly
- Drive smoothly
- Turn smoothly
- Lightweight
- Easy upkeep
- Simple to implement

Unlike the project requirements, which were defined with individual metrics, these points were used to compare different wheel options against each other as seen in the Pugh chart included in the next section.

Types of Wheels

In order to optimize the above listed drivetrain requirements, the team considered seven different types and orientations of drive systems as shown in Figure 11.

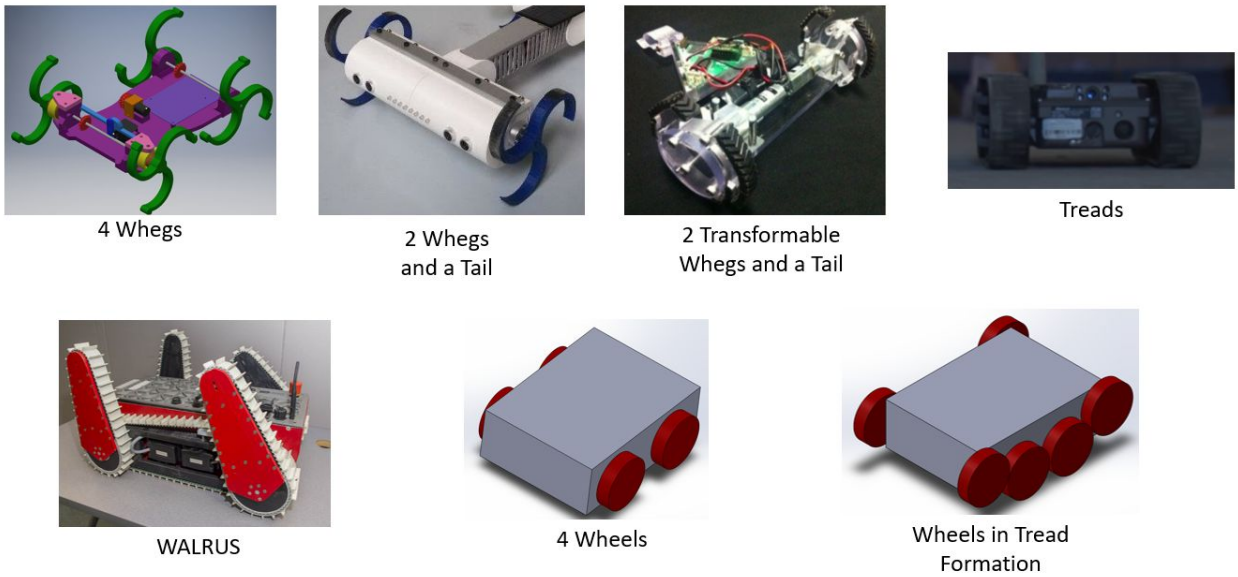

Figure 11. Drive systems considered for final robot

Two layouts involving standard round wheels were considered: a standard 4-wheel drive setup, and 6-8 wheels (per side) in a mirrored formation, as seen in Figure 11. The main benefit of a basic four-wheel drive was simplicity of implementation, both in construction and driving. The main benefit of the double-sided formation of 12-16 wheels would be the ability for the robot to drive immediately after being deployed independent of which side it landed on. The robot would have no designated top or bottom, and would be able to function in either direction. Of the options considered, the main benefits of standard round wheels were their stability for providing smooth sensor feedback and their broad commercial availability (wheels are available for purchase in many sizes and materials). The primary drawback to basic wheels is their inability to absorb impacts from being dropped. Vehicles that must cope with uneven surfaces and impacts, such as all-terrain vehicles, use inflated tires to absorb impact forces. However, tires are not a feasible solution within a fireground because of the risk of melting or even explosion if a tire gets too hot. Wheels used on a firefighting robot would have to be entirely rigid and likely made of metal, which are likely to be damaged or break their axles if the robot is deployed roughly. Without tires, wheels also cannot scale obstacles taller than the radius of the wheel. As shown in the Pugh chart below, the options with wheels ranked high for smooth driving, ease of turning, and speed, but ranked poorly for obstacle navigation/avoidance.

Two types of treads were considered because of their ability to scale obstacles and uneven terrain. The first style considered was continuous track, commonly known as tank treads. When oriented in a trapezoidal shape, the raised front and back allow a vehicle to scale uneven terrain and small obstacles. A tank-driven robot also drives fairly smoothly and is relatively easy to turn. The second tread-based configuration was modeled after the WALRUS Rover (Water and Land Remote Un-manned Search Rover) built by a team of WPI students in 2014-2015. The WALRUS Rover has four independently driven and actuated treaded “pods” as seen in Figure 11 which allow for very effective obstacle navigation. However, the WALRUS Rover was a full-year project and would likely be very difficult to implement and maintain within the restraints of this project. In addition, neither of these options would be able to effectively absorb the impact of a drop or rough deployment, neither is particularly fast, and both require significant maintenance as their belts wear down. These traits are weighted accordingly in the Pugh chart.

The third type of drive system considered was whegs. “Whegs,” a combination of wheels and legs, utilize the obstacle-clearing advantages of legs and feet in the rounded shape of a wheel (Figure 11). Their individual legs can absorb impact (especially when they are curved) while their round shape comprised of multiple spokes can be attached to an axle and driven like a wheel. The primary issue with whegs is the result of a trade-off; having more legs reduces obstacle scaling potential, but having fewer legs causes increasingly uneven, wobbly driving. The team considered a 4-wheg configuration ,which would yield the most erratic driving, as well as a triangular 2-wheg configuration, with a “tail” in the rear (first two designs in Figure 11).

Both wheg options were ranked highly for obstacle avoidance, but scored poorly for smoothness of drive and ease of turning.

The final option considered was a modified wheg, called a transformable wheg, which has legs that can expand to scale obstacles but is able to transform back to a rounded wheel. This option allows for the versatility of whegs, but also allows for smoother driving (and thus smoother sensor feedback) whenever possible. The research published about transformable whegs showed them used in conjunction with a tail on a triangular chassis, which was the final configuration considered in the Pugh chart (Table 2). All Pugh chart ranks were chosen and all drivetrain decisions were made together by the team in an open-discussion meeting.

Table 2. Pugh chart used to decide wheel type

Ranking	Criteria	Weights	4 Whegs	2 Whegs with Tail	Wheels Transform to Whegs with Tail	Treads	Walrus	4 Wheels	Wheels in Tread Formation (6-8)
2	Smooth Drive	1 - Wobbly; 5 - Smooth	2	3	4	5	5	4	4
1	Ease of Turning	1 - Hard; 5 - Easy	1	3	5	4	3	5	4
2	Weight	1 - Heavy; 5 - Light	4	5	4	2	1	3	2
3	Obstacle Avoidance	1 - Can't Climb; 5 - Can Climb	5	5	5	4	5	1	3
1	Ease of Implementation	1 - Hard; 5 - Easy	4	4	3	3	1	5	4
2	Speed	1 - Slow; 5 - Fast	3	3	4.9	2	2	5	5
3	Droppable	1 - 0m; 5 > 3m;	4	3	2	1	1	5	5
1	Upkeep	1- Hard; 5- Easy	5	5	4	1	1	5	4
		TOTAL	55	58	**58.8**	41	39	57	58

The speed of the transformable whegs was given a 4.9 rating because it was thought that they would be slightly slower than wheels since the trigger leg has a gap. The colors in the bottom row indicate how each drivetrain scored. The highest scores are indicated in green, the middle scores are yellow, and the lowest scores are indicated in red.

Best Options and Final Choice

The weighted sums in the Pugh chart yielded “2 whegs and a tail,” “Transformable whegs,” and “Wheels in a tread (tank) formation” as the best options. After an in-depth discussion, the team chose a drive configuration of two transformable whegs with an omniwheel tail. The multi-wheel design was ultimately ruled out because even though it allowed for a reversible chassis, there was no reliable way to absorb impacts. The transformable whegs were chosen over standard whegs for their increased smoothness of drive because, as a mobile sensing platform, the goal of our robot is to return the best possible sensor data.

Passive Transformable Wheg Design

Using the design of a passive transformable wheg developed at the Seoul National University [29], the mechanical team created a transformable wheg to suit the needs of a compact firefighting robot. Transformable whegs are terrain adaptable, utilizing both the obstacle-scaling ability of whegs and the smooth drive of normal wheels as needed.

Each wheg has five components: three legs and two side plates (see Figure 12). The curvature of the legs forms the perimeter of the wheg while a series of slides, pins, and springs controls the movement of the legs in relation to the side plates. One side plate, called the wheel-base, has a tri-point shape; its center hole fits a D-shaft axle to drive the wheg. All three legs are bolted to the wheel-base and rotate about these joints when "deployed." When an obstacle is no longer actively keeping the whegs deployed, a torsion spring at the trigger leg's joint pulls the legs back into wheel formation.[5] The design published by the Seoul National University team utilized a torsion spring around the trigger leg/wheel-base joint, and a metal wheg would need the force of the torsion spring to keep the legs in a closed position. However, the 3D printed prototype whegs used on the robot were lightweight and had enough internal friction that their default position was the wheel configuration. Each wheg has two follower legs and one trigger leg.

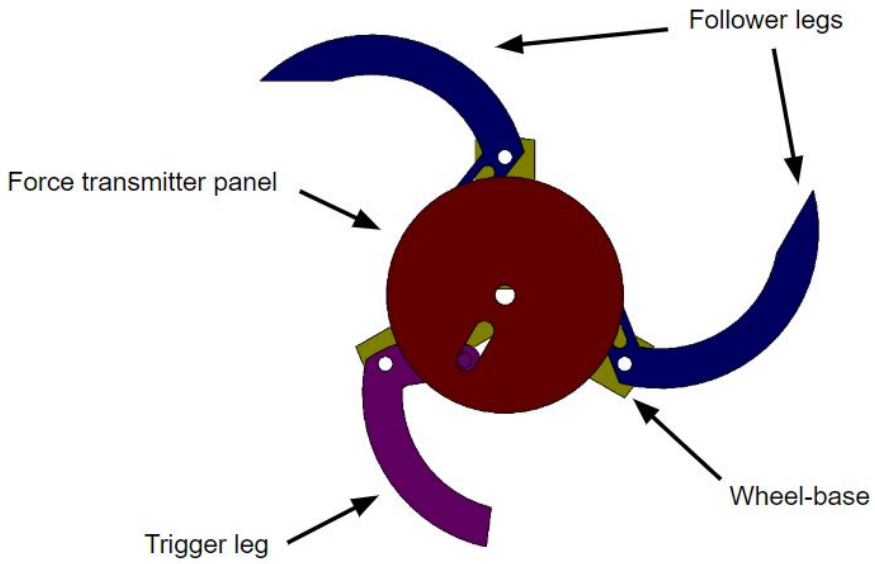

Figure 12. Labelled transformable wheg

[5]The use of springs rather than actuators is what makes the whegs passively transformable; active transformable whegs would be heavy.

The trigger leg has a sharply angled edge that forms a notch in the perimeter of the wheel. When the notch catches on an obstacle such as a step, it forces the leg out. A peg on the trigger leg rotates the force transmitter side panel which slides the other two legs into their open positions as well, hence the name trigger leg. The second side panel, which functions as a force transmitter, has an oblong cutout that acts as a slide for the peg on the trigger leg. The force transmitter itself also has two pegs facing inward, which move in similar slides on the follower legs to open them. The rotation of this panel utilizes the force from opening the trigger leg to opening the follower legs, thus deploying the wheg (Figure 13).

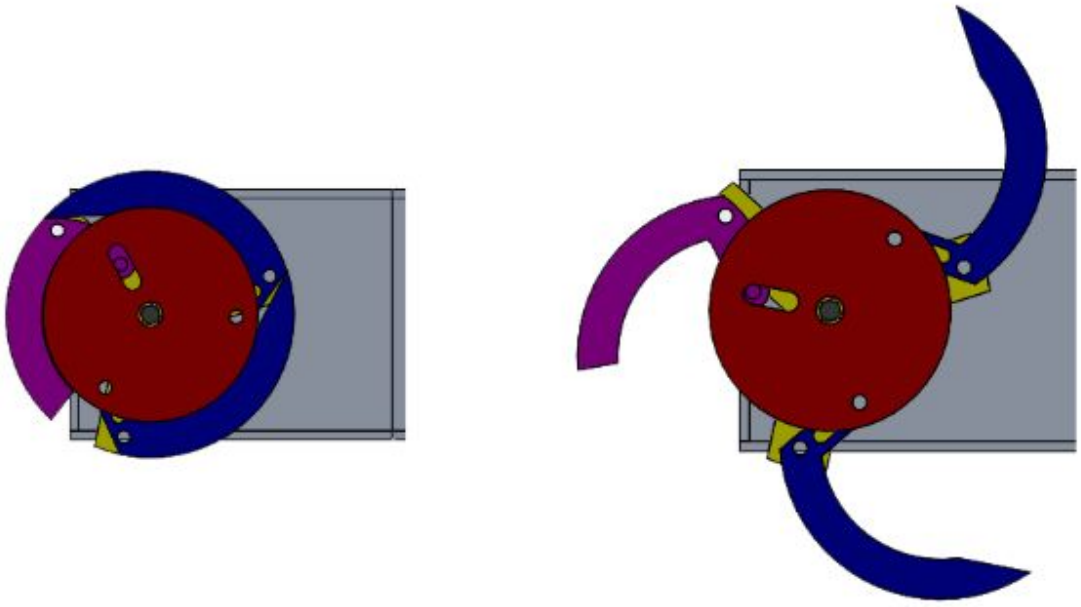

Figure 13. (left) collapsed transformable wheg, (right) expanded transformable wheg

The designs from the Seoul National University publication were manufactured from CNCed polycarbonate, with strips of anti-slip rubber padding on the legs' contact surfaces. Due to the high temperature environment, heat-treated aluminum from which to machine the whegs was selected. Each leg is half an inch thick to increase strength and surface contact area. For prototyping and testing, multiple iterations of the whegs were 3D printed. The final whegs have a diameter of four inches in wheel form and extend to a six inch diameter in wheg form. All whegs were assembled with #8-32 bolts and nyloc nuts.

Chassis Design

To determine the overall shape of the robot, the four designs shown in Figure 14 were considered. These designs follow the drive configuration of two transformable whegs with an omniwheel tail The red circles indicate wheel positions.

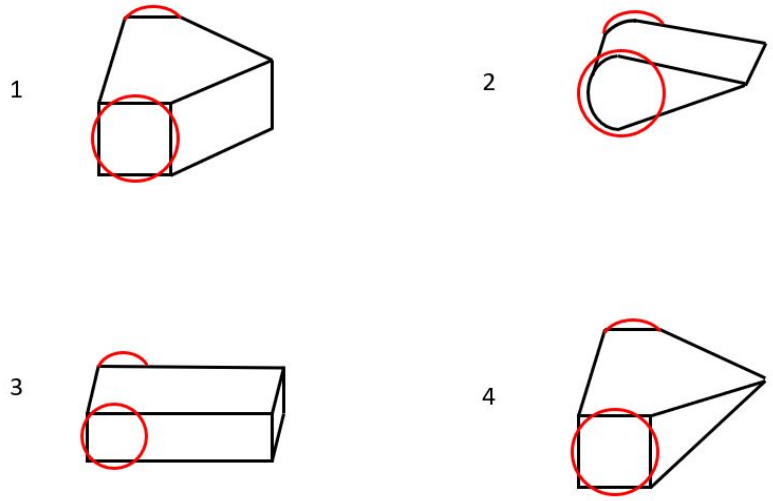

Figure 14. Initial chassis designs

Design 1 was chosen as a baseline for the shell of the robot because it is compact, streamlined, and easy to manufacture. Out of all the designs, design 3 was ruled out because it is the least fluid dynamic and not as compact. Because the interior of the robot holds the battery, motors, and electronics, it is necessary to have enough interior space in the chassis. Both design 4 and 2 were ruled out because they decreased the interior space too much. Although design 2 is very fluid dynamic, the curved design was not implemented since it would be difficult to manufacture.

Design 1 was modified to be more square at the back, so an omni-directional wheel could be attached to make the driving more smooth. Originally, the robot was going to be designed to be "flippable" where it could drive upside down or right side up, but the largest omni-directional wheel that could be bought and survive the environment was four inches in diameter. To fit all the electronics inside the robot, the robot would need to be more than four inches tall, so the "flippability" of the robot was removed. Additionally, to make the chassis more fluid dynamic and in case something were to fall on top of the robot, a curved shield was attached to the top of the shell. Figure 15 shows the final shape of the chassis in SolidWorks. The left picture is the chassis shape without the aluminum shield and the right is with the aluminum shield.

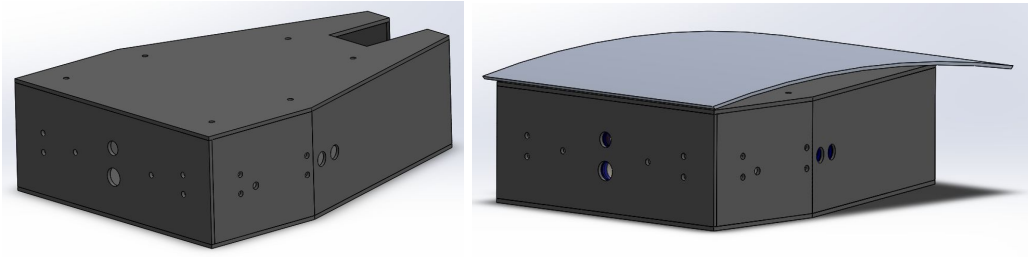

Figure 15. Finalized chassis shape with (right) and without (left) the aluminum shield

Material Layering System

The interior of the robot must remain below 60°C (140°F) while the robot is operating in order for the battery to discharge effectively and the rest of the electronics to function properly. The robot will have to survive a high-heat environment, and the electronics will increase the interior temperature while the robot is operating. Different materials with low thermal coefficients were layered to decrease the speed of heat flow to the interior of the robot. Active cooling was not a viable option because the robot will be operating in a high-heat environment, so there would be no way to release the hot air from inside the robot.

Research showed an effective way to keep the interior of the robot cooler for longer was to layer different materials with low thermal coefficients [30]. In "A New Concept for Indoor Fire Fighting Robot," the layers of the robot are outlined as follows:

1. **silver coating**: an excellent thermal reflector which reflects most flames and high temperatures reducing the thermal energy by 50% upon passing through the first protective layer.
2. **aluminum board** (2mm): protects the robot from falling objects and obstacles, but it is not a good thermal insulator.
3. **non-flammable materials** (1.5mm): a non-flammable, cloth-like material with low thermal conductivity.
4. **air space** (5mm): greatly reduces any heat that has made it through the case thus far from the outside.
5. **insulation board** (13mm): nonflammable, non-heat conductive of and easy to process, maintained in the shape of Styrofoam.

The layering system described above keeps the interior temperature of the robot at 70°C (158°C) and can survive in an environment up to 700°C (1292°F) for about one hour.

CES EduPack was used to help find the materials to use for the robot. The "Limit" function was used to narrow down materials. The following limits were set for the following properties:

1. Maximum Service Temperature: minimum 150°C
2. Price: maximum $20/kg
3. Specific Heat Capacity: minimum 750 J/kg*°C
4. Water Durability: Excellent

Based on the materials that still remained, a spreadsheet (shown in Figure 16) was used to compare certain properties of each material.

name	cost ($/kg)	fracture toughess (MPa*m^0.5)	max service temp (deg C)	specific heat capacity (J/kg*degC)	thermal expansion coeff. (microstrain/degC)	durability in water	density (kg/m^3)	Thermal conductivity (W/m.degC)
alumina	18.3-27.4	3.3-4.8	1.08e3-1.3e3	790-820	7-7.9	Excellent	3.8e3-3.98e3	26-38.5
epoxies	2.26-2.91	0.4-2.22	140-180	1.49e3-2e3	58-117	Excellent	1.11e3-1.4e3	0.18-0.5
silicon carbide	14.5-20.7	3-5.6	1.4e3-1.7e3	663-800	4-4.8	Excellent	3.1e3-3.21e3	80-130
teflon	9.32-11.3	1.32-1.8	250-270	1.01e3-1.05e3	126-216	Excellent	2.14e2-2.2e3	0.242-0.261
phenolics	1.65-1.87	.787-1.2	200-230	1.47e3-1.53e3	120-125	Excellent	1.24e3-1.32e3	0.141-0.152
silicone elastomers	4.57-6.26	0.03-0.5	227-287	1.05e3-1.3e3	250-300	Excellent	1.3e3-1.8e3	0.3-1
Cast Al-alloys	1.99-2.15	18-35	130-220	900-995	16.5-24	Excellent	2.5e3-2.9e3	80-160
rigid-polymer foam	15.3-19.6	0.0066-0.0486	66.9-157	1.12e3-1.91e3	20-70	Excellent	78-165	0.027-0.038

Figure 16. Material comparison chart

In Figure 16, bright green indicates the property exceeds requirements. The green indicates the property meets the requirements. Yellow indicates that the property meets one end of the requirements, and red means it does not meet requirements. A material (first column) was given a color based on the average color of their columns. For example, if a material's columns were mostly green and yellow it was given green. If there was any red, it was given yellow. All the green materials were then search for to see if they could be purchased. Based on availability and actual price, the materials were then chosen.

The robot in "A New Concept for Indoor Fire Fighting Robot" was significantly larger and heavier than the robot created for this project, so fewer layers were used in this project. Layers for the robot include:

1. **Aluminum shield** (⅛"): for protection and is lightweight
2. **Reflect-A-Cool**: thermal reflection layer
3. **Teflon** (⅛"): low thermal conductivity, robust, relatively light-weight
4. **Air space** (¼"): blocks heat conducted through the Teflon
5. **Rigid foam** (½"): nonflammable, light-weight, and nonconductive

The amount of each material needed was determined by a Computer Aided Design (CAD) model in SolidWorks. The CAD model was designed from the inner layer to the outer layer to ensure the electronics would fit. The width of the front of the robot was determined using the motor length of both motors while the length of the robot was determined so the robot would remain within a one cubic foot volume. Figure 17 shows the dimensions of the robot shell from the top (the outer shell is 3 ⅝ inches tall), and Figure 18 is a sectional view of the robot with labelled materials.

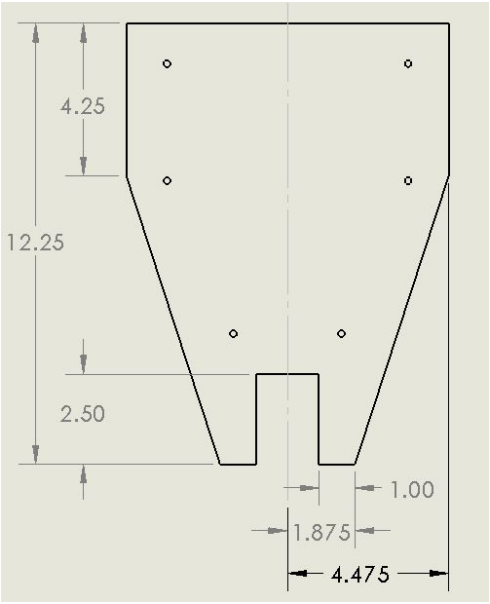

Figure 17. Dimensions of outer shell in inches

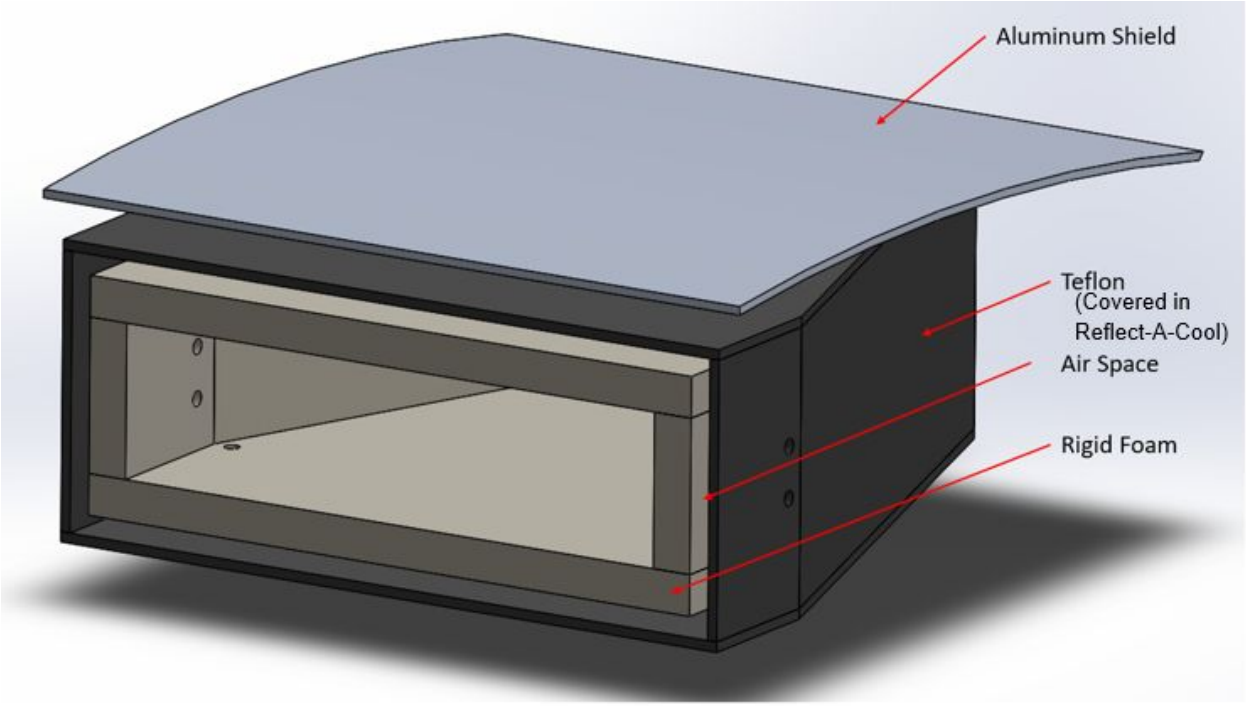

Figure 18. Section view of robot with labelled layers

As shown in Figure 18, the top shield was chosen to be aluminum because of its light-weight and durable properties. If an object were to fall on top of the robot, the aluminum shield would help protect it. Additionally, the curved shield allows for water runoff and smoother heat flow around the robot. Ceramic spacers were used to separate the aluminum shield from the teflon to prevent

the aluminum from melting the teflon. The teflon layer was chosen because of its maximum service temperature, low thermal conductivity coefficient, and low density. A layer of Reflect-A-Cool was placed on top of the teflon to reflect radiating heat. A layer of air was used to act as a thermal insulator. To create the air layer, spacers between the teflon and the foam layer were 3D printed using PLA to reduce costs. PLA is inexpensive and has a melting temperature between 180°C (356°F) and 220°C (428°F) which would keep the robot intact during operation. The rigid foam was chosen as the inner layer to protect the electronics because of its light weight and low thermal conductivity coefficient.

Once the materials were chosen, the amount of time it would take to heat the interior of the robot to 60°C (140°F) was calculated using the thermal coefficients and specific heats of each material. To calculate the amount of time for the interior to reach 60°C (140°F), the thermal resistance of all the layers was calculated to be 1.974 °C/W (35.55°F/W). The amount of energy transferred through all the layers was calculated to be 65.87 W. In order to calculate the total time, an assumption that when the foam reaches 70°C (158°F) the interior of the robot will be at 60°C (140°F). Using this assumption, the amount of time the interior of the robot will stay below 60°C (140°F) when the robot is operating in 150°C (302°F) environment was calculated to be 6.16 minutes. See Appendix A for the full thermal calculations.

Final Chassis Construction

The following steps were used to construct the final robot shown in Figure 19.

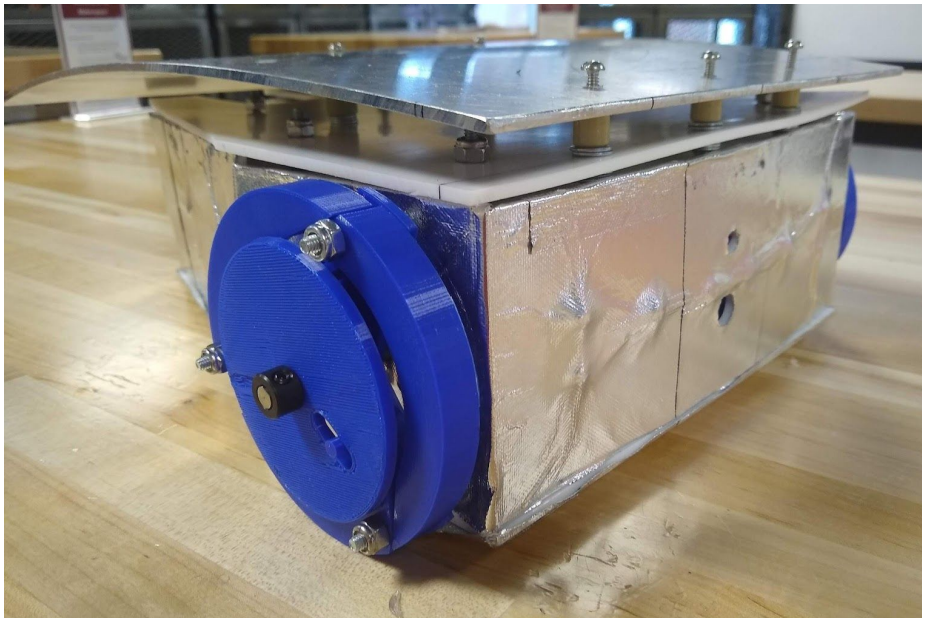

Figure 19. Robot fully constructed

1. Cut the materials
    a. Rigid foam and Teflon were cut using a bandsaw
    b. Aluminum shield was cut using a jigsaw
2. Bend the aluminum shield using rollers
3. Drill holes for spacers, axles, motor mounts, and lens holders
4. Assemble the foam layer using J-B Weld ExtremeHeat Temperature Resistant Metallic Repair Paste (referred to as "thermal paste") to bind the sides together (top foam piece excluded from pasting so that the interior could be easily accessed)

Figure 20. Foam layer drying after application of metallic thermal paste

5. Press fit the bearings into their respective holes with thermal paste for reinforcement

Figure 21. Bearing press fitted with thermal paste

6. Attach the Teflon side and front pieces using #8-32 stainless steel machine screws and #8-32 Nylon lock nuts, with #8 zinc washers on either side of the foam layer for support, and 2 machine screw nuts (size #8-32) per bolt functioning as spacers

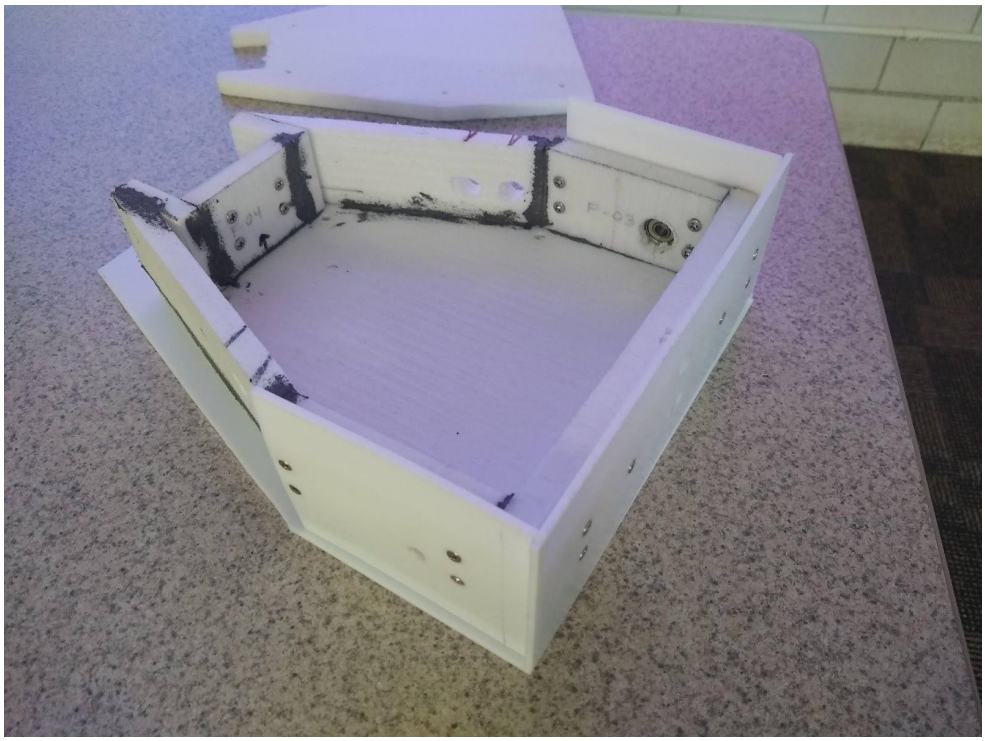

Figure 22. Foam layer with front side panels attached and lined up on unattached bottom Teflon panel

7. Mount the motors to the 3D printed motor mounts, then secure the mounts to the bottom foam piece before attaching the bottom Teflon piece

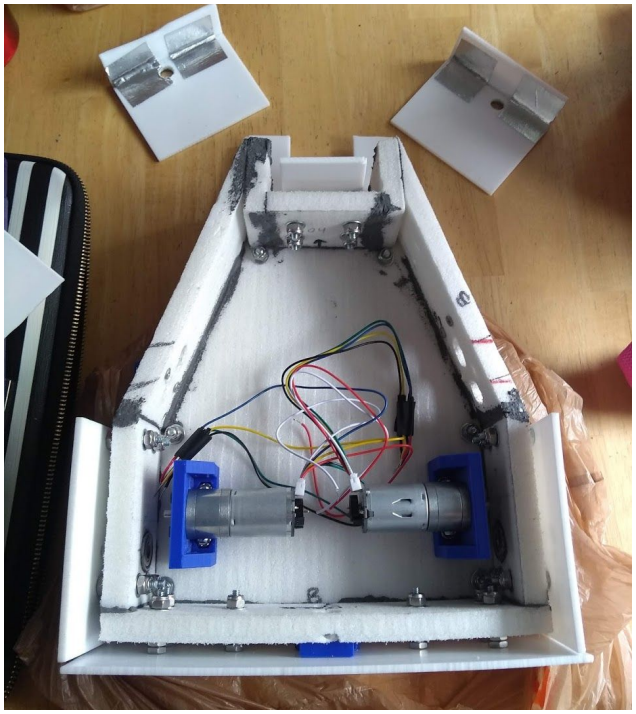

Figure 23. Chassis with front and side Teflon panels attached and secured motor mounts

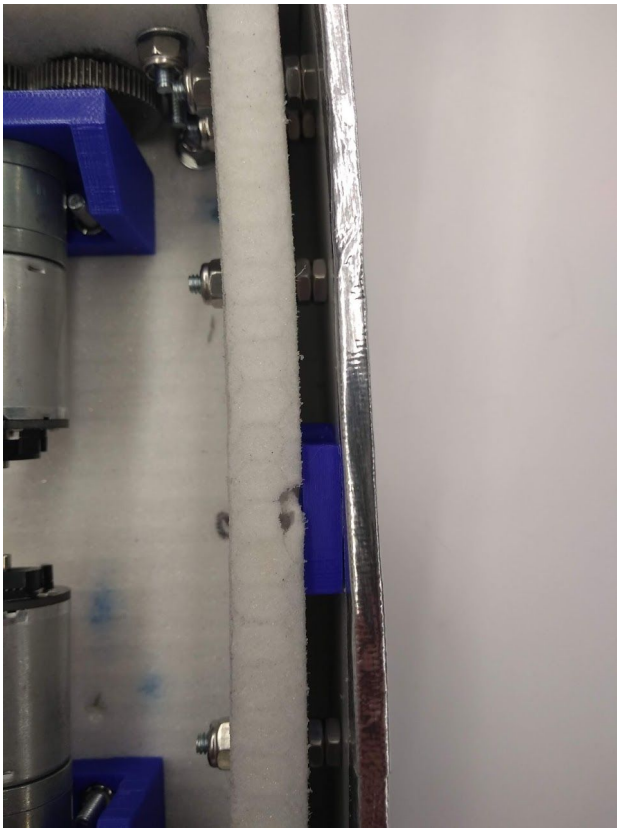

Figure 24. Spacer system

7. Glue back Teflon pieces that surround the omnidirectional wheel together using 100% RTV Silicone adhesive. Once cured, reinforce it with strips of Reflect-A-Cool and attach to the foam using bolts and spacers

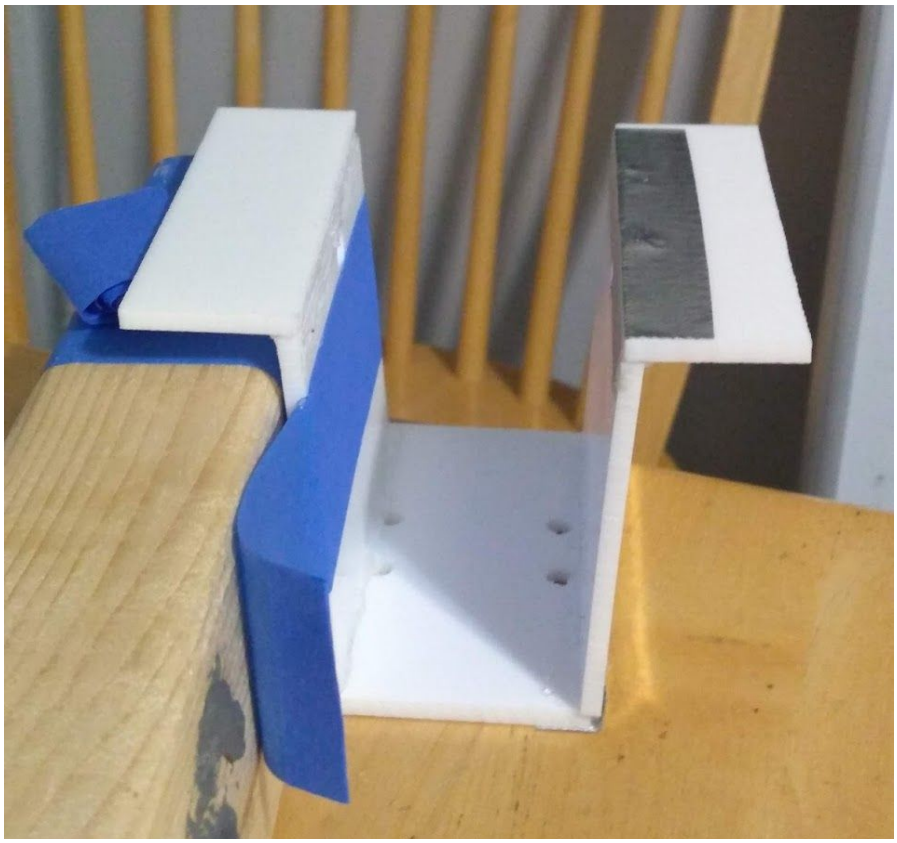

Figure 25. Teflon panels supported in a right angle while curing

8. Attach angled side pieces of Teflon to foam using spacers and machine screws
9. Place lenses inside lens holders as shown below and then mount lens holders between the Teflon and foam layers

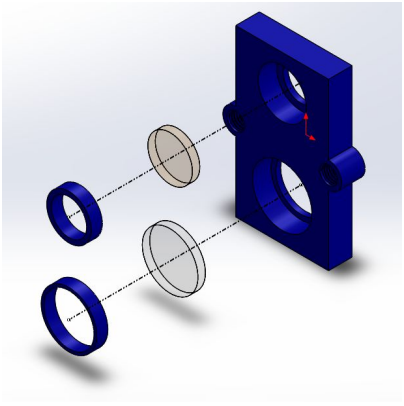

Figure 26. Lens holder mount

10. Drill holes in the aluminum shield so it can be attached to the top Teflon piece
11. Attach top Teflon piece to top foam piece using #8-32 bolts, nylock nuts, and machine screw nuts as spacers. Then attach aluminum shield to Teflon piece using machine screws and ceramic spacers

The omnidirectional wheel was not mounted to the robot because the back of the robot was not strong enough to support it. The silicone adhesive used to glue the pieces together did not bond well to the surfaces due to Teflon's slick surface. The weight of the omnidirectional wheel was enough to pull the silicone joints apart.

System Design

This section contains the complete electrical system design of the firefighting robot. Prior to the implementation stage, it is vital that the correct choices are made to ensure optimal functionality of the device. Using the requirement specifications and the background research, a high-level block diagram was designed (Figure 27).

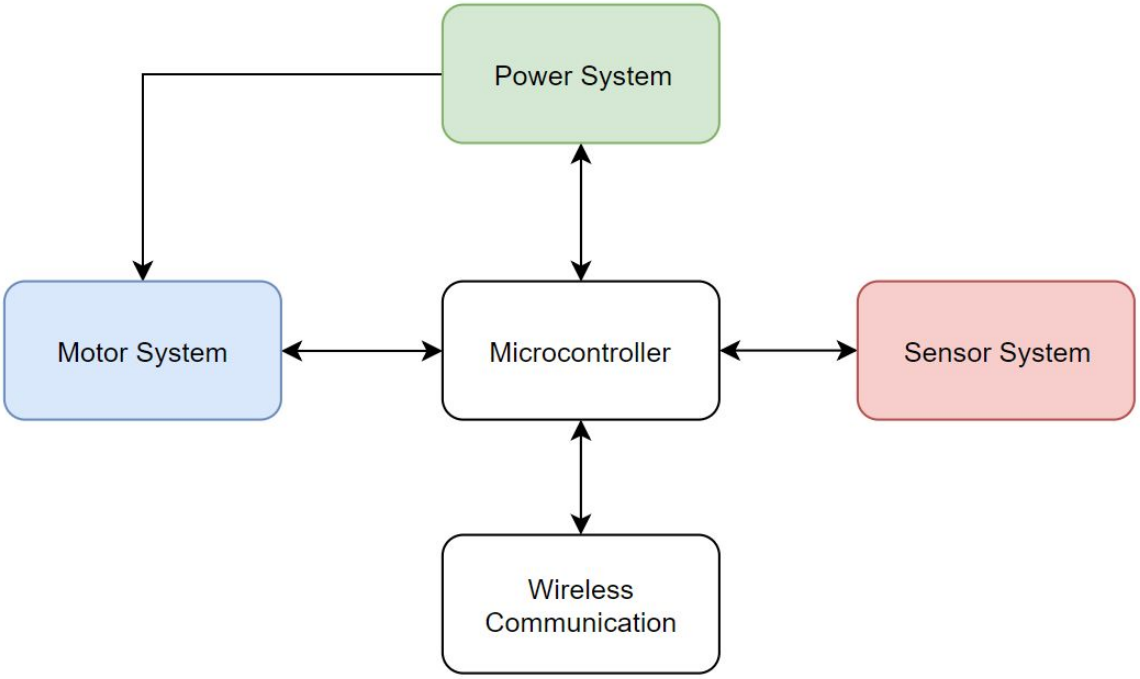

Figure 27. High Level Block Diagram

As shown in the figure above, the high-level block diagram is composed of five different modules: a microcontroller unit (MCU), a power system, a motor system, a sensor system, and wireless communication. In the following sections, the design choices of each module will be thoroughly described using pre-made assumptions, comparison charts, and scientific reasoning.

Sensor System

As specified previously, the robot must:

1. survive a high temperature environment of 300°F for 15 minutes;
2. detect the temperature and heat flux of its environment;
3. and provide a 2D heat map overlay of the environment it is traversing.

Given that the robot will be teleoperated and a map of the room will be provided, the sensor system will be composed of two different subsystems – an external sensor system that is used to detect information from the environment, and an internal sensor system that is used to detect changes in the robot.

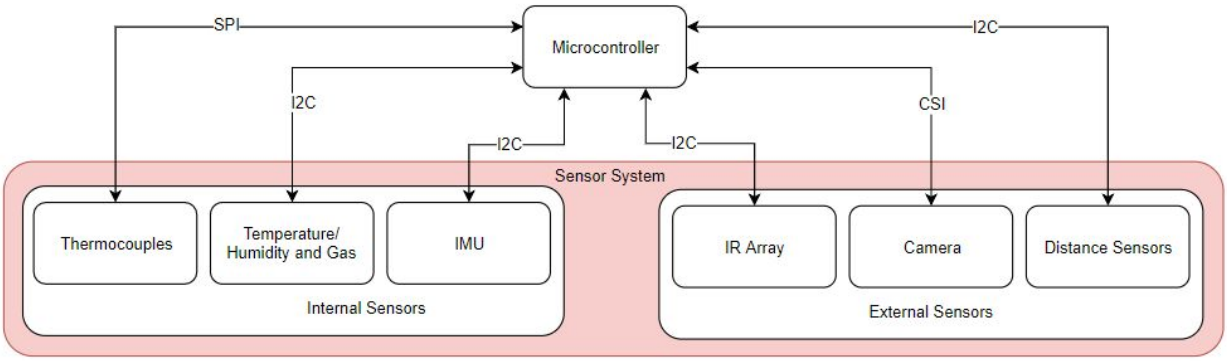

Figure 28. Sensor System Block Diagram

External Sensor System

The external sensor system is made up of three main types of sensors: a camera, distance sensors, and infrared (IR) arrays. Figure 29 is a depiction of the external component configuration on the robot. Since the robot will be remote controlled from outside the building, it is necessary that the driver has a means to visually perceive the environment. Therefore, a camera on the front of the robot will be utilized. Although the robot is teleoperated and a map of the field is provided, distance sensors are necessary for localization. These will be placed on the front and sides of the robot to help understand where the robot is located relative to its position on the map.

The IR array sensors will be used to detect both room temperatures and hotspots, and they will be placed around the robot. The front IR array will mainly be utilized to aid the driver in identifying areas by temperature.

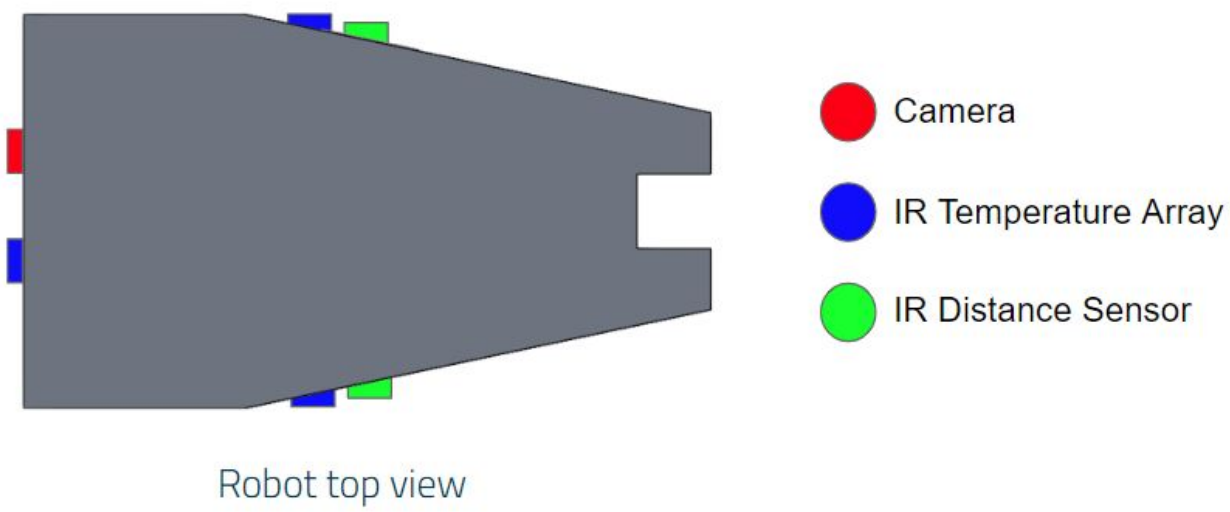

Figure 29. External Sensor Configuration

Camera

As mentioned, a camera is a necessary component for the firefighting robot. Not only will it be used for remote controlling the robot in an unknown environment, but it can also be used in future projects to identify the structural integrity of a building or the victims of a fire through computer vision.

In choosing the camera, the main specifications were the resolution and the sample rate. However, considering the microcontroller that was selected (see the Processors section), the camera that was chosen was a Raspberry Pi Camera. Unlike its predecessors, it has an 8-megapixel Sony IMX219 image sensor and supports high resolution video formats such as 1080p30 and 720p60[6]. This was the ideal choice as it has high quality footage, is inexpensive, and is compatible and easy to integrate with the processor.

[6] 1080p30 represents a video feed of 1920 x 1080 pixels at 30 frames per second. On the other hand, 720p60 is 1280 x 720 pixels at 60 frames per second.

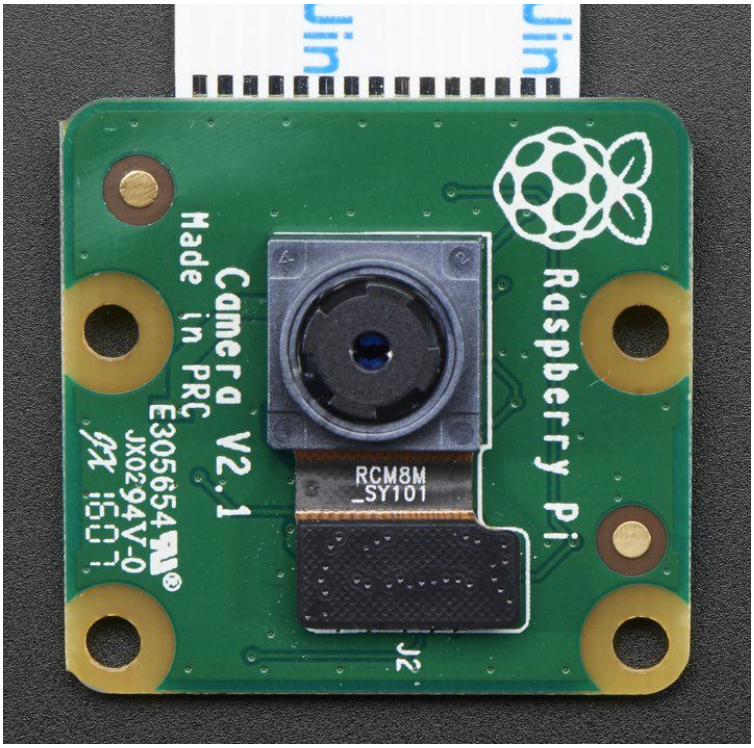

Figure 30. Raspberry Pi Camera Board v2 - 8 Megapixels [31]

Distance Sensors

A proximity sensor can detect the distance it is from an object without any physical contact [32]. This is an important sensor to have as it can help localize the robot relative to a map of its environment. With a distance sensor, the robot will be able to determine where it is as it creates the 2D heat map overlay. For future cases, the proximity sensor can also be used for localization in autonomous driving and map generation. There are many types of proximity sensors; however, due to the cost and complexity, a Time of Flight sensor will be utilized.

Research on range finding in fire-smoke environments show that longer wavelength sensors usually tend to fail to operate in certain fire environments [33]. J.W. Starr conducted an experiment to test different types of range finding sensors in two fire-smoke environments. The table below represents a summary of his findings.

Table 3. Summary of Range Finding sensors in Fire-Smoke environments [33]

Sensor	Dense Smoke, Low Temperature	Light Smoke, High Temperature
Electromagnetic Sensors		
LIDAR Sensors	Attenuation at 4 m visibility; failure at 1m visibility	No effect
Visual Cameras	Attenuation at 8 m visibility; failure at 1m visibility	No effect
Kinect™ Depth Sensor	Poor results even with >8m Visibility (Combination of particle blocking and sensor being flooded by light from fire)	Sensor flooded by light from fire during whole test
Night Vision	Failure at about 4m visibility	Sensor flooded by light from fire during whole test
Thermal Cameras	No effect	No effect
Radar	No effect	No effect
Other		
Sonar	Some attenuation with temperature change	Attenuation with temperature change

Considering the robot will mainly be used to explore areas unknown to firefighters, it is expected and therefore assumed that the environment will have light smoke and high temperatures. As shown in table 3, sonar, night vision, and the Kinect Depth sensor are eliminated since the results were poor during testing. Although both thermal camera and radar have no effect in both environments, due to the complexity and cost, the thermal camera is dismissed as a possible proximity sensor. Bearing in mind that the robot will be looking for hotspots, it is essential that the distance sensor chosen can "see" through fires. LIDAR (Laser Imaging, Detection And Ranging), which in this case has no effect in the robot's presumed environment, can effectively "see" through a fire [34]. However, due to its high price, going with a Time of Flight (ToF) sensor, which makes up the LIDAR, is more ideal.

ToF sensors enable accurate distance ranging by directly measuring the distance to an object based on the time for emitted photons to be reflected. Other proximity sensors such as infrared (IR) technology can only measures signal strength, and thus the measurements are affected by the object's reflectivity. Not only are they accurate, but they also have low power consumption, low cost, and easy integration making it the most ideal proximity sensor for the robot [35].
Since the robot is expected to traverse through rooms and hallways, it is important to consider the distance range for the sensor to measure. Because this sensor will be used for localization, it should measure very close ranges as well as up to a meter in length. The most suitable device is the VL53L0X Time of Flight sensor which can measure between 30mm to 1000mm [36].

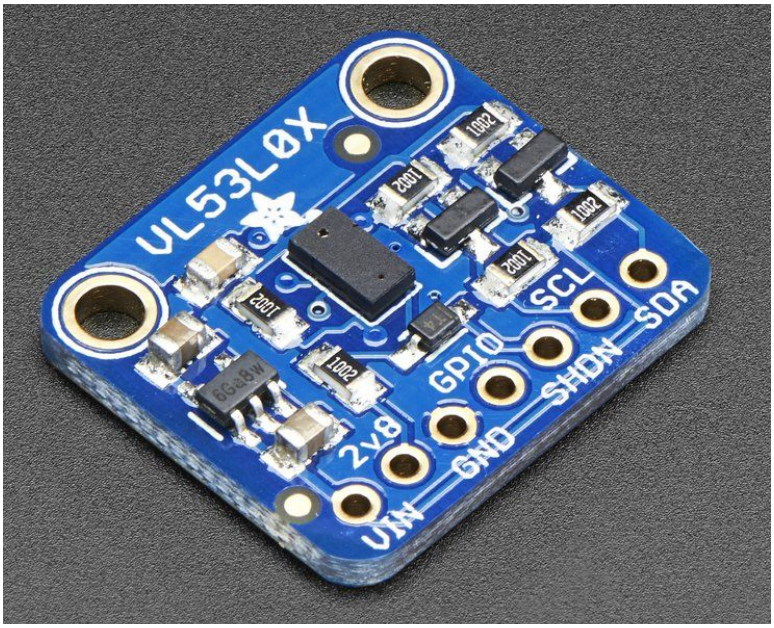

Figure 31. VL53L0X Time of Flight sensor [36]

Infrared (IR) Arrays

It is vital to measure temperature in a fireground as it will be used to give firefighters a better understanding of how the current environment is developing. Since the robot is driven on the ground, the temperature measured using a simple ambient temperature sensor will not be an accurate representation of what is occurring in the room. Instead of using a thermopile IR sensor, which is a single point temperature sensor, the robot will utilize multiple IR arrays.

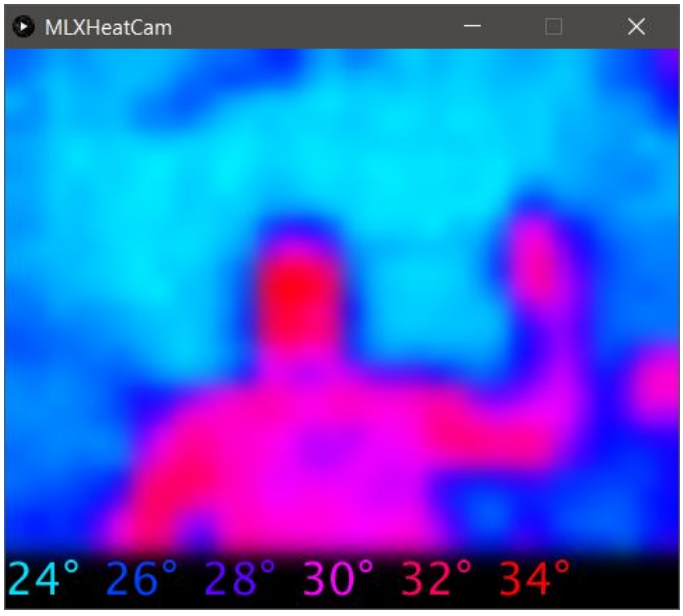

Figure 32. Infrared array sensor readings in degree celsius [37]

An IR array uses an array of thermopile sensors to image the temperature of a whole area rather than a single fixed point. It is essentially a low-cost and low-resolution thermal camera. Although commonly used in many firefighting technologies, thermal cameras are not only expensive, but they are also complex to integrate and not found to be beneficial in this project. Initially, a thermal camera was going to be used in the front of the robot to assist the driver in finding hotspots. However, since high resolution is not a priority, IR arrays will be used. The combined cost of three IR arrays is much less than the cost of a cheap FLIR thermal camera. Thus, by placing the IR arrays around the whole robot, the sensors will allow for autonomous hot spot detection, human detection, and temperature and heat flux measurement.

As shown in Figure 33, the IR array chosen is a 32x24 RES Melexis MLX90640 that can measure temperatures from -40°C (-40°F) to 300°C (572°F) at an accuracy of 1°C (33.8°F). Table AD2 in Appendix B demonstrates that this sensor was preferred over the Panasonic Grid-EYE IR array sensor since it had a higher pixel resolution, accuracy, and temperature detection range as well as a lower cost per unit.

Figure 33. MLX90640 Infrared Array Sensor [38]

Window Lens Materials

To protect the device from the scorching environment, a lens is used for each external sensor to allow for detection of the environment. However, since each sensor works in different types of wavelengths, different window materials will be used to complete the task.

Camera Lens

The onboard camera will be protected by a fireproof lens designed for cameras used in extreme temperature environments and can withstand up to 510°C (950°F) [39].

IR Array and Distance Sensor Lens

The IR arrays from Melexis are sensitive to a wavelength between five to fourteen micrometers (um) which is in the Long Wave Infrared (LWIR) range. It is necessary to choose a lens material that is sensitive to the desired wavelength as it will alter and completely affect the expected results. As shown in Figure 34, possible lenses for the IR array sensors are Germanium, Zinc Selenide, Barium Fluoride, Sodium Chloride, and Potassium Bromide. Salts like Barium Fluoride, Sodium Chloride, and Potassium Bromide can be eliminated as they are extremely fragile, water soluble, and tend to deform under heat and pressure – all necessary aspects for a suitable window lens in the robot's environment.

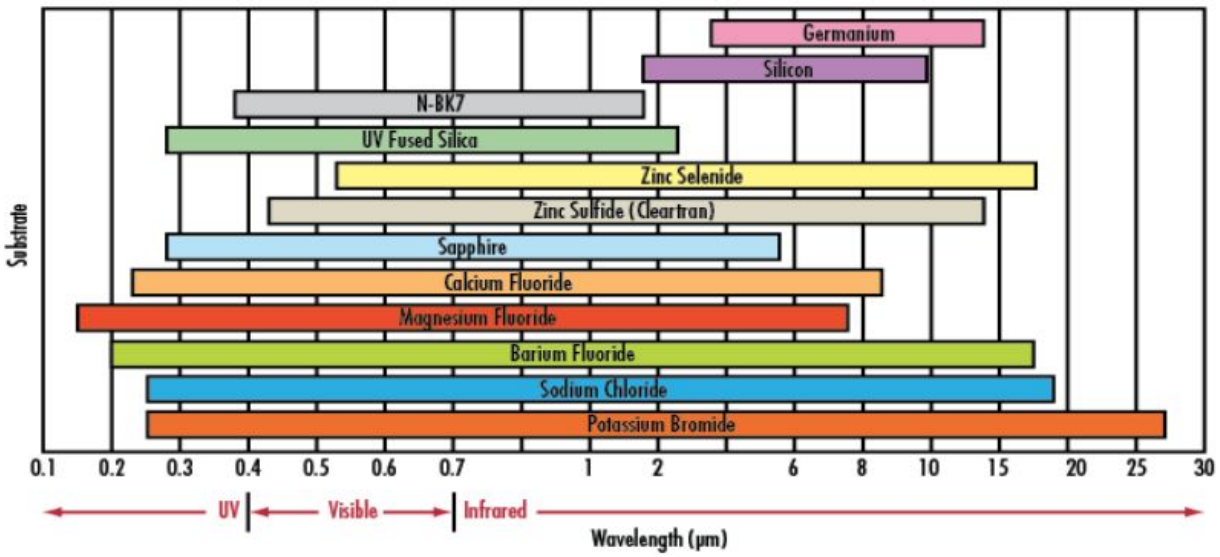

Figure 34. Lens Substrate vs. Wavelength Graph [40]

Although germanium fits within the sensitivity range, it is not a suitable material since it is subject to decreasing transmission as a function of temperature and is only suitable for operational conditions less than 100°C (212°F) [41]. In contrast, Zinc Selenide (ZnSe) is an ideal

material as it is within the LWIR sensitivity range, insoluble in water, and can withstand temperatures up to 250°C (482°F). Nevertheless, a downside to ZnSe is that it has a 70% transmission rate. However, through sensor testing, this can be compensated for in programming [42][43].

The following figures show a transmission graph and how the transmission is affected by temperature for a ZnSe lens. As shown by Figure 35, the wavelength used by the ToF distance sensors also fall within the range of ZnSe. Therefore both the IR arrays and ToF sensors will use the same type of lens.

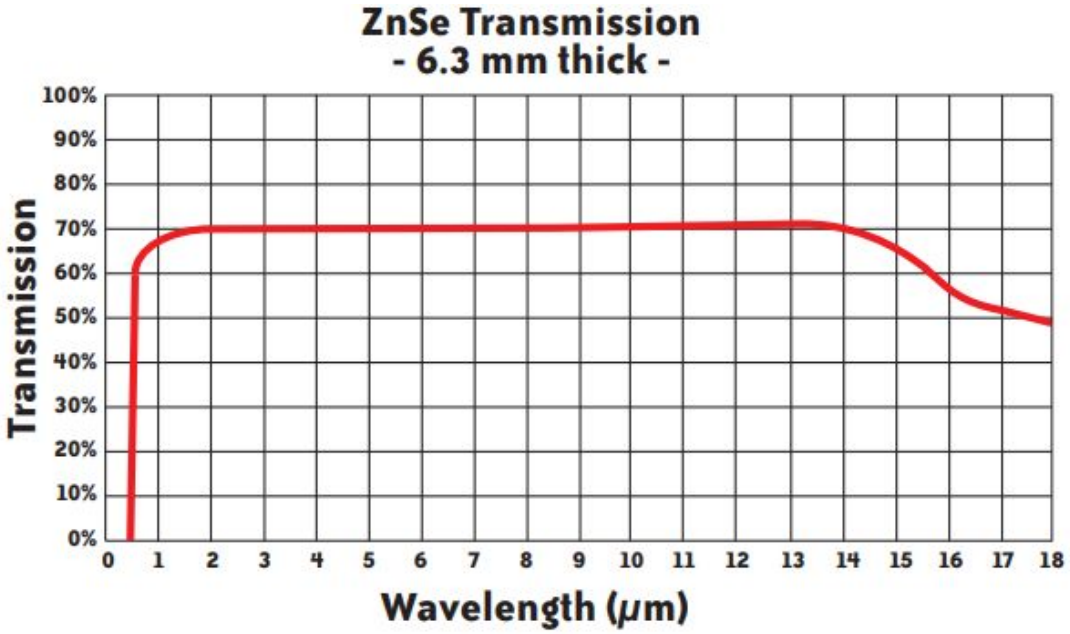

Figure 35. Zinc Selenide Transmission Range [44]

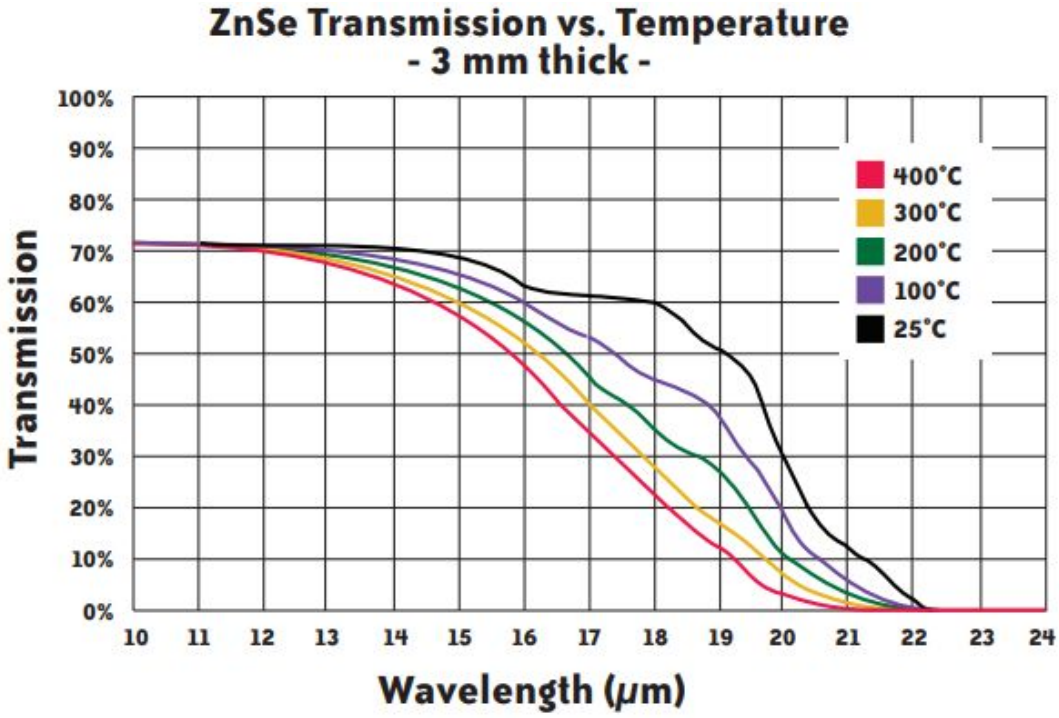

Figure 36. Zinc Selenide Transmission vs. Temperature [44]

Internal Sensor System

The internal sensor system is composed of three sensors: an Inertial Measurement Unit (IMU), thermocouples, and a combined temperature, humidity, and gas sensor. The IMU will be used for localization, navigation and to determine the orientation of the robot. The thermocouples and combined sensor device will function to identify the health of the robot as it operates in the fireground. Although the robot must withstand a specified external temperature of 300°F, for it to truly survive the fireground, the interior of the robot must be kept below a certain temperature not to damage any of the electronic components.

Inertial Measurement Unit (IMU)

An inertial measurement unit (IMU) is an electronic device that fuses accelerometer, gyroscope, and magnetometer data to measure and report orientation, velocity, and gravitational forces. They are fundamental components in the field of robotics as they are used for position tracking, control and stabilization, and navigation and correcting [45].

Although this firefighting robot will be teleoperated, since it must generate a thermal heat map of the environment, it is necessary for it to *know* its position relative to the environment. For this firefighting robot, the IMU assists in relative localization. By combining data from the distance sensors and encoders, the data collected by the IMU allows the robot to understand where it is

positioned by its velocity and orientation. Without the sensor fusion of these devices, the robot will return inaccurate thermal map data of its environment.

In future implementations where autonomous features may be integrated, an IMU will be a necessity as the robot will have to autonomously traverse through its environment without the help of human guidance. The robot will be efficient if it can accurately represent its relative and absolute positioning.

The main issue in programming the IMU will be fusing the accelerometer, gyroscope, and magnetometer data to obtain usable information. The accelerometer measures acceleration, the gyroscope measures rotational motion, and the magnetometer assists in direction orientation. By themselves, they are very limited and cannot give context to what is occurring [46]. To counter this problem, the Bosch BNO055 absolute orientation sensor was chosen. Unlike many other IMU sensors, the BNO055 outputs sensor fused data such as quaternions, Euler angles, rotation vectors, and linear acceleration.

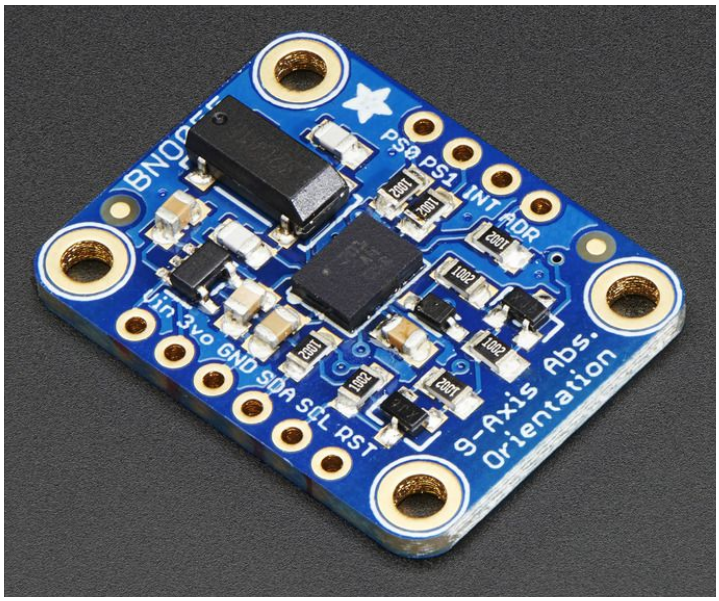

Figure 37. Bosch BNO055 Absolute Orientation Sensor [47]

Thermocouples

As mentioned previously, it is essential to track the internal health of the robot for it to fully survive its environment. Because the robot will have multiple layers of insulating material to protect the electronics, by understanding the amount of heat transferred per layer, the robot can monitor the risk of overheating. This prediction can be made using thermocouples between each layer.

A thermocouple is a device that measures temperature. It consists of two different conductors joined together at one end to form a junction which is placed on the surface that is being measured. As the temperature changes, the two dissimilar conductors begin to deform, thus outputting a voltage signal as the resistance of each wire is altered [48].

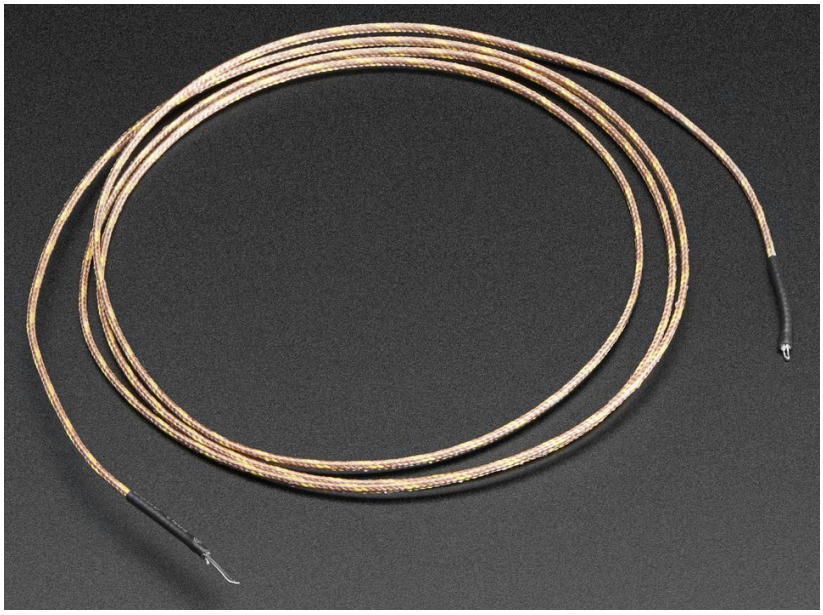

Figure 38. K-Type Thermocouple with Glass Over-Braiding [49]

A thermocouple is desirable in measuring the temperature of each layer since they are very low cost, simple to use, capable of providing accurate readings, and best used to measure temperatures that go above 100°C (212°F). The thermocouple chosen for this project is a K-type thermocouple with glass over-braiding which is good for measuring temperatures up to 500°C (900°F). To output readable data, a 14-bit thermocouple-to-digital converter (MAX31855) will be used. For more ideal applications, a 16-bit resolution would be preferable.

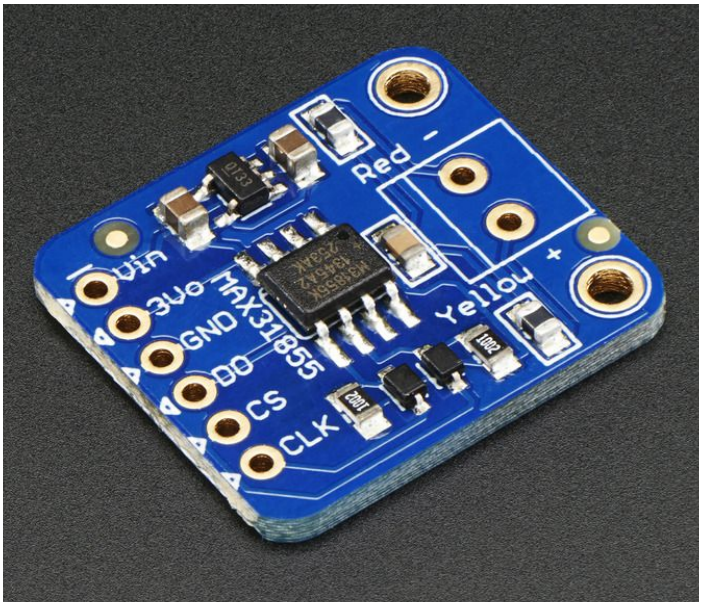

Figure 39. MAX31855 Thermocouple-to-Digital converter [50]

Initially, every thermocouple would have been placed between every layer to obtain more data on the heat transfer of the robot. However, since there are a total of three thermocouples in the current system, they have to be placed efficiently. Figure 40 shows how the thermocouples will be displaced internally in the system to optimize data collection on the heat transfer through the robot.

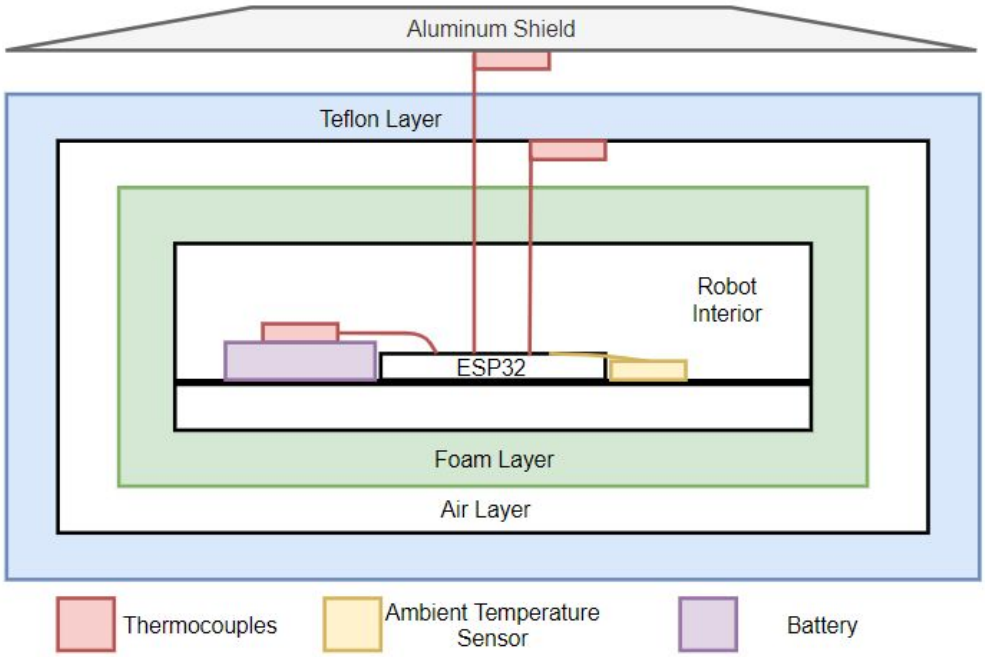

Figure 40. Thermocouple Internal Configuration

A thermocouple attached to the aluminum shield will serve to measure the exterior temperature of the robot. Another thermocouple will be attached to the battery since there is no circuit to measure the temperature of the battery. The last thermocouple is placed in the middle of the robot within the air layer. A thermocouple does not need to be placed within the foam layer because there is already a temperature sensor to measure the interior of the robot. This configuration would provide a better understanding of how the robot is reacting to its environment, and with the right algorithm, it can detect when the robot interior will reach a critical temperature of 60°C (140°F). As shown in the experimental evaluation chapter, a similar configuration was used to test the robot for fire resistance.

Temperature, Humidity and Gas

The survivability of the robot not only depends on the exterior shell but also on the internal electronic system. Every component is rated with a specific range of operating temperatures; thus, it is important to keep track of the ambient temperature of the system. If a layer becomes damaged and causes leaks, a humidity and gas sensor will be useful in also determining the deteriorating health of the robot. This information, as well as the thermocouple data, is necessary in identifying the survivability rate of the robot.

Instead of using separate sensors, the Bosch BME680 environmental unit was used as it integrates gas, pressure, humidity and temperature sensors in one device. This sensor is preferred over using individual sensors because of its functionality, low-cost, and low-power consumption.

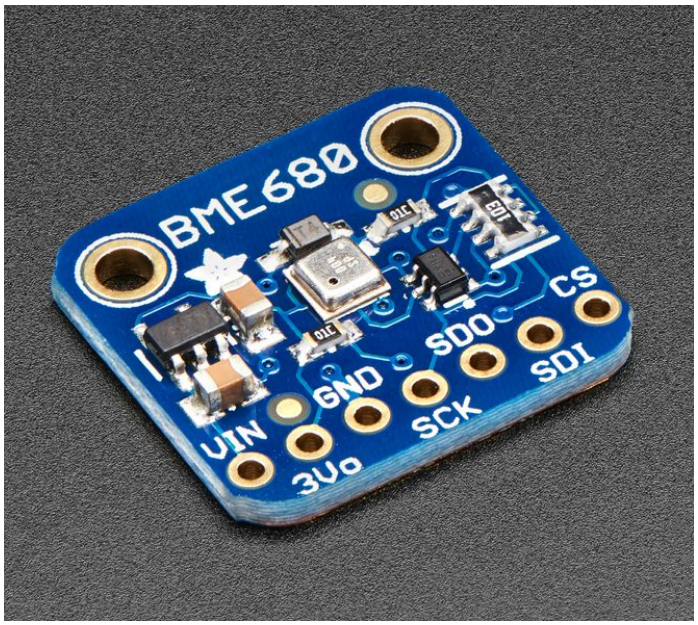

Figure 41. Bosch BME680 Environmental Unit [51]

Communication Protocols

To communicate to the sensors, this system utilizes three different communication protocols: an Inter-Integrated Circuit (I^2C), a Serial Peripheral Interface (SPI), and a Camera Serial Interface (CSI). The CSI is used to get data from the camera to the Raspberry Pi processor.

From the sensors chosen, some of them can only communicate via I^2C, while others can only communicate via SPI. Although SPI supports much higher speed communication than I^2C, it is more expensive to implement as each sensor takes up a single general purpose input/output (GPIO) port. As shown in the table below, a majority of the sensors will communicate via I^2C, whilst the thermocouples will use SPI.

Table 4. Sensor Communication Protocols

Sensor	**Quantity**	I^2C	**SPI**
Time of Flight	2	x	
Infrared Arrays	3	x	
Inertial Measurement Unit	1	x	
Thermocouples	3		x
Temperature, Humidity and Gas	1	x	x

Although I^2C can support multiple sensors on two lines (clock and data), depending on the amount of data being retrieved from every sensor, there may be latency in receiving the accumulated data information. Therefore multiple processors will be utilized. As shown in the Processors section, the ESP32 retrieves all the information via I^2C while the Raspberry Pi handles it.

Power System

The most important aspect in the electronic system is the battery since it allows the entire robot to function. The power system is divided into two sub-sections: a battery management system and a power distribution system.

Battery

This section will function to determine the type of battery that will be used in the robotic system. First, the current consumption, nominal voltage, and power requirements must be retrieved from

each component in the system. Second, a set of requirements are listed in order to find the desired battery. Third, a variety of batteries are described, and their pros and cons are listed. Lastly, from the requirements and by researching each battery, the most optimal type of battery is chosen.

Component Voltage and Current Consumption

The table below reveals the operating voltage and total current consumption of the robot by looking at the two power hungry components of the robot: the motors and the processor. The data was taken from each of the corresponding datasheets (see the Motors and Processors section).

Table 5. Current consumption and operating voltage of every component

Components	**Motors**	**Raspberry Pi**
Max Operating Voltage (V)	12	5
Current Consumption (mA)	2000	2500

From the motors chosen, the no-load current is 20mA while the stall current is 5.5 A. On average, each motor consumes 1000 mA. Therefore, since the Raspberry Pi processor consumes 2.5 A and the motors consume 2 A, the total current consumption is equal to 4.5 A. From the voltage requirements, it would be ideal to have a battery that can supply more than 12V.

Specification Requirements [52]

In order for the robot to function optimally in the environment, a set of requirements were created: maintenance, capacity, nominal voltage, weight, protection, and discharge rate.

Maintenance: long lasting and rechargeable

The robot must be of low maintenance. This robot should not be a hassle for firefighters to use. Therefore, in order for it to be low maintenance, it would be ideal if the robot could last long (both in capacity and life-time).

Capacity: 5500 mAh and 6000mAh

The customer requirements state that the robot must survive 15 minutes in a 300 degrees Fahrenheit environment. However, it would be practical if the robot can be used up to five times on a full battery since firefighters may constantly be in missions. It is best to have a robot that is functioning most of the time as any mission can be unpredictable.

Therefore, assuming that the internal temperatures are kept within a safe range, the capacity of the battery is determined below:

$$4500\ mA \cdot 15\ minutes \cdot 5\ uses$$
$$4500\ mA \cdot 1.25\ hours = 5625\ mAh$$

Rounding it up, a battery capacity between 5500 mAh and 6000mAh is necessary to meet the specified needs.

Nominal Voltage: 12V - 15 V Battery

Having chosen a 12V motor to drive the robot, the battery has to be more than or equal to 12V to efficiently power the system. In order to reduce the amount of current drawn from the battery, it is important that the voltage is dropped down rather than boosted up.

Weight: 2 lbs

Considering the whole robot must be under five pounds (lbs), then it would be ideal if the battery is under two lbs.

Protection: Metal casing

Since the robot is in a spontaneous and dangerous environment, it is possible that the robot can get knocked over or get crushed by falling objects. If the robot shield is not strong enough to handle some impacts, the battery may become impacted if not protected well. The impact on the battery could blow it up, damaging the robot and anyone in its vicinity. Therefore, a metal casing is much more preferred than a pouch.

Discharge Rate: 2C to 3C rating

The discharge rate is a measure of the rate at which a battery is discharged relative to tits maximum capacity. A 1C rate means that the discharge current will discharge the entire battery in an hour [53]. The current consumption in the table above already considers the maximum current consumption for each component. However, it is critical to have this rating be much higher than the typical current drawn since the battery may get ruined if it draws more than it can handle [54]. Therefore, its ideal to obtain a battery with a discharge rating of 2C-3C or above.

Other:

Although not necessary for the scope of this project, in between fire fighting missions, it may be important to be able to charge the robot quickly. Therefore, a battery that can support safe quick charging would be of interest.

Battery Types and Considerations [55]

This section will describe potential battery types that may be used. Lead-acid batteries are not considered since they do not like charging/discharging cycles. Nickel cadmium batteries are also

not considered since their toxic. Other batteries that are not considered, are either way too expensive, difficult to buy or difficult to charge.

Battery type	**NiMH**	**Li-Ion/Li-Poly** high energy type	**Li-Ion/Li-Poly** high current type	**Li-Ion/Li-Poly** high safety type
Chemistry	NiMH	$LiCoO_2$ $LiNiMnCoO_2$	$LiMn_2O_4$	$LiFePO_4$
Nominal cell voltage	1.2V	3.6 - 3.7V	3.7 - 3.8V	3.2 - 3.3V
Operating cell voltage range	1.0 - 1.4V	3.0 - 4.2V	3.0 - 4.2V	2.5 - 3.65V
Max voltage for charging	1.4 - 1.6 V	4.2 - 4.3V	4.1 - 4.2V	3.65V
Max charging current*	0.1C or 1C (only with ΔV/ ΔT)	~1C	up to 3C	up to 4C
Max discharging current	1C - 30C	1C – 2C	5C - 30C	1C - 40C
Charging method	CC with timer or ΔV/ ΔT (faster)	2 stages: CC and then CV	2 stages: CC and then CV	2 stages: CC and then CV
Specific energy	40 - 120Wh/kg	150 - 250Wh/kg	100 - 150Wh/kg	90 - 120Wh/kg
Specific power	100 - 1000 W/kg	100 - 400W/kg	400 – 5000 W/kg	200 - 7000 W/kg
Internal series resistance for a single cell	5-50 mΩ (for 18650 size)	15-100 mΩ (for 18650 size)	10-50 mΩ (for 18650 size)	6-60 mΩ (for 18650 size)

Figure 42. Battery type and specifications [55]

Lithium Polymer

Li-Poly (lithium polymer) is exactly the same as Li-ion (lithium ion) except that it does not need a metal enclosure. However according to the requirements, a metal enclosure would be ideal for extra protection. Therefore Li-Poly is removed from consideration since it is rarely used in a cylindrical enclosure.

Nickel-Metal Hydride

Nickel-Metal Hydride (NiMH) and Li-ion are both commonly used in cylindrical battery shapes of a metal enclosure. From the battery requirements, although NiMH is safer and easier to charge, it is more compatible for smaller robots. The NiMH battery tends to have smaller nominal voltages, and a more reduced specific energy and specific power than some of the lithium based batteries. Furthermore, unlike some lithium-ion based cells, NiMH has a much lower energy density. These downsides make this battery type unfit to be used in the firefighting robot.

Specific Energy vs Specific Power [56]

Specific Energy or Energy Density (Wh/kg) is a measure of how much energy a battery can hold. The higher the energy density, the longer the runtime will be.

Specific Power or Power Density (W/kg) indicates how much power a battery can deliver on demand. The focus is on power bursts such as drilling through heavy steel rather than runtime.

From these two definitions and from the requirements, it is crucial to achieve a good mix of both. Not only is it important that the robot can run for longer times, but it is also essential that the robot can overcome certain obstacles. However, from this description specific energy seems to be more important than specific power as power bursts may not be as frequent.

Taking this into account, lithium ion batteries with cobalt cathodes offers highest energy densities, while Manganese and phosphate-based lithium ions, as well as nickel based chemistries are among the best performers for specific power.

Battery for F.R.E.D.

From the research above, and from the research in Appendix C, the ideal battery for this robotic system is the Lithium Nickel Manganese Cobalt Oxide (NMC) as it offered a higher energy density and proved to be a commonly used material in electric vehicles similar to the firefighting robot. The battery was obtained from the manufacturer Battery Space, and is rated for 14.4 V with a capacity of 5 Ah which is more than enough for the robot.

Figure 43. 14.4V 5Ah LiNiMnCo 26650 Battery [57]

Battery Charging and Management

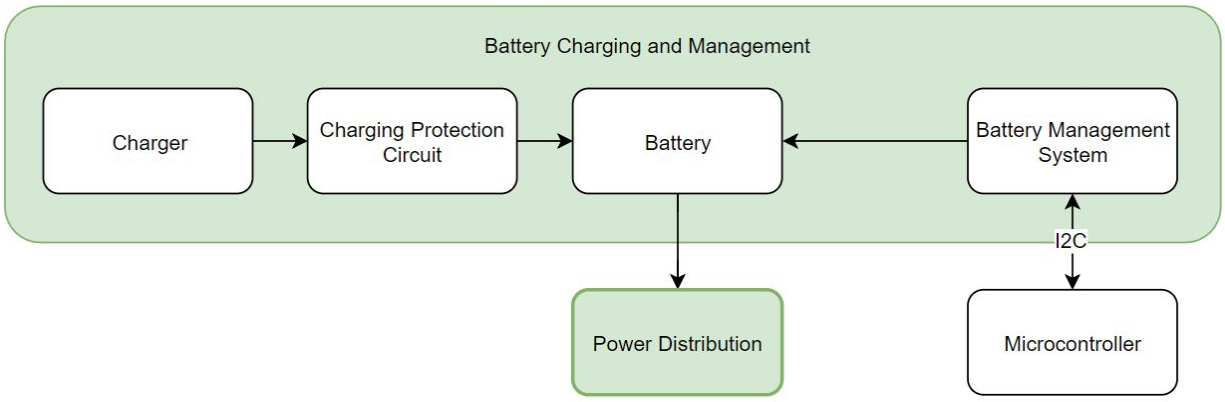

Figure 44. Battery Management Power System

Because the robot must operate in a high-temperature environment, the battery should always be well-protected. That includes protection circuits for both charging and discharging of the battery. Likewise, to understand how the battery is withstanding the environment, the microcontroller can receive information from a battery management system (BMS) to determine the health of the battery.

Battery Management System (BMS)

A battery management system (BMS) is a powerful tool that can measure and monitor battery voltage, state of charge (SoC), state of health (SoH), temperature and other critical measurements. Lithium ion batteries have a high power density, and overcharging can cause thermal runaway and combustion, so a BMS is a necessity when using this battery material to reduce the likelihood of fires and explosions [58][59].

Although a BMS is the safest and most optimal option for monitoring the robot's battery, it will not be implemented within the scope of this project because it would require either modifying the battery or designing a custom one. While not as efficient, the battery pack has a protection circuit module (PMC) that is designed to protect the battery against overcharge, overcurrent, and short circuits. It has a cell balance function that helps prolong the lifespan of the batteries. Unlike a BMS, the PMC only protects the battery; it does not monitor the health and safety of the battery pack. With this approach, the temperature of the battery will be directly measured via a thermocouple [60].

Battery Management Enclosure and Schematic

As shown in the schematic in Figure 45, there are three different connector jacks: the battery jack, the charger jack and the power jack. The battery jack is where the battery will be connected to. Using the switch, the robot system can be turned ON or OFF. When the switch faces the power jack, power is distributed to the electronics. A 0.01 µF ceramic bypass capacitor is connected to the rails of the power jack to short any AC (analog current) signals to ground. This removes any AC noise in the DC (direct current) supply, thus producing a cleaner DC output. As an indicator that the system is ON, a green light emitting diode (LED) is connected to the power jack. To light up an LED with a forward voltage of 2.1V, twenty milliamps (mA) is needed. Therefore a 680 ohm resistor is placed in series with the green LED to light it up completely.

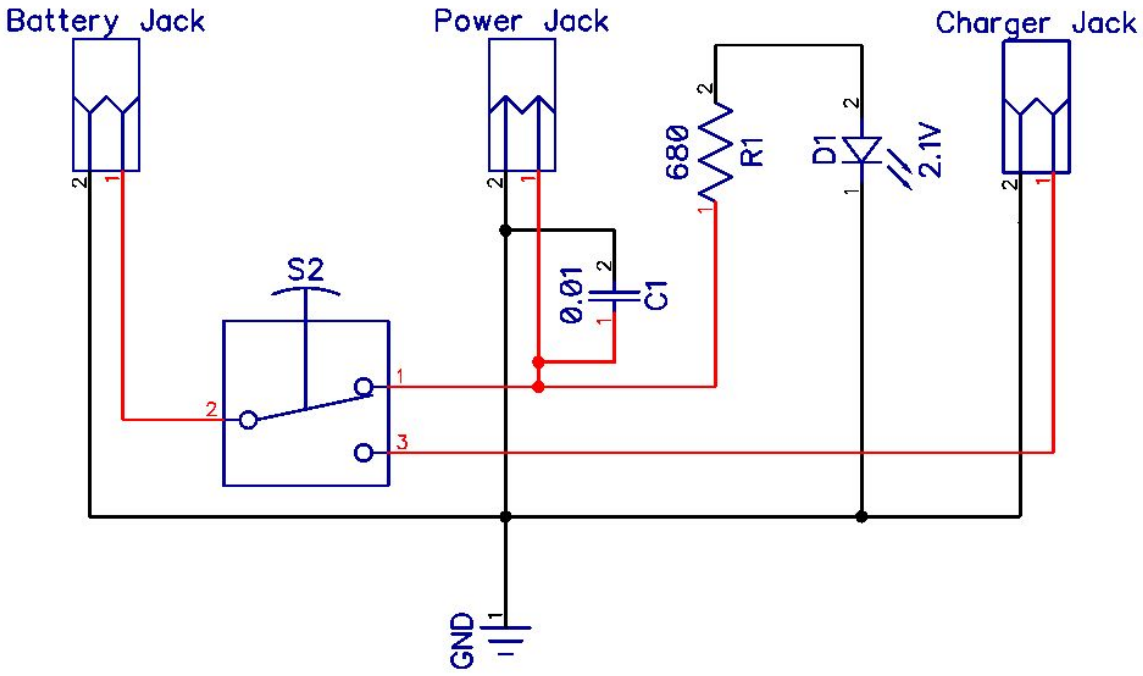

Figure 45. Battery charger and power to board schematic

When the power is OFF, the switch is directed to the charger jack. While disconnected the battery does not dissipate any power. However, once the charger is connected to the charger jack, the battery begins to charge. The simplicity of this system allows the battery to easily power the robot and get charged. Using male and female DC power jack plug adapters, each jack can be connected and disconnected effortlessly and safely. This is shown in Figure 46.

Figure 46. Prototype of battery charger and power to board

Finally, to hide any open wires, a 3D printed enclosure was designed to hold the electronics. As shown in Figure 47, the circuit would be placed above the battery, therefore the enclosure was designed as thin as possible to fit within the interior robot height.

Figure 47. Enclosure of battery charger and power distribution

Power Distribution

As shown below, the robot's power distribution system involves regulating the voltage supplied by the battery to the motor system and microcontroller. Since both systems require different operating voltages, DC to DC converters will be utilized. Although unnecessary on the field, LED indicators will be used for troubleshooting purposes.

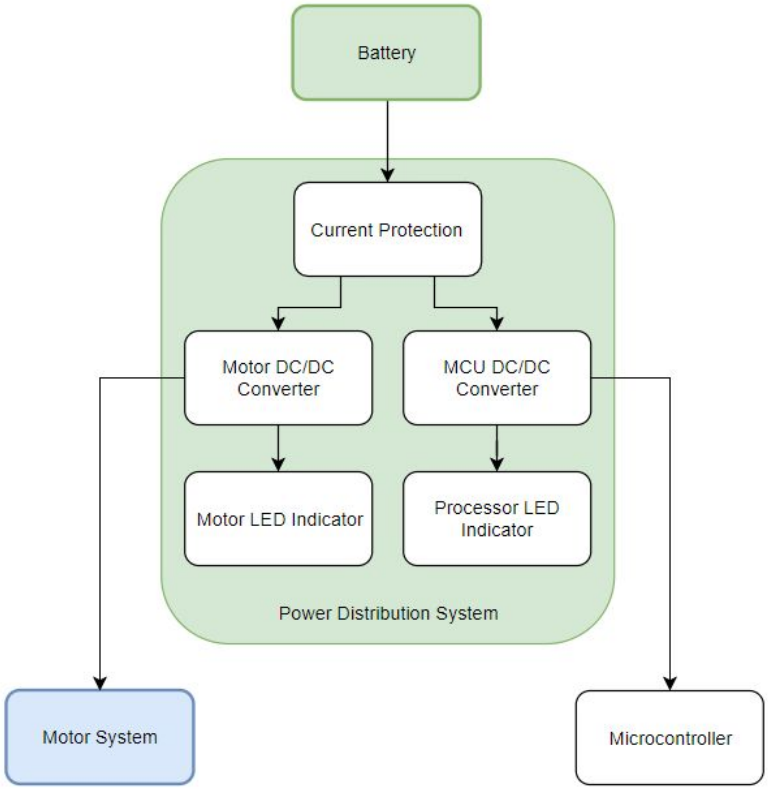

Figure 48. Power Distribution Power System

Current Protection

Implemented in the protection module circuit (PMC) of the battery, the practice of current limiting imposes an upper limit on the current to the load and protects electronic circuits from harmful effects due to short circuits or problems in the load [61].

DC to DC Converters

A DC to DC converter converts a source of direct current (DC) from one voltage level to another. There are two types of DC to DC converters: linear and switched.

A linear regulator uses a resistive load to regulate the output voltage. However, this method is only great for powering low powered devices, where the difference between the input and output

voltage is small. As shown in the equation below, this is because the power dissipation from a linear regulator depends on the product of the voltage difference between the input and output, and the load current. Although it is cheap and simple to implement, this is an inefficient solution as it is important that the power dissipated by the electronics is minimized and conserved to avoid heat generation.

$$P_{dissipation} = \Delta V \cdot I_L = (V_i - V_o) \cdot I_L$$

On the other hand, a switching regulator uses a switching element to transform the input voltage into a pulsed voltage which is smoothed by using capacitors, inductors and other elements. By turning a MOSFET switch on and off, power is supplied to the output once the desired voltage is reached. Unlike the linear regulator, although the circuit is more complicated, it is very efficient as dissipates little to no power. A switching regulator will be utilized to efficiently manage the power to the motors and processors by reducing the power dissipated by the circuit which minimizes the heat generated by the electronics [62][63][64].

LED Indicators

For troubleshooting purposes, the LED indicators are necessary to implement to determine whether there is power to the motors and processors. It is a visual indicator of power being supplied to the load.

Switching Regulator

As shown in Figure 49, the DC to DC converter chosen is a switching regulator that can step down a DC voltage from 3V to 40V, to a DC voltage of 1.23V to 37V. It can output a max of 3 Amps, which meets the current consumption requirements of both the motors and processors. The circuit has a built-in LED indicator to determine whether power is being supplied to the output of the buck converter.

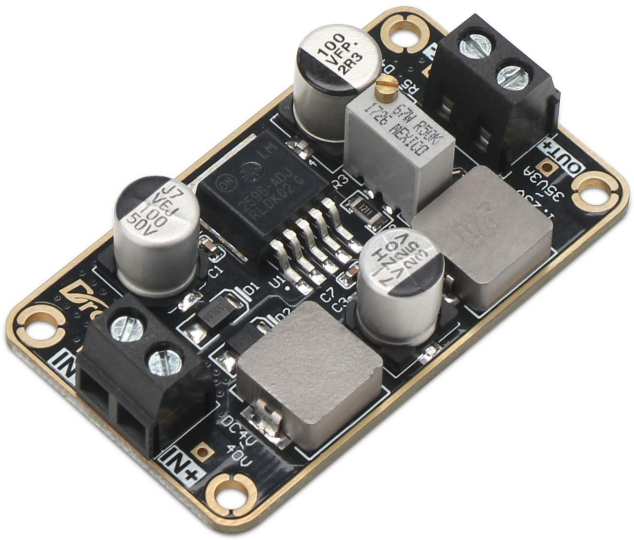

Figure 49. DROK Switching Buck Converter

Motor System

The motor system is essential to drive the motors and get feedback from the encoders. As shown in the block diagram below (Figure 50), the motor system is composed of a motor controller and a motor.

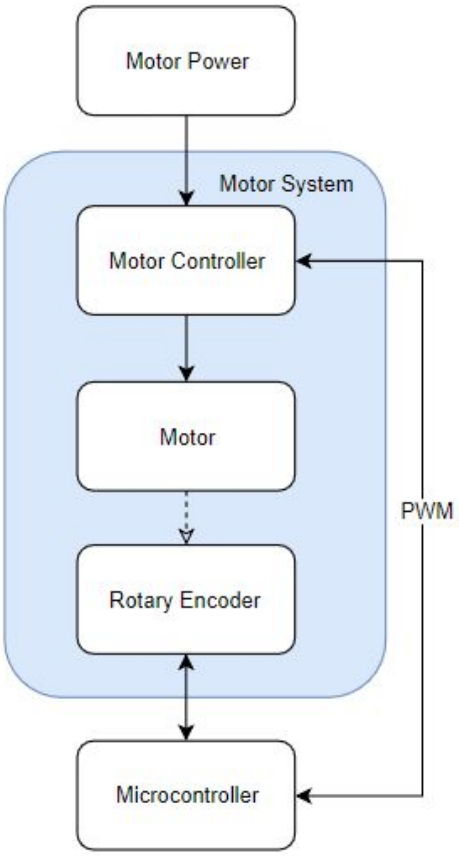

Figure 50. Motor System Block Diagram

The system is powered by a regulated voltage from the power system, whilst the motor is controlled via the microcontroller through a PWM signal. To further aid in determining relative and absolute positioning of the area the robot is in, rotary encoders will be integrated into the motor.

Motor

This subsection explores the necessity of a rotary encoder and determines the motor for the system by a set of specification that is created using a static system of the robot.

Encoder

Essentially, a rotary encoder is a position sensor. It is attached to a motor to determine the angular position of a rotating shaft. For the purposes of this project, it is important that the motor system has an encoder to further localize itself in the environment. Alone, it can be subject to many problems on the field. However, with the use of an IMU and distance sensors , if a robot were to get stuck it would be able to determine that.

Motor Specifications

In order to select motors for the drive system, the maximum torque required from the motors during the robot's use had to be found. To determine this, a model of the system was devised which attempted to represent the worst case scenario for the robot. The following assumptions were made for this model:

- The robot is climbing a height of six inches, the maximum height the wheels would allow
- The robot weighs ten pounds
- The entire weight of the robot would be at the axles
- The support provided by the back wheel is ignored
- The robot is at a point in its climb where the axles are at the height of the ledge

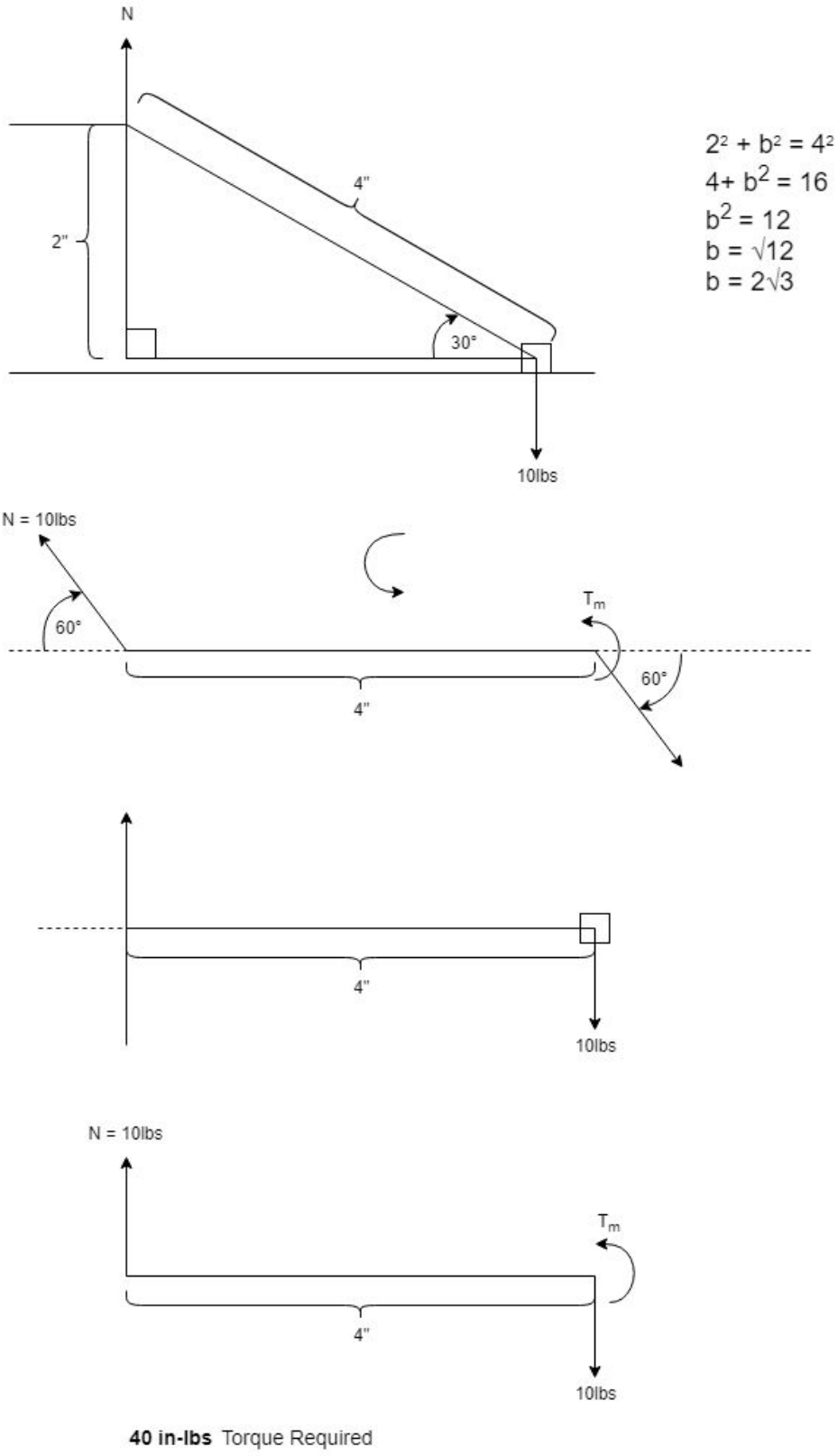

Figure 51. *Motor Torque Calculations*

Based on these assumptions and as shown in Figure 51, the motors would need to overcome a force of ten pounds on a torsion arm four inches long, for a total of forty inch-pounds. This is shared by two motors, so each required twenty inch-pounds.

In addition to torque, motor speed needed to be determined. The desired top speed was 0.5 meters per second. With four inch diameter wheels, this required the motors to have a rotational speed of at least 94 rotations per minute.

From the calculations and requirement metrics, the motor specifications are as follows:

1. Revolutions Per Minute: ≥ 94 RPM
2. Stall Torque: > 20 in-lbs
3. Encoder: Yes
4. Nominal Voltage: 12V

A 12V motor was chosen as there were no 6V motors that met the speed and torque requirements specified above.

PWM vs. CAN

Using the controlled area network (CAN) bus allows for closed-loop feedback control which can precisely control the driving mechanism of the robot. Although a CAN bus is utilized in industry for automation, due to its complexity and high-cost of integration, a pulse width modulated (PWM) signal will be sent to the motor controller through a microcontroller.

Motor Controller

A motor controller acts as an intermediary device between the motors, the power supplied and the microcontroller. This device is necessary because the microcontroller cannot provide the amount of current necessary to operate each motor. Since two motors will be utilized in this robotic system, the Cytron dual channel DC motor driver was chosen.

Figure 52. Cytron Motor Controller [65]

This motor controller can support the nominal voltage of the motor, can supply high current up to 10 Amps continuously, and can drive two motors on its dual channel.

Processors

Due to the nature of wirelessly transmitting large amounts of sensor data as well as a real-time video stream, a sufficiently powerful processor was needed to be able to perform all of these tasks simultaneously. Initially a modular processor/sensor system named Tinkerforge (Figure 53) was considered, as it was powerful enough for our purposes while also sporting several sensor packages that would have made integration seamless. Unfortunately costs and delivery times ruled this as a non-option.

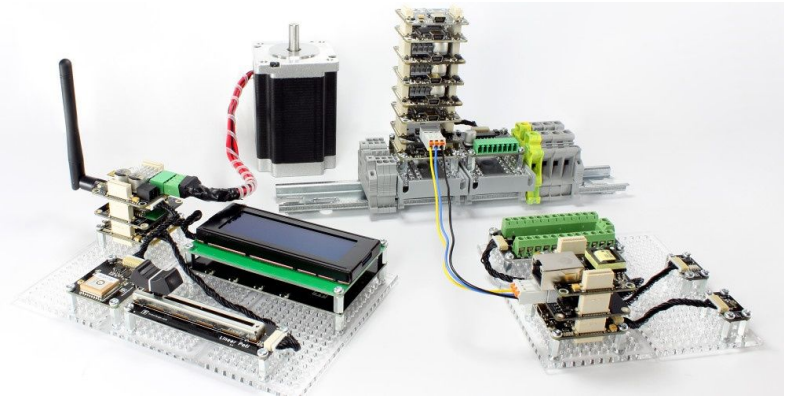

Figure 53. Generic Tinkerforge system [66]

It was eventually decided to use a Raspberry Pi 3 Model B+ (Figure 54) as the master microcontroller given its permanence in the hobbyist robotics community and therefore wealth of documentation and resources, as well as its 1.4Ghz quad-core processor being more than enough to handle the necessary tasks. It was later decided to include an ESP-32 (Figure 55) as a co-processor to handle the direct sensor communications over I²C. Many of the sensors chosen had libraries written for Arduino-like devices, making programming for them much simpler on the ESP-32.

Figure 54. Raspberry Pi 3 Model B+ [67]

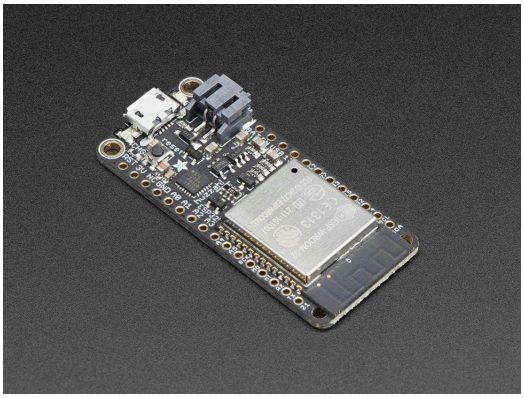

Figure 55. ESP-32 Feather [68]

Final Sensor Configuration

Using the Fritzing tool, the final electronic component configuration was created as shown in Figure 56. This includes both the Raspberry Pi processor and the ESP32 processor connected via serial. While all sensors are connected to the ESP32 via I^2C, the Raspberry Pi controls the motors and retrieves odometry data. The motors are controlled through the Raspberry Pi since its the core processor of the robotic system and the motors must be controlled in real-time.

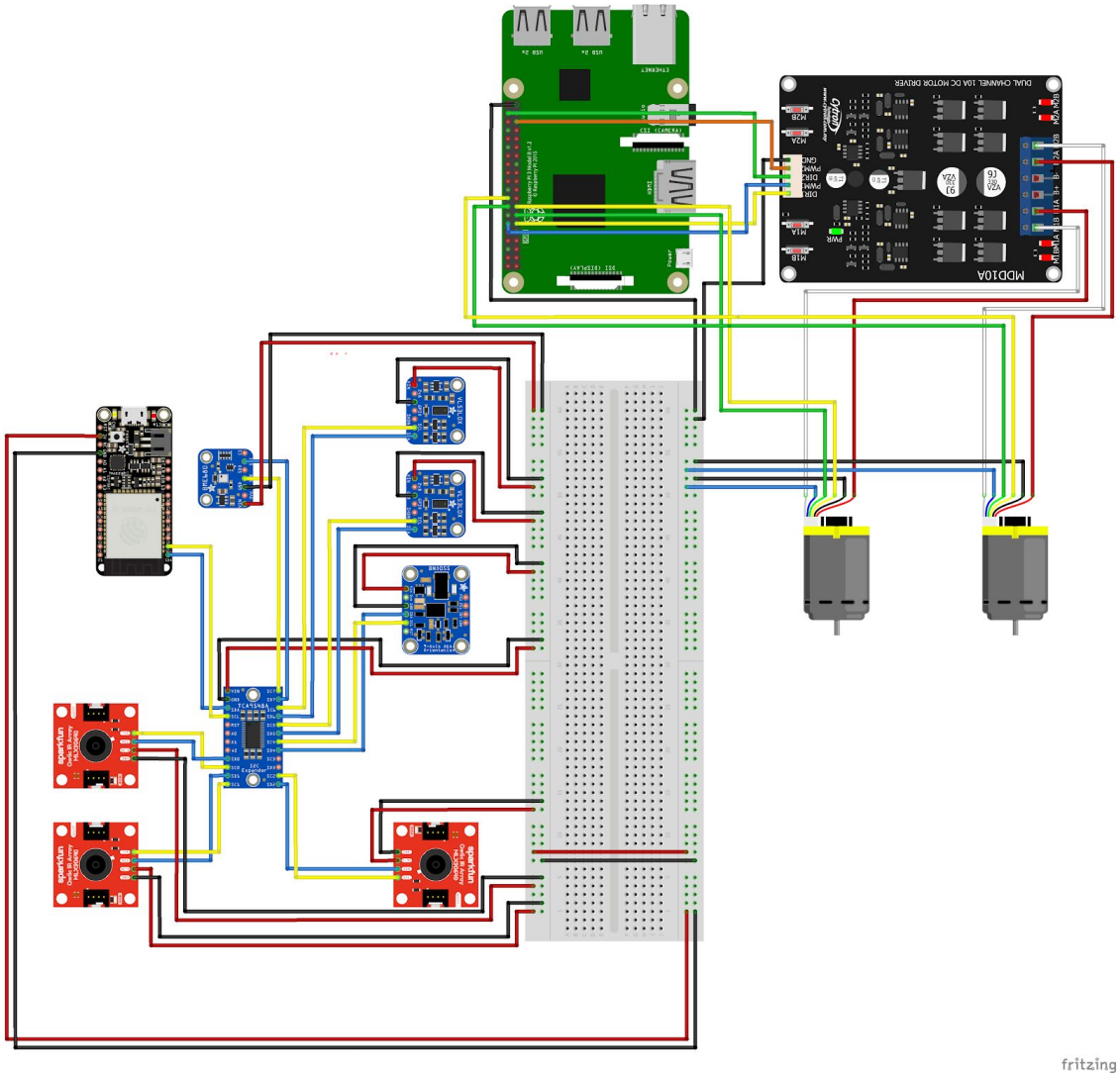

Figure 56. Final electrical system configuration

Communication

Communication between each of the robot's processors and the operation device was done over WiFi and managed by the Robot Operating System (ROS) [69].

ROS

ROS is an open source, high-level program focused on handling communications between different components in a robotic system. Each component is represented by a node, typically a python script or C++ program that handles a specific task, sensor, or actuator. A ROS core node is run on one device and manages all other nodes using a publish and subscribe system. Nodes that collect or produce data publish it to a specific topic, and nodes that utilize or act on this data subscribe to the topic. The core node acts as a message board where packets are posted by publishers and read by subscribers.

ROS and F.R.E.D.

ROS is used to handle communication between the three major processors in the system: the Raspberry Pi, the ESP-32, and the operation device. The operation device is whatever device is used to display gathered data and send user input. Ideally, this would be an iPad for ease of use by firefighters, but for this implementation, a laptop running Ubuntu was used. The operation device, being the most powerful processor in the system, runs the ROS core. Communication between the operation device and the Raspberry Pi is done via WiFi. The Raspberry Pi in turn communicates with the ESP-32 via serial over a USB port, and passes data it has gathered along to the operation device over WiFi. Figure 57 shows the different devices and how they communicate with each other.

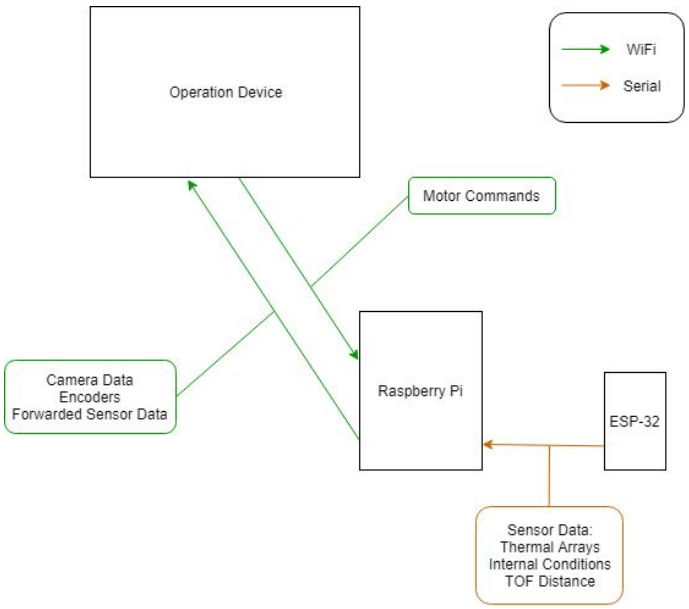

Figure 57. Diagram of Inter-Processor Communication

User Interface

The purpose of this robot is to gather and present data useful to firefighters during an incident. The presentation portion is fulfilled by the user interface (UI), which, as mentioned above, will be handled by an application running on a remote device. The intended UI design (Figure 58) was meant to be simple and intuitive to the operator and other firefighters. Data is readily available and displayed in such a way that can be interpreted at a glance.

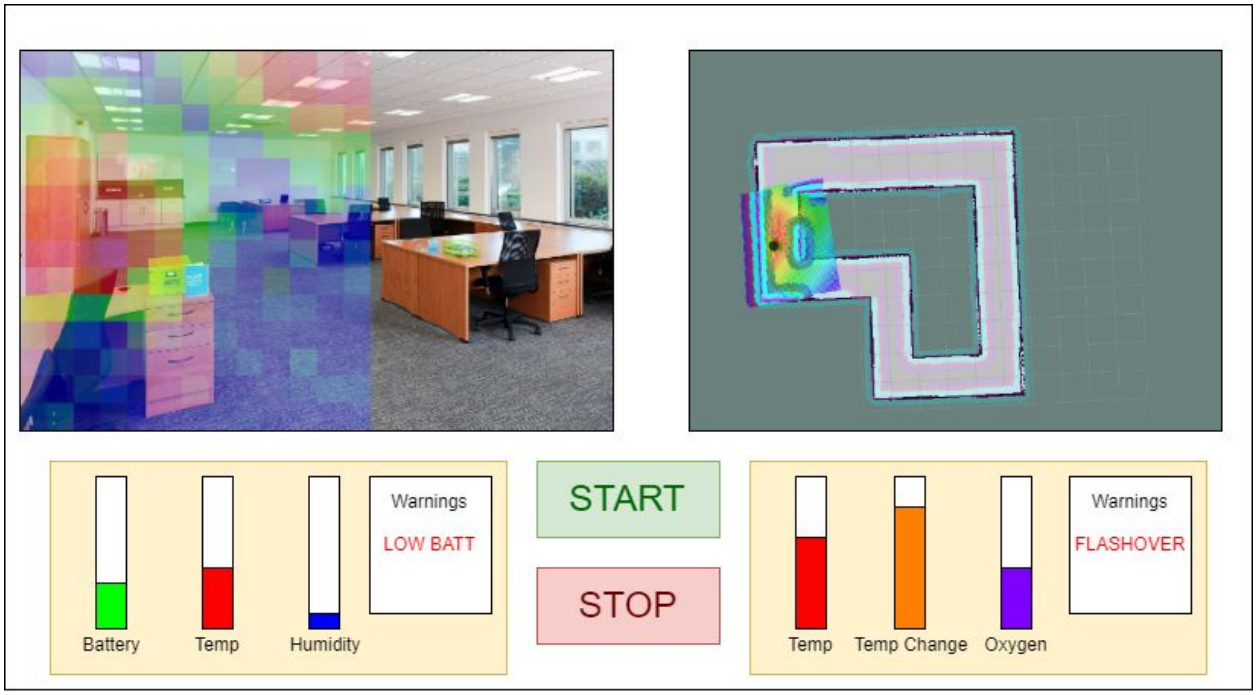

Figure 58. Early Mockup of Potential User Interface

The left side of the UI features data about the robot itself, while the right side features data about the environment. The top left corner has the video feed from the front mounted camera. Optionally, using a button on the operator's controller, an overlay of the front mounted infrared array sensor can be added to the video for a visual thermal display. Under the camera feed is various readings and warnings pertinent to the robot, such as battery and internal temperature. The top right features a map of the robot's operation space, which becomes populated with thermal data as the robot traverses it. For the purposes of this project, it is assumed a map of the space already exists, and the robot simply adds thermal data to the existing map. Below the map display is readings and warnings regarding the environment, such as temperature and rate of change of temperature. These readings can be used to assist in predicting dangerous fireground events such as backdraft and flashover. Finally, the bottom center features start and stop buttons for controlling the robot mainly for emergency use.

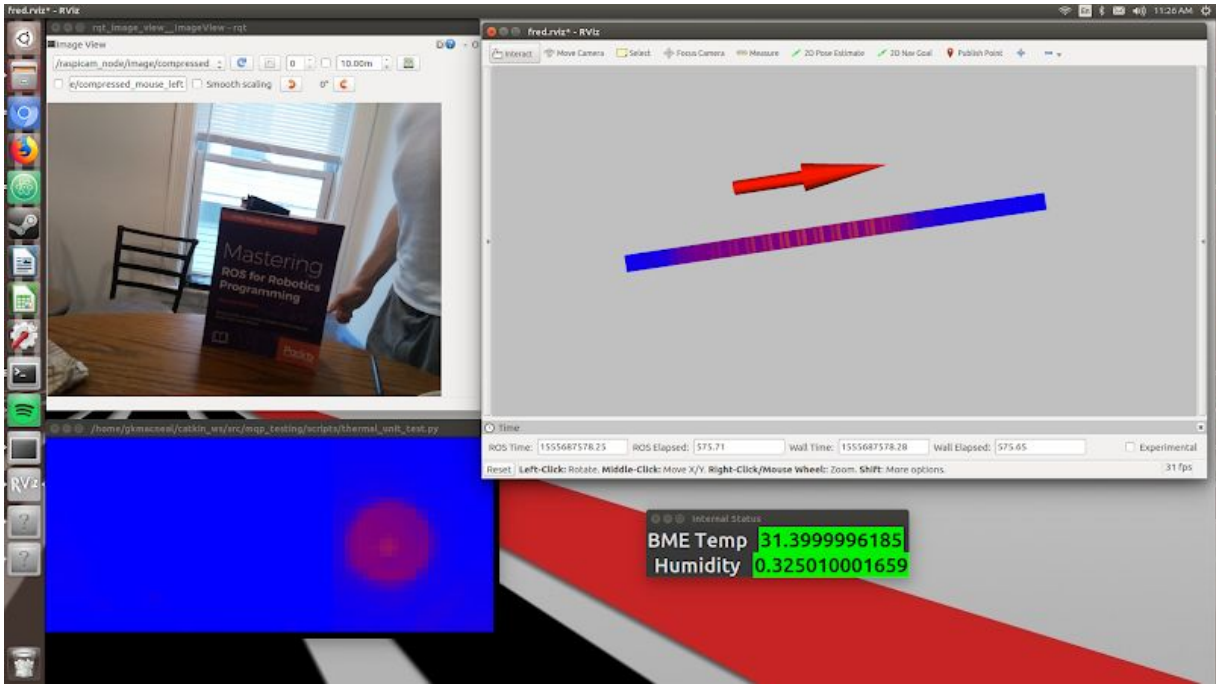

Figure 59. Final User Interface Implementation

The final version of the User Interface as implemented in this project is seen in Figure 59. It lacked some of the desired features but did display most of the desired relevant information. The UI is comprised of four windows. In the top left, the output of the camera feed from the Raspberry Pi Camera is shown. The bottom left window is the visualization of the three thermal array sensors, side by side with each other. The center and left sensors are not detecting anything of interest in this screenshot, but the right sensor is pointed at a heated frying pan for display purposes. The top right window is the thermal mapping display. The red arrow represents the robot, and the blue and red line represents the temperatures of the wall to the right of the robot. By using the same color scheme for both thermal displays, objects in the thermal array sensor are easy to recognize as they appear on the map; here, the frying pan that appears on the right thermal array also appears in the map directly to the right of the robot. Finally, the small bottom right window is data from the BME680 environmental sensor, specifically the internal temperature and humidity of the robot.

Code Structure

Generally, the use of ROS guides the structure of code across the robot system. Each device or processor is responsible for particular nodes, each corresponding to a script or program.

Operation Device

The operation device handles the ROS core, driving commands, and data display. The ROS core is the first node to be initialized and is handled by the ROS libraries. Two nodes, each a python

script, handle driving commands. One accesses the Xbox 360 controller via hardware systems and publishes the state of each of the inputs as a Joy message to the `/joy` topic. The other subscribes to these messages, calculates the appropriate linear and rotational velocity of the robot, and publishes these as a Twist message to the `/cmd_vel` topic. These are split into two separate nodes so the joystick controls can be used by other nodes as well. Data display is handled by a handful of nodes which each subscribe to one or more sensor messages and provide a visualization of the data on the device's screen.

Raspberry Pi

The Raspberry Pi runs nodes for motor control, sensor readings, and serial communication with the ESP-32. Motor control is done by a python script node which subscribes to the `/cmd_vel` topic, calculates the motor speeds to produce the requested velocities, and sends the speeds to the motor controller via PWM signals. Various sensors, including the camera, are connected directly to the Raspberry Pi. Each one has a node to read from the device and publish the sensor data to the corresponding topic. In order to interface the ESP-32 with ROS, the Raspberry Pi runs a pre-built node which communicates with the ESP over serial and passes its messages along to the core.

ESP-32

Most of the robot's sensors transmit data directly to the ESP-32 via the I^2C protocol. This includes the thermal IR arrays, the distance sensors, and the BME temperature and humidity sensor. Unlike the other processors, which are capable of running multiple python scripts, the limited memory space and processing power of the ESP-32 only allows it to run a single Arduino program. This one program initializes and takes readings from all connected sensors, then publishes the data to the appropriate topics via its serial connection with the Raspberry Pi. This program required extensive optimization in order to refresh the sensor data as often as possible. This was done through modification of the thermal array libraries, which were the most intensive sensors to implement.

Thermal Mapping

In order to demonstrate the robot's capability to determine the surrounding environments temperature, it was necessary to generate a map of the desired area. This was accomplished through the use of a 3rd generation TurtleBot, which comes equipped with a 360° LIDAR. This was needed as the robot's onboard sensors are not capable of properly performing localization without being given pre-existing environmental constraints.

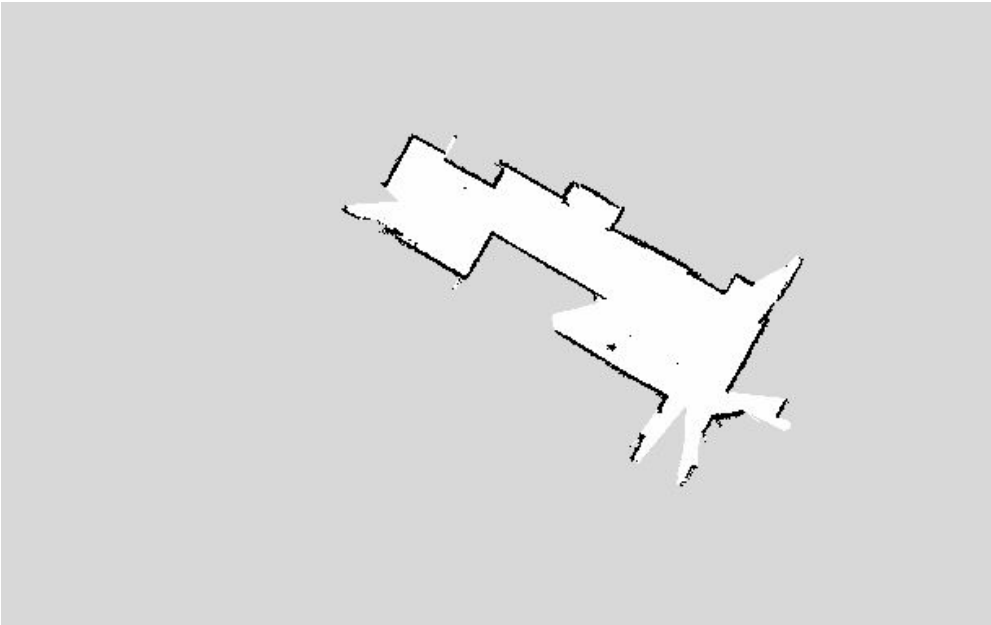

Figure 60. Map generated by TurtleBot

To accurately display the surface temperatures of the environment, the robot used the left and right facing thermal IR arrays and distance sensor in tandem. This is done by scaling the outputted temperature image from the array based on the distance from the robot to the surface, which were then averaged and overlaid two-dimensionally on top of the generated map, creating an effective thermal outline of the robot's surroundings as shown in Figure 60.

Driving

As discussed in Code Structure section, driving is handled by three distinct python scripts, each a different node which interacts with ROS and/or device hardware. The first pulls data from the controller using the `/dev/input/js0` file in Ubuntu, which is the default utility for controller input on that operating system. This data is then published for the use of the next node, which interprets the joystick data. To try to increase ease of use, the script allows for three different control schemes:

- "Tank" - each joystick independently controls each motor
- "Arcade" - one joystick controls forward and reverse, the other controls steering
- "Rocket" - based off of the video game Rocket League™, the triggers control acceleration and one joystick controls steering

These can be toggled using the right bumper. Because the ROS Twist message type requires linear and rotational velocities, the "arcade" and "rocket" styles map directly. The "tank" control requires finding the average of the two joysticks for linear velocity, and the differential of the two for rotational.

The final node in the process controls the motors themselves. This is done via the GPIO library for python. To determine the appropriate motor speeds to produce the desired linear and rotational velocities of the robot, forward kinematic equations are used:

$$V_r = w \cdot (R + \tfrac{l}{2})$$
$$V_l = w \cdot (R - \tfrac{l}{2})$$

Where V_r and V_l are the right and left wheel velocities, *omega* is the rotational velocity, R is the radius of turning, and l is the distance between the wheels. R can be determined from the linear and rotational velocities. In addition to these calculations, the incoming Twist messages arbitrarily range from -1.0 to 1.0 without specific units, so constants (100 for linear velocity, 1/1.1 for rotational velocity) were determined via guess and check methods to scale the speeds appropriately.

Localization

Localizing the robot is a necessary process as it gives the user the ability to determine the location of the robot as well as being a crucial step in retrieving environmental thermal data. Localization was accomplished through the 9-DOF IMU by means of extensive calibration where the robot was slowly moved through a wide range of motion and varying orientations in order to determine its bearings.

Chapter 4. Experimental Evaluation

Though the robot was designed to meet certain requirements, the final prototype was subjected to multiple tests to determine whether the goal criteria were met. The following sections describe the series of tests, each designed to test the robot's survival and performance in a fireground.

Test Setup

The following sections describe how each completed test was setup to determine if the project requirements were met.

Affordability

The cost of each of the robot's components (not including shipping) were added together to determine the total cost of the robot. The total sum was then compared to the requirement metrics.

Fire Resistant

With the help of the WPI Fire Protection Engineering (FPE) department, the thermal integrity of the robot was tested using a Screening E119 Furnace (Figure 61). The testing was split into two parts based on the test temperature, and a procedure document was drafted for the FPE department's approval (see Appendix D for thermal testing protocols).

Figure 61. Screening E119 Furnace

Preparation

In addition to writing the test protocols for approval by the FPE lab staff, the team prepared for the thermal testing by sealing the robot thoroughly, as intended for an actual firefighting scenario. Three thermocouples were secured between layers on the lid of the chassis: one on the outer surface of the Teflon, one on the inner surface of the Teflon (within the air layer), and one on the inner surface of the foam. This distribution of thermocouples, as seen in Figure 62 and Figure 63, allowed for data to be collected regarding the rate at which heat penetrated each layer of the chassis.

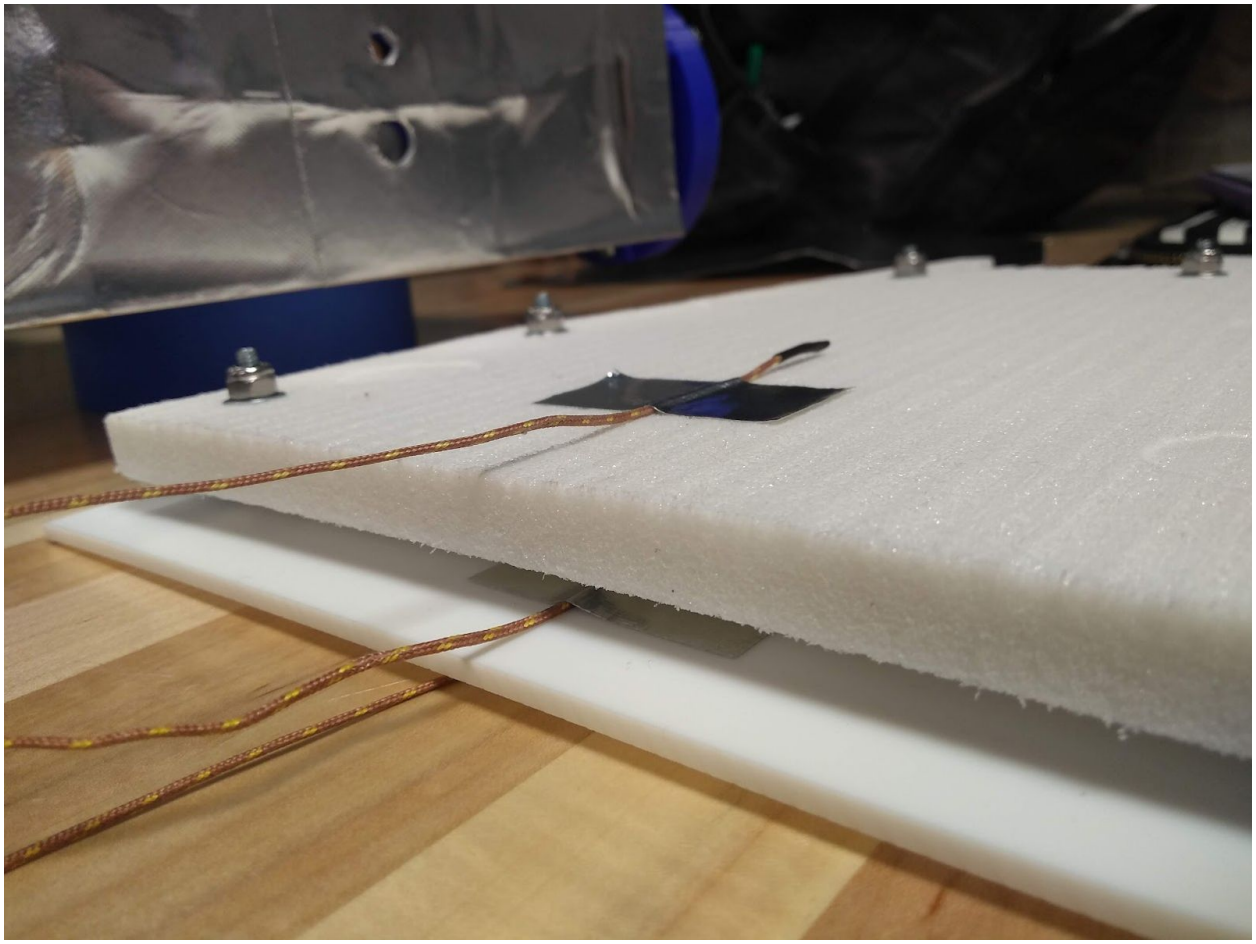

Figure 62. Thermocouple arrangement for thermal testing

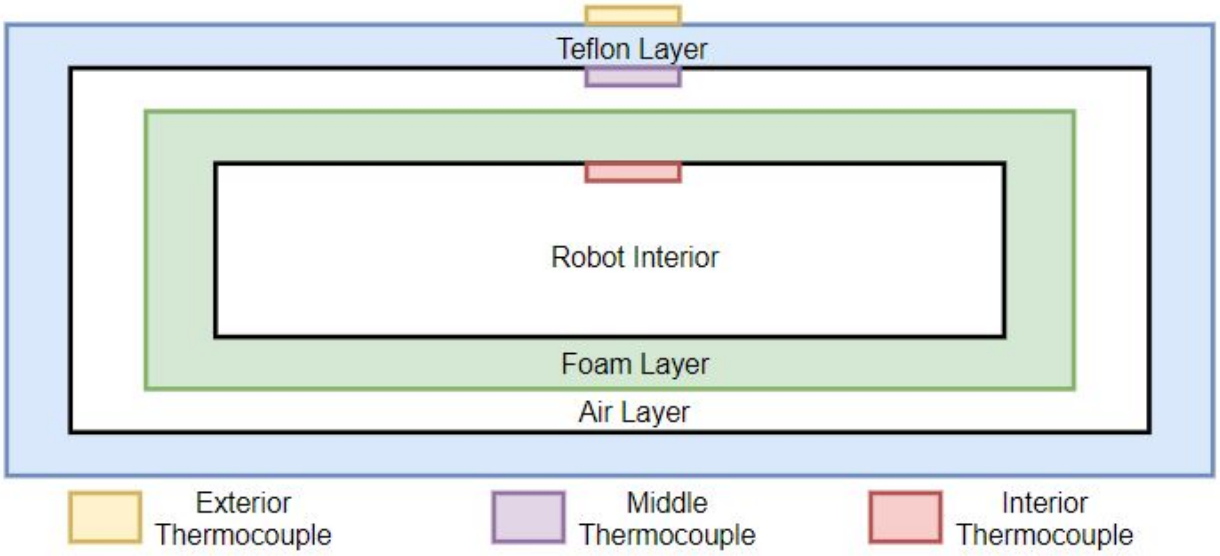

Figure 63. Conceptual Thermocouple Arrangement for Thermal Testing

All the electronics were removed from the interior of the robot to avoid damaging them, with the exception of the motors and their mounts, which were left in place because removing them would have required disassembling the bottom layers of the chassis. The lid of the robot was then secured in place using strips of Reflect-A-Cool. (Individual strips were used rather than a continuous strip around due to a shortage of Reflect-A-Cool discovered the day prior and because the lid fits snugly into the rest of the chassis as it is.) The whegs were removed because at the time of testing, they were 3D printed prototypes and the PLA would have deformed at the testing temperatures. The axles remained in the chassis. At the time of the thermal test, the aluminum shield was not yet secured to the robot due to lack of correctly sized hardware. The state of the robot as prepared for testing can be seen in Figure 64.

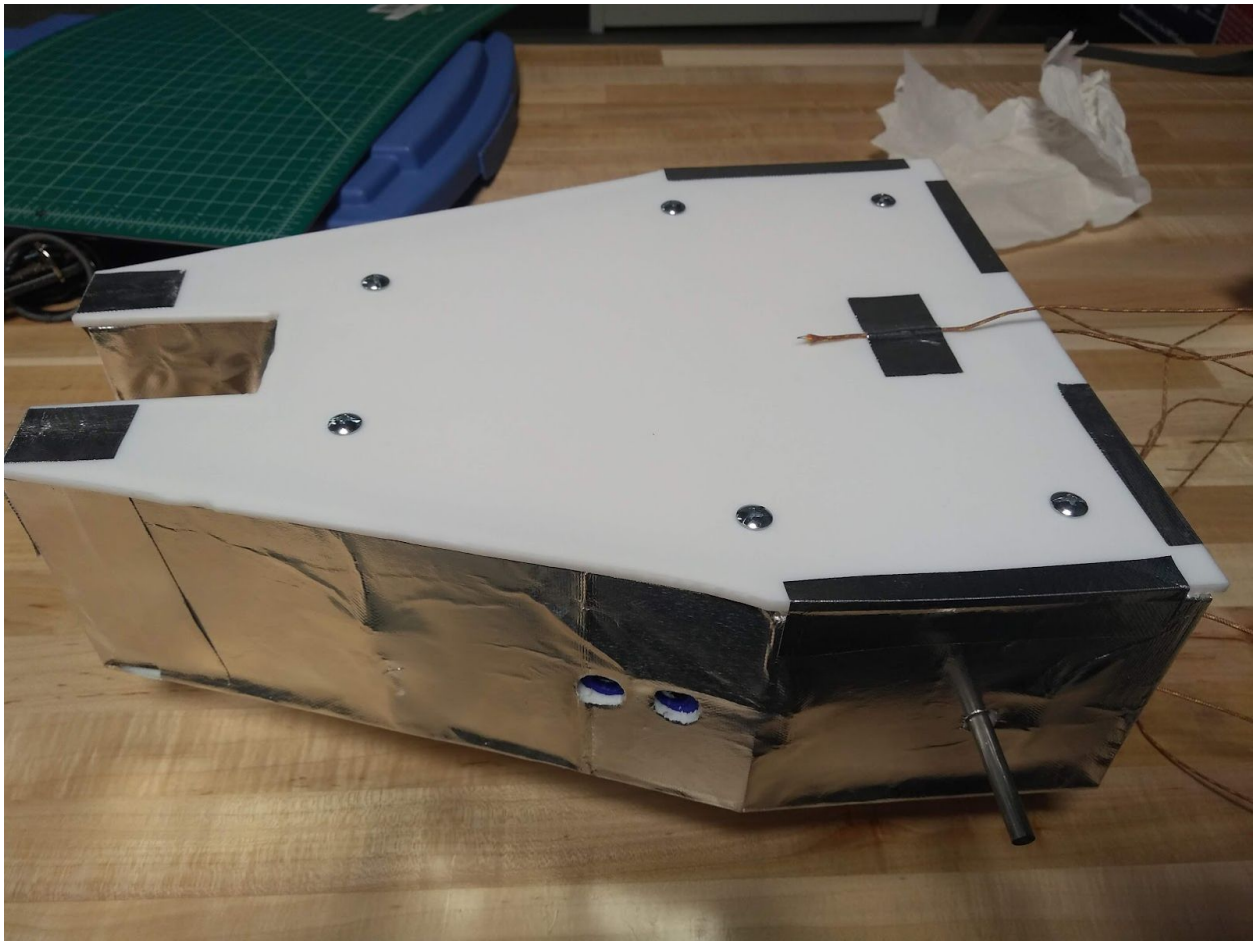

Figure 64. Chassis prepared for Thermal Testing

Data Collection

To collect thermocouple data from the tests, the ESP8266 microcontroller read the temperature of each thermocouple approximately five times per second, and directly outputted real-time data to an Excel spreadsheet. To output real-time data from the serial port to an Excel spreadsheet, a

modified version of the Parallax Data Acquisition Tool (PLX-DAQ) was utilized because it could support the baud rate of the ESP8266 serial port (115200). See Appendix D to view the thermal test data collection code.

Thermal Test

The thermal test was conducted at a temperature of approximately 300°F (149°C). The Screening E119 Furnace is intended to operate at temperatures over 1500°F (816°C), so its control at temperatures as comparatively low as 300°F (149°C) is somewhat imprecise. The FPE lab manager explained this, and said that the furnace temperature remained between 275°F (135°C) and 300°F (°C) for the duration of the experiment. The robot was placed in the furnace for a total of 18 minutes. Upon removal, the robot was left on the ground to cool for approximately 13 minutes, then the team removed the top of the robot to allow the interior to cool more quickly.

Water Resistant

To determine if the robot was water resistant, five gallons of water were poured onto the top of the robot without the electronics inside. Paper towels were placed inside the robot (both between the Teflon/foam layer and within the foam layer) to indicate whether any water entered the chassis. As shown in Figure 65, the robot was placed on the ground, and the water was poured on the top center of the aluminum shield from a height of one meter.

Figure 65. Water Test Setup

After the five gallons of water were poured onto the robot, the top of the robot was then removed to see if the paper towels remained dry.

Impact Resistant

To test if the robot was impact resistant, a jug of water filled with different amounts to meet different masses (0.5kg, 1 kg, 1.5kg, and 2kg) was dropped onto the center of the robot's aluminum shield from four different heights: 10in, 20in, 30in, and 40in. A spring scale was used to weigh the jug of water as shown in Figure 66.

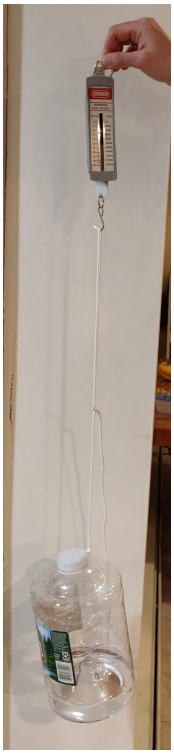

Figure 66. Weighing the weight using a spring scale

The test was completed outside with the robot on the ground, and a tape measure was used to measure the height at which the weight was dropped as shown in Figure 67. To reduce the impact on the axles, the robot was placed on a 2x4 piece of wood, so the axles were not touching the ground. The axles were not tested at this time since there was a higher chance that the axles could break from the stress. After each weight was dropped, the aluminum shield and internal structure of the robot was inspected to see if it was dented or damaged in any way.

Figure 67. Impact test setup

Accurate Environmental Data

The two sensors that gather environmental data are the distance sensors and IR arrays. The distance sensors were tested with and without the Zinc Selenide (ZnSe) lens to determine their accuracy.

As shown in Figure 68, to test the distance sensor, the measured distance from the sensor readings was compared to the actual distance measured with a ruler. Keeping the sensor in place, a large flat non-transparent object was placed in front of the component. For every inch, the measured distance was recorded and the object was then placed an inch further. This was repeated until the object was 40 inches away from the sensor. This experiment was conducted two times: without the lens and with the lens. As the distance between the sensor and the object increased, the readings became more noisy. To reduce the noise, 10,000 readings were sampled and averaged.

Figure 68. Distance sensor test setup

Without a test fixture, the lens was directly placed on the distance sensor with sticky putty.

Figure 69. Distance sensor with lens configuration

Results and Discussion

This section goes through the results of each completed test and discusses the performance of the robot.

Affordability

Tables 6, 7, and 8 contain the costs of all the components (electrical, materials, and hardware respectively) used for this project to build one robot.

Table 6. Costs for electronic components

Component	Cost ($)	Quantity	Total ($)
Adafruit 9-DOF Absolute Orientation IMU Fusion Breakout - BNO055	34.95	1	34.95
Adafruit BME680 - Temperature, Humidity, Pressure and Gas sensor	22.50	1	22.50
Raspberry Pi 3 - Model B+ - 1.4GHz Cortex-A53 with 1GB RAM	35.00	1	35.00
SparkFun IR Array Breakout - 110 Degree FOV, MLX90640 (Qwiic)	69.95	3	209.85
Adafruit HUZZAH32 - ESP32 Feather Board (pre-soldered)	20.95	1	20.95
Raspberry Pi Camera Board v2 - 8 Megapixels	29.95	1	29.95
SanDisk 64GB Ultra microSDXC UHS-I Memory Card with Adapter - 100MB/s, C10, U1, Full HD, A1, Micro SD Card - SDSQUAR-064G-GN6MA	11.99	1	11.99
12V DC Motor 350RPM w/Encoder (12kg*cm)	29.00	2	58.00
Cytron 10A 5-30V Dual Channel DC Motor Driver	19.25	1	19.25
Adafruit VL53LOX Time of Flight Distance Sensor - ~30 to 1000mm	14.95	2	29.90
Thermocouple Amplifier MAX318555 breakout board	14.95	3	44.85
Thermocouple Type-K Glass Braid Insulated K	9.95	3	29.85
Premium Female/Female Jumper Wires - 20 x 3" (75mm)	1.95	1	1.95
Premium Male/Male Jumper Wires - 20 x 6" (150mm)	1.95	1	1.95
Premium Female/Female Jumper Wires - 20 x 12" (300mm)	3.95	1	3.95
Qwiic Cable - Breadboard Jumper (4-pin)	1.50	5	7.50

Buck Converter, DROK LM2596 Immersion Gold Voltage Regulator DC 3V-40V 24V Step-Down to DC 1.23V-37V 5V 9V 12V Volt Reducer Board 3A Power Supply Transformer Module	9.99	2	19.98
LiNiMnCo 26650 Battery: 14.4V 5Ah (72Wh, 10A rate, 4S/S)	64.95	1	64.95
USB DIY Connector Shell - Type Micro-B Plug	0.95	1	4.75
[Real 18AWG 43x2pcs Wires] 10 pairs DC Power Pigtail Cable 12V 5A Male & Female + 10 Pairs DC Power Jack Plug Adapter Connector for CCTV Home Security Surveillance by MILAPEAK (2.1mm x 5.5mm)	12.89	1	12.89
Smart Charger (3.0A) for 14.8V Li-ion/Polymer Battery Pack. Output Terminal: CH-L1483SM: 5.5x2.1mm Male	36.95	1	36.95
500SSP1S2M2QEA; SWITCH SLIDE SPDT 5A 120V	2.89	1	5.78
LTL2P3KGKNN; LED GREEN CLEAR T-1 3/4 T/H	0.285	1	2.85
TCA9548A I^2C Multiplexer	6.95	1	6.95
Total cost for electronics			717.49

Table 7. Costs for materials

Material	Cost ($)
Reflect-a-Cool - Heat Reflective Sheet	33.75
5052 H32 Aluminum Sheet	16.01
Teflon- Natural PTFE Sheet	106.12
PET Foam Core Rigid Sheet	36.59
Bullet HD Pro 2 Fireproof Glass Replacement lens	25.00
Five 12mm Dia ZnSe Focus Lens	45.85
J-B Weld ExtremeHeat™ High Temperature Resistant Metallic Paste (4 bottles)	38.88
ASI 502 High Performance 100% RTV Silicone adhesive	7.48
PLA for Motor Mounts	0.64
PLA for Whegs	2.62
Total cost for materials	312.94

Table 8. Costs for hardware used for robot

Product	Cost Per Unit ($)	Quantity	Total Cost ($)
RND STANDOFF #6-32 CERAMIC 3/4"	4.00	2	8.00
RND STANDOFF #6-32 CERAMIC 3/8"	3.06	3	9.18
6mm D-shaft	1.80	2	3.60
6mm Bore Size, Steel, Set Screw Shaft Collar	2.62	2	5.24
70 Tooth gear	26.27	2	52.54
24 Tooth gear	13.22	2	26.44
Bearing 6x19x6 Shielded Miniature	2.49	2	4.98
#8-32 x 1 ¼" Trusshead Machine Screw	0.12*	~40	4.96
#8-31 x 1" Round head Machine Screw	0.15	9	1.35
#8-32 Nylon Lock Nut	0.32	~50	16.00
#8-32 Machine Screw Nut	0.08*	~70	5.60
#8 Flat Washer, Zinc	0.04*	~100	4.24
Total Cost for hardware			142.13

*Purchased in a package of 50+

The total cost to make one robot is $1,172.56.

The requirement metric for affordability was met as the total cost of the robot was "less than $2,000." The unit cost of creating a robot could be improved by designing a printed circuit board (PCB) that utilizes all of the necessary components and circuits. As shown in Table 9, the unit cost per sensor is shown. Unlike the cost of development, the cost to make a custom circuit board is reduced by a factor of 2.4. Designing custom electronics and embedded systems reduces the total cost to less than $1,000 per robot.

Table 9. Cost to make custom electronic circuit

Component	Cost per 100 units ($)	Quantity	Total ($)
Sensors			
BNO055	6.776	1	6.776
VL53L0X	3.721	3	11.163
MLX90640	44.177	3	132.531
BME680	8.099	1	8.099
MAX31855	4.877	3	14.631
Thermocouple Type-K	9.95	3	29.85
Actuators			
12V DC Motor 350RPM with Encoder	29.00	2	58.00
PCBs[7], Miscellaneous Hardware[8], and Assembly[9]			
(20cm x 20cm) PCB	4.75	1	4.75
Miscellaneous Hardware	5.00	1	5.00
Assembly	5.00	1	5.00
Total cost for custom electronics			275.8

Fire Resistant

The interior and exterior thermocouples gathered sufficient information throughout the test. Unfortunately, due to a misconnection, the data collected from the middle thermocouple was not usable. As shown in Figure 70, the interior of the robot reached 60°C (140°F) after 11 minutes and 36 seconds. Although this is less than the 15 minute requirement, this was an accomplishment as it was not expected to survive that long based on the thermal calculations. The discrepancy between the thermal calculations and actual result is due to the assumption that when the rigid foam reached 70°C (158°F), the interior of the robot reached 60°C (140°F). The

[7] Using JLCPCB, a 200mm by 200mm PCB costs $400 with shipping for 100 boards. Using PCBWay, it costs roughly $550. Therefore the cost provided is the average of the two costs.
[8] Miscellaneous Hardware are extra components necessary to create the PCB. It is an estimate that includes the cost of headers, wires, terminals, etc.
[9] Assembly costs are the costs to solder components to the PCB and to create enclosures for the PCBs.

data collected shows the robot heating at 150°C (302°F) and cooling at 15°C (59°F). The sudden drop of temperature (at around 1000 seconds) on the exterior thermocouple is the time when the robot was removed from the furnace.

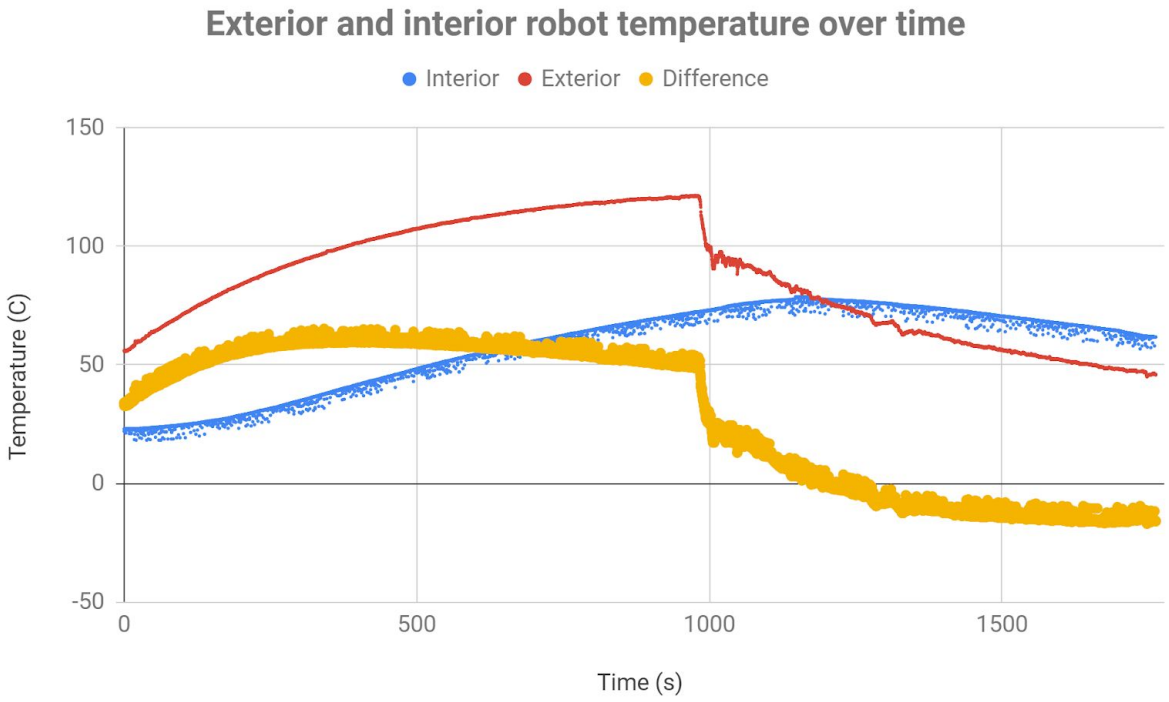

Figure 70. Exterior vs. Interior temperature over time

After the robot was removed from the furnace, the interior heated by 10°C (50°F)until it started to cool (i.e. when the interior and exterior lines cross). This emphasizes the critical temperature of the robot. The critical temperature is the temperature at which the robot should be removed from the environment. In order to survive, the interior of the robot, where the electronics are housed, must remain below 60°C (140°F). Therefore if the internal temperature keeps rising after it is removed from the fireground, the critical temperature should be set to 5 °C (122°F). By determining the heat transfer through the robot, it is possible to determine the time it takes for the interior to reach its critical temperature when it is operating in a fireground.

An observation when the robot was removed from the furnace was that the Teflon softened on the top and the sides. This suggests that another layer should be placed around the Teflon to further protect the Teflon and to increase the time until the interior reaches its critical temperature.

Water Resistant

After the five gallon pour on the robot, there was moisture present in the air layer between the Teflon and the foam. The inside of the foam, where the electronics are housed, remained dry. We hypothesize that this was the result because there were small gaps on the Teflon layer that allowed water to enter as shown in Figure 71. The image on the left, which does not include the lid of the robot, shows that the edge of one Teflon panel does not line up evenly with the adjoining panel, leaving a gap when the lid is placed on. The image on the right shows that the 3D printed lens holder was not wide enough to fully cover the holes cut for the sensor windows.

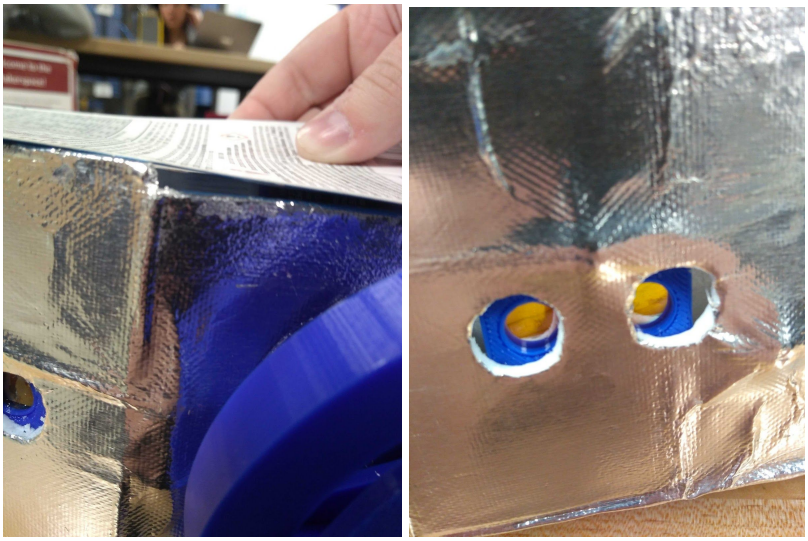

Figure 71. Gaps present in robot during water test

The paper towels indicated whether there was water present between the layers, however they could not quantitatively indicate how much water was present. To provide better data on the water resistance of the robot, sensors should be utilized to measure moisture and humidity. The international protection (IP) marking system could be used in future water tests to evaluate the water resistance of the robot [70].

Impact Resistant

Figure 72 is a comparison between the shield before any weights were dropped onto it and the shield after the last weight was dropped onto it during the impact test.

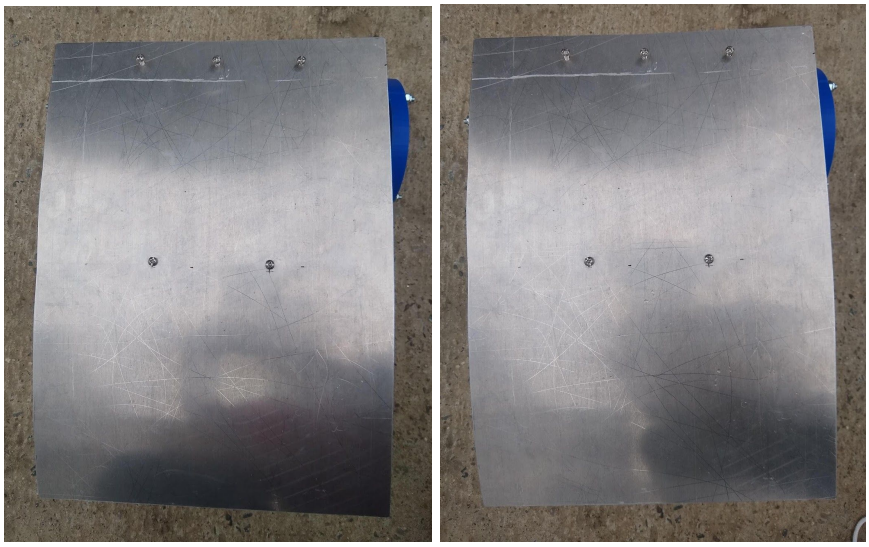

Figure 72. (left) aluminum shield before impact test; (right) aluminum shield after impact test

There is no visible difference between the two pictures. When the heavier weights (1.5kg and 2kg) were dropped from greater heights (30 and 40 inches), the top of the robot was jostled out of place because it was not secured to the body of the robot. (The lid was not secured because there was not enough Reflect-A-Cool left after the thermal and water testing.)

An improvement to this test would be to secure the top to the rest of the robot, so it does not pop out during the test. Additionally, the front bolts were too long and should have been cut down so that the aluminum shield would be more secure. Another improvement would be to incorporate sensors that can measure impact. This type of quantitative data would give a better understanding of how the internal structure of the robot reacted to certain weights and could possibly determine the structural integrity of the robot. Similarly, it is important to determine the impact on the wheel axles so the robot can traverse the fireground correctly.

Accurate Environmental Data

For future iterations, a test fixture should be designed to hold the lens at varying distances. This can help identify where the sensor can be placed within the robot to get the most accurate measurements possible of the environment.

Measured from 0 inches to 40 inches, the following figures show the accuracy of the distance sensors with and without a ZnSe lens. Without the lens, the measured distance of the time of flight sensor is relatively linear to the actual distance.

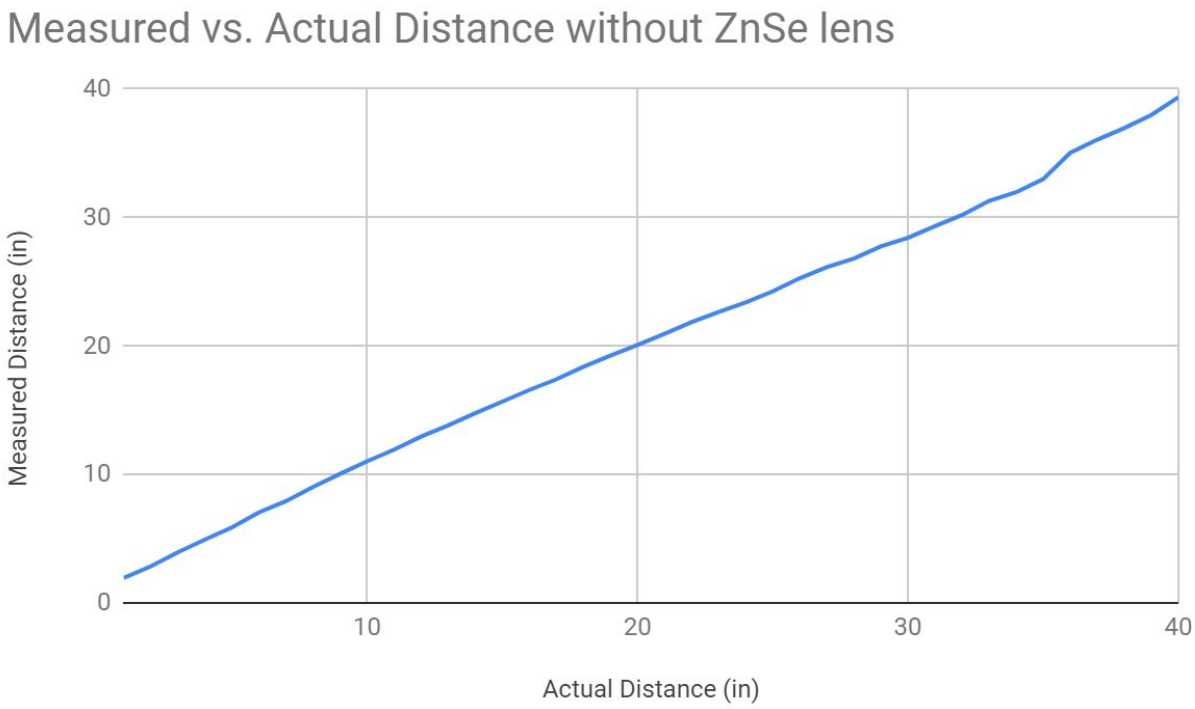

Figure 73. Measured vs Actual Distance without lens

As soon as the lens is integrated, the error increases exponentially. This is possibly due to refraction from the converging lenses. As shown in Figure 74, a measured distance of 6 inches, corresponds to an actual distance of 5 inches and 28 inches. This creates a great discrepancy in measuring accurate distances.

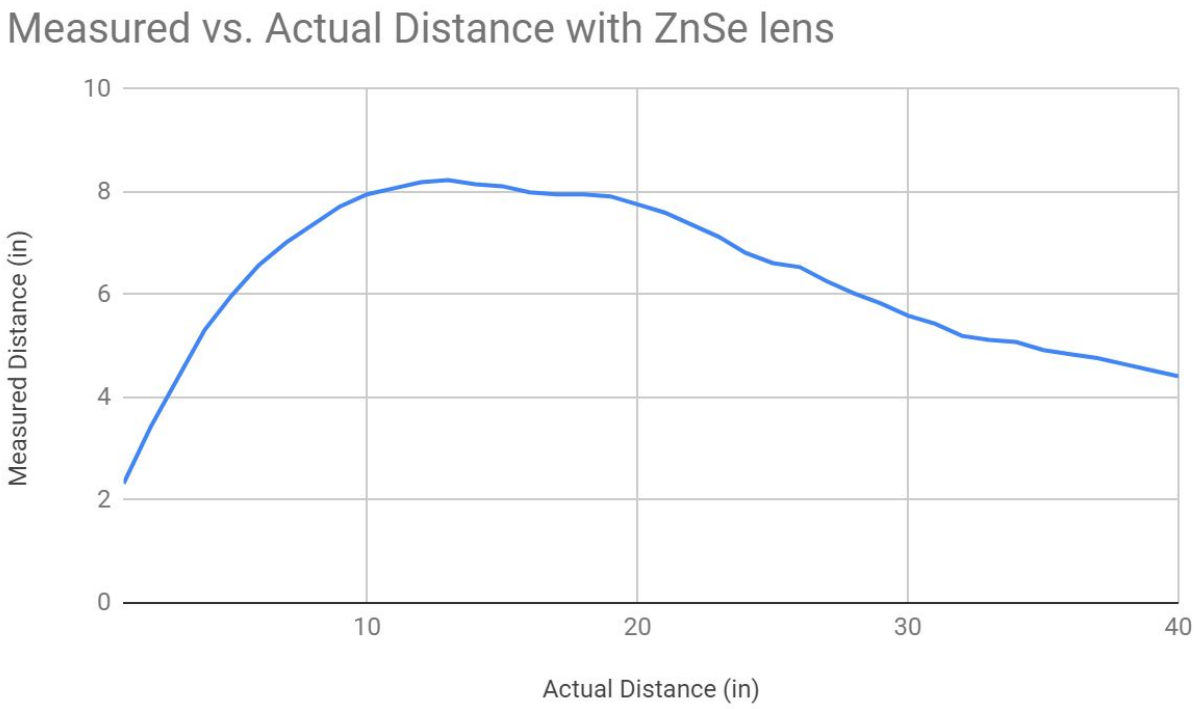

Figure 74. Measured vs Actual Distance with lens

Chapter 5. Conclusion

From the background research about fireground hazards to the prototyped chassis and wheels, this project encompasses the development and creation of a mobile sensing platform for firefighting applications. The FRED robot, or Firefighting Remote Exploration Device, is outfitted with a camera, thermal sensors, and wireless capabilities as well as a robust chassis and drive system to function in a hostile fireground. The robot weighs less than 10 pounds making it human-portable, and has an affordable price for fire departments as it cost less than $1,500 to create a prototype. Additionally, the passive transformable whegs make for smooth driving for data collection and better obstacle avoidance compared to other drivetrains.

Multiple tests were conducted throughout development to determine the effectiveness of our design decisions; the water resistance testing and impact resistance testing yielded favorable results, but thermal testing proved that the chassis was not adequately insulated. FRED was able to perform basic localization and thermal mapping providing the beginnings of a very useful data display for firefighting. Though the chassis and whegs are prototypes with plenty of room for improvement, FRED serves as a functional proof of concept for further compact firefighting robots. This chapter contains lessons learned throughout the project, as well as suggestions for future tests and improvements to create more effective robots in the future.

Lessons Learned

A major lesson learned while completing this project was creating a fire resistant robot on a budget is very difficult. Fire resistant materials are expensive, and some materials have high shipping costs. Another lesson learned was not all sensors integrate with the Raspberry Pi over I^2C due to a clock stretching bug in the Raspberry Pi's firmware. The third lesson learned during this project was localization and mapping is challenging when there are not enough sensors present to accurately locate the robot within its operating environment. Given enough time and money, these difficulties would be trivial to overcome.

Future Work

While the robot created for this project was successful in many aspects, there are a lot of improvements and additions that can be made to make this robot more useful for firefighters. Below is a list of possible improvements to be made in further iterations of the project, followed by an in-depth explanation of why the current iteration is inadequate in these areas and how it could be improved.

1. Utilize an interior time algorithm
2. Implement phase change cooling
3. Add another layer of insulating material outside of the Teflon layer
4. Develop a system to keep whegs deployed when dropped
5. Implement autonomous functionalities
6. Improve sensor system
7. Correct for sensor lens refraction
8. Design a custom battery with a power management system
9. Refine user interface
10. Implement automatic launch of scripts on robot boot
11. Complete requirement metric testing

Interior Time Algorithm

Although it is important to keep track of the health of the robot in a fireground, it is more useful to understand when deteriorating conditions can become a problem. Providing firefighters with information as to when the robot will reach critical conditions can help plan an optimal interior attack and reduce the risk of the robot exploding and harming more property or life. The most crucial component in FRED is the battery which must be kept under 60°C (140°F) while discharging. By finding the heat transfer from the exterior to the interior of the robot, a model of the interior time can be derived for the specific environment. The interior time is an estimate of the time it takes the interior of the robot to reach its critical temperature. The critical temperature is the temperature the robot should be removed from the environment to ensure the interior does not heat up over its max operating temperature. To better understand the heat transfer at different environments, the thermal test should be repeated at different temperatures ranging from 60°C (140°F) to 500°C (932°F). Further, the amount of heat the electronics dissipate should also be tested. Both of these heat sources should be considered when coming up with an efficient algorithm.

Phase Change Cooling

Phase change cooling is a method that can be implemented to increase the time the interior of the robot remains below 60°C (140°F). A phase (solid, liquid, or gas) can be placed in the interior of the robot to absorb energy and change to another phase before the temperature increases. For example, a contained ice pack can be placed inside the robot to absorb the heat that has entered the robot. The ice pack will absorb the energy until it reaches its melting point in which the ice will start to change phase. Phase change materials could be used such as Paraffin wax or hydrated salts since there is a chance the water will start to condense on the ice pack which may damage electronics. Therefore, the electronics would have to be properly sealed in order for a phase change to be used.

Additional Material Layer

To improve the material layer system and ultimately the robot's thermal protection, another material should be added between the Reflect-A-Cool and Teflon. Teflon outgasses at approximately 316°C (600°F), which is a temperature that the robot could encounter while operating in a fireground. Therefore, to avoid outgassing, another material layer should be added so that the Teflon is subjected to less intense temperatures. This layer could be added to the material system in two ways:

1. Directly on top of the Teflon;
2. With a small air layer between the Teflon and new layer.

If the first option is chosen, the material should have a similar thermal expansion coefficient to avoid stress between the two materials. Additionally, the thermal coefficient and specific heat of the material should be compared with Teflon so that the added material does not heat up too quickly and subject the Teflon to high temperatures. The advantages of the second method are that adding another air layer to the system adds an additional layer of insulation, and also a larger variety of materials can be chosen for the new outer layer.

Wheg Deployment

If the robot were to be dropped from waist height for faster deployment, the axles would likely break from the impact because, in their current state, the transformable whegs would remain collapsed and the force of the impact would be transferred directly to the axles. A method to improve the impact resistance of the robot would be to keep the transformable whegs in wheg form during deployment. The curved nature of the wheg legs would help absorb the force of impacts if the robot were to be dropped, instead of breaking the axle.

Autonomous Capabilities

In a real fire fighting situation, all personnel already have important tasks designated to them. Therefore, for the robot to be useful to firefighters in the future, it will need to be able to operate autonomously. In addition, there will rarely be a pre-generated map available to the robot, so it will need to create its own as it explores the environment. Luckily, both of these tasks are well supported by ROS using the built in navigation stack. This allows developers to provide sensor data to the stack, which then handles mapping and navigation on its own.

In addition to adding new autonomous capabilities, improvements to the existing ones can be made as well. In particular, the thermal mapping system is still in a very basic state, and could stand to be improved greatly. This could involve matching thermal data more accurately to walls as they exist in the map, and accounting for the robot's positioning in relation to structures in the map. Thermal mapping in general is a difficult problem with significant ongoing research in the field, and this project only attempts to dip into it.

Improve Sensor System

A significant factor that prevented this project from reaching its full potential was the limited array of sensors at our disposal. Implementing sensors such as a 2D-LIDAR, a second camera, or adding depth sensors to the existing camera would allow for the robot to generate its own map for navigation, which when combined with the encoders and IMU would allow for significantly more accurate localization as well as autonomous capabilities.

It is difficult to implement additional or more complex sensors because protecting them from the high temperature environment is challenging. For some sensors, this simply requires more lenses, but for others, far more complex solutions are needed. For example, a 2D-LIDAR is the most appealing for accurate localization; however, this is an expensive sensor that requires an infrared laser to rotate 360 degrees around the robot to collide with its surroundings and return to the sensor. Therefore, a lens such as the ones used for the distance and thermal sensors in this project iteration would be required, but the lens would need to cover the 360 degree path of the infrared laser. This entails contracting a custom part to be manufactured of an expensive material, which will drive the cost up further.

Sensor Lens Distortion

Due to the difficulty of operating under such strict budgetary restrictions given the robot's task, we were forced to compromise on the material used for the external sensor lenses. This resulted in a non-insignificant decrease in sensor accuracy. This could be solved through the purchasing of a less distorted sensor lens material or determining a method of correcting for the distortion.

One method that can help reduce the distortion is by identifying the optimal distance between the sensor and the lens. As shown in the distance sensor test setup, the Zinc Selenide (ZnSe) lens was placed directly on the sensor. This test can be improved by designing a test fixture that can easily change the distance between the sensor and the lens and keep them aligned at all times. The same can be done for the IR array, however the field-of-view must be considered.

Custom Battery and Battery Management System

The size and weight of the battery proved to be the biggest obstacle in driving and fitting the electronics in the robot. Similarly, monitoring the health of the battery is essential to keep FRED functioning properly. It is hard to find pre-made battery packs that meet specific requirements; therefore, to combat this issue, a custom battery should be designed. Creating a custom battery has two benefits:

1. The weight of the battery can be distributed in the robot more evenly and can thus make more space for the electronics to fit;

2. It can reduce the likelihood of fires and explosions using a battery management system (BMS).

A BMS can be easily integrated to measure and monitor the battery voltage, the state of charge (SoC), state of health (SoH), temperature and other critical measurements.

Refine User Interface

Presently, the user interface (UI) is functional, but far from ideal. Some additional features are described in the User Interface section (Chapter 4), such an option to overlay thermal visualization over the camera feed, sections for warnings, and adding detail and visuals for some sensor data. The UI would ideally also be unified into a single application window, rather than split into multiple as it is currently. Beyond these simple upgrades, there is also room to add much more complex features that could prove incredibly valuable to firefighters. Using just the camera and thermal arrays, it should be possible to identify a human that is trapped in the fireground, likely with the assistance of machine learning, and mark the person on the map to aid search and rescue. Similarly, with some improvements and additions to the sensor package, it would likely be possible to detect and display common fireground hazards such as flashover and backdraft.

Launch Scripts on Robot Boot

A simple way to drastically improve robot deployment time is to add instructions for the Raspberry Pi to automatically launch the appropriate scripts for robot operation as soon as it boots up. Currently, these scripts are each run manually via accessing the Raspberry Pi's operating system with a monitor, keyboard, and mouse, opening a terminal, typing in the command, and running it. This amount of additional deployment time and required hardware would be inexcusable if the robot was to see use in an actual fire situation.

Testing

More intensive tests should be run to determine if project requirements have been met. Due to time, weight, and equipment constraints we were unable to complete these tests during this project iteration. The following tests should be run in future iterations of the project:

1. Robot deployment
2. Operation speed
3. IR array data collection
4. Additional thermal test
5. Low power consumption
6. Long range communication

Robot Deployment

A formal test of robot deployment time was not performed due to timing restrictions and other tasks taking higher priority. However, working with the robot enough allowed the team to estimate that the robot takes about thirty seconds to boot. At this time, the operator must log in to the robot and run the appropriate scripts on the robot before it is ready to operate. This is user-dependent, so an estimate of the timing of this would not be useful. In addition, this user login would ideally be removed in favor of necessary scripts being automatically launched on boot, which would eliminate this additional time.

The final weight of the robot was about 8.35 lbs. This weight is not particularly difficult for a human to transport over short distances. No sort of handle or other hardware specifically for carrying the robot was added, but the robot can be carried comfortably for distances greater than what would be expected in a fireground by placing a single hand and forearm under the robot.

Once firefighters arrive at a fireground they can take less than two minutes to prepare. Since this robot can be used to explore a fireground ahead of firefighters, the robot must be quickly deployable. The deployment is dependant on two factors: whether it is human-portable or whether it has a fast boot time.

To test the boot time, the operation device should be ON prior to booting the robot. Using a stopwatch, the time the robot takes to boot and connect to the operation device can be measured. The human portability aspect of the robot can be determined by the weight and ease of carrying the robot. The weight can be found by placing the robot on an adequate scale. Ease of carrying is subjective, but can be evaluated based on comfort and travel time.

Operation Speed

An accurate test for operating ahead of firefighters was unable to be completed. This was due to the fact that the chassis was too heavy on the back because the omnidirectional wheel was not attached and that the whegs did not have enough traction to carry the robot. To test driving and other software functionalities, a testbed was 3D printed for the electronics to be mounted to. The gears were not transferred over to the testbed, so the motors were not geared down like they would be in the actual chassis. Additionally, the testbed was significantly lighter than the actual chassis, so if the testbed were used for this test, the results would not have accurately represented the actual chassis.

The robot must not interfere with normal fire operations. Therefore, the robot should remain ahead of firefighters when it is deployed. The speed at which the robot moves should be tested. This can be done by timing how long it takes for the robot to travel 2 meters. A start and a finish

line should be marked off and a stopwatch can be used to keep time. The robot should start 0.25 meters behind the start line, so it can get up to speed before crossing the start line. The stopwatch should be started when the front of the robot crosses the start line and stopped when the front of the robot crosses the finish line. This test should be repeated five times to get an average speed.

Infrared (IR) Array Data Collection

To test the IR arrays, all three sensors should be placed in a configuration to face the same object. This configuration can be used to determine whether all sensors are receiving the same data. To verify the data retrieved, a thermocouple should be placed on the object and its temperature readings should be compared to the readings returned by the IR arrays. Because it is hard to determine the accuracy of the temperature readings of the environment, this test aims to determine the accuracy among the sensors within the robot. If the thermocouple read 60°C (140°F), the IR arrays should have also retrieved values around 60°C (140°F). This experiment should then be repeated with the ZnSe lens.

Thermal Test 2

A second thermal test was planned to be three minutes long at 260°C (500°F), but during the heating process, one of the system's safety failsafes was triggered, which extinguished the furnace.

The second thermal test should use the same setup as the thermal test completed at 150°C (300°F) , but it should be conducted at approximately 260°C (500°F) for three minutes. Since the maximum temperature of the Teflon is 260°C (500°F), it is vital that the robot is removed immediately after three minutes of exposure.

Low Power Consumption

The test for low power consumption was unable to be completed as the electronics did not fit within the chassis. Additionally, due to a lack of time and resources, recreating a fireground in a compartmentalized building is hard. Nonetheless, this test should be completed in future iterations to get a better understanding of how long the robot can last on the field.

To test the power consumption of the robot, the robot should run for 15 minutes in a compartmentalized building that may represent a common fireground. Prior to the experiment, the battery charge should be measured as a control variable. After 15 minutes, the battery charge should be measured and compared to the initial controlled value. Knowing the capacity difference and the time it took to discharge, the amount of current drawn can be calculated which will determine the average power consumption of the robot.

Long-Range Communication

Multiple separate tests should be run to test long range communication. The first test should test the camera by itself. The camera should be placed in one spot, and the speed of the video feed transfer should be examined as the computer receiving the data is moved farther away from the camera. Once the frames per second (fps) sent reaches less than 24 fps, measure the distance between the computer and the camera. This test should be repeated with a wall between the camera and computer, and possibly repeated again with multiple walls between the camera and computer. The next test should incorporate the robot. While driving the robot around, move the computer further away from it. Once the video feed reaches less than 24 fps or the robot no longer responds to the controller, measure the distance between the computer and the robot. This test should be repeated with one wall between the computer and robot and again with multiple walls between the robot and computer.

References

1. Bryner, N. P. & Grant, C. & Hamins, A. P. & Jones, A. W. & Koepke, G. H. (June 11, 2015). Research Roadmap for Smart Fire Fighting. NIST. Retrieved October 20, 2018, from https://nvlpubs.nist.gov/nistpubs/SpecialPublications/NIST.SP.1191.pdf
2. (2016, August 11). Firefighter: $46,870 - Americas 10 most dangerous jobs - CBS News. Retrieved October 20, 2018, from https://www.cbsnews.com/media/americas-10-most-dangerous-jobs/6/
3. (2018, August). NFPA statistics - Home fires. Retrieved October 20, 2018, from https://www.nfpa.org/News-and-Research/Fire-statistics-and-reports/Fire-statistics/Fires-by-property-type/Residential/Home-fires
4. Fahy, R. F & LeBlanc, P. R. & Molis, J. L. (2018, June). NFPA report - Firefighter fatalities in the United States - 2017. Retrieved October 20, 2018, from https://www.nfpa.org/News-and-Research/Fire-statistics-and-reports/Fire-statistics/The-fire-service/Fatalities-and-injuries/Firefighter-fatalities-in-the-United-States
5. Owen, C. (Ed.). (2014). Human factors challenges in emergency management : enhancing individual and team performance in fire and emergency services. Retrieved from https://ebookcentral-proquest-com.ezproxy.wpi.edu
6. (2017, September). Trends in Home Structure Fires and Fire Deaths. Retrieved October 20, 2018, from https://www.nfpa.org/-/media/Files/News-and-Research/Fire-statistics-and-reports/Fact-sheets/TrendsHomeFiresFactSheet.pdf
7. (n.d.). A Comparison of Modern & Legacy Fires - Belmont Fire Department. Retrieved October 20, 2018, from http://www.belmontfiredepartment.com/files/Page_5_and_6_Jumpseat_Jargon.pdf
8. (2016, September 7). Smoked Out: Are Firefighters in More Danger than Ever ... - EHS Today. Retrieved October 20, 2018, from https://www.ehstoday.com/emergency-management/smoked-out-are-firefighters-more-danger-ever
9. [jarHead96]. (2010, December 17). New vs Old Room Fire Final UL [Video File]. Retrieved October 20, 2018 from https://www.youtube.com/watch?v=aDNPhq5ggoE
10. Mora, W.R [2005, June]. "UNDERSTANDING AND SOLVING FIREFIGHTER DISORIENTATION." Fire Engineering: 103,104,106,109-110,112-114. ProQuest. Web. 17 Sep. 2018
11. (2009, July 22). Basement fires, or cellar fires, are some of the most difficult ... - Firehouse. Retrieved September 17, 2018, from https://www.firehouse.com/operations-training/article/10471100/basement-fires-or-cellar

-fires-are-some-of-the-most-difficult-challenging-and-dangerous-operations-you-will-ever-encounter-lots-of-basement-fires-result-in-loss-of-buildings-and-loss-of-life-lets-take-a-look-at-the-challenges-we-face-and-how-we-may

12. Feasibility Study of Rotorcraft Fire Fighting for High-Rise Buildings. (2010). Journal of Aerospace Engineering, 23(3), 166–175. https://doi.org/10.1061/(ASCE)AS.1943-5525.0000021
13. (2016, February 22). Compartmentalizing A Facility With Fire Barriers - Life Safety Services. Retrieved October 20, 2018, from http://news.lifesafetyservices.com/blog/compartmentalizing-a-facility-with-fire-barriers
14. Cahill, A. (n.d.). Compartmentation of buildings – What does it mean? - Fire Safety .... Retrieved October 20, 2018, from https://firesafetyservices.co.uk/compartmentation-of-buildings-what-does-it-mean/
15. (2010, December 3). Worcester Cold Storage Warehouse Fire 1999 | Command Safety. Retrieved October 20, 2018, from http://www.commandsafety.com/2010/12/03/worcester-cold-storage-warehouse-fire-1999/
16. (2010, December 17). Development of a Portable Flashover Predictor - Worcester .... Retrieved October 20, 2018, from https://www.wpi.edu/sites/default/files/docs/Research/WPI_AFG_2008_Fire-ground_Environment_Sensor_-_Scientific_Report.pdf
17. Hartin, E. (2008, March 30). Fire Behavior Indicators and Fire Development - Part 1 - Firehouse. Retrieved October 20, 2018, from https://www.firehouse.com/operations-training/article/10494291/fire-behavior-indicators-and-fire-development-part-1
18. (2008, March 1). Extreme Fire Behavior: Backdraft - Firehouse. Retrieved October 20, 2018, from https://www.firehouse.com/operations-training/article/10499828/extreme-fire-behavior-backdraft
19. (2010, November 17). Fire Dynamics | NIST. Retrieved October 20, 2018, from https://www.nist.gov/el/fire-research-division-73300/firegov-fire-service/fire-dynamics
20. [KillTheFlashoverProj]. (2013, April 11). Kill the Flashover 2013 Fire Growth as seen from Thermal Imager [Video File]. Retrieved October 20, 2018 from https://www.youtube.com/watch?v=W1jUGxLjgak
21. (2009, November 9). What Is Robotics? | NASA. Retrieved October 20, 2018, from https://www.nasa.gov/audience/forstudents/5-8/features/nasa-knows/what_is_robotics_58.html
22. (n.d.) Firefighting Robots. Retrieved October 20, 2018, from http://www.allonrobots.com/firefighting-robots.html

23. (2009, September 21). 지방판 - 愛國言論 실시간 더타임즈. Retrieved October 20, 2018, from http://www.thetimes.kr/news/article.html?no=4856
24. tmdwl. (n.d.) Home [Youtube Channel]. Retrieved October 20, 2018, from https://www.youtube.com/channel/UCkaHZ3xGItVGyCa-ra8cCqA
25. hoyarobot. (n.d) Home [Youtube Channel] Retrieved October 20, 2018, from https://www.youtube.com/channel/UCTBs23LUlRiGbo_bBJXtuyA
26. [hoyarobot]. (2010, March 7). HOYAROBOT(PR) [Video File]. Retrieved October 20, 2018 from https://www.youtube.com/watch?v=wMPf48i64Zc
27. (n.d.). AchiBot - M - Welcome to DRB Fatec. Retrieved October 20, 2018, from http://www.drbfatec.com/frd_center/fighting_m.htm
28. (n.d.). IZ Holding Security Division. Retrieved October 20, 2018, from http://www.izholding.com.sg/security/firos.htm
29. (n.d.). Wheel Transformer: A Miniaturized Terrain Adaptive ... - Biorobotics. Retrieved April 24, 2019, from http://biorobotics.snu.ac.kr/wp-content/uploads/2014/05/2013_ICRA_Wheel-Transformer-A-Miniaturized-Terrain-Adaptive-Robot-with-Passively-Transformed-Wheels.pdf
30. (n.d.). New Concept for Indoor Fire Fighting Robot - Science Direct. Retrieved April 24, 2019, from https://www.sciencedirect.com/science/article/pii/S1877042815036708
31. (n.d.). Raspberry Pi Camera Board v2 - 8 Megapixels ID: 3099 - $29.95 .... Retrieved April 24, 2019, from https://www.adafruit.com/product/3099
32. (n.d.). What is a Proximity Sensor? - Definition from Techopedia. Retrieved April 24, 2019, from https://www.techopedia.com/definition/15003/proximity-sensor
33. (2015, November 30). Rangefinding in Fire Smoke Environments Joseph ... - VTechWorks. Retrieved April 24, 2019, from https://vtechworks.lib.vt.edu/bitstream/handle/10919/73780/Starr_JW_D_2016.pdf?sequence=1
34. (2018, August 8). NIST Shows Laser Ranging Can 'See' 3D Objects Melting in Fires | NIST. Retrieved April 24, 2019, from https://www.nist.gov/news-events/news/2018/08/nist-shows-laser-ranging-can-see-3d-objects-melting-fires
35. (n.d.). Proximity Sensors - STMicroelectronics. Retrieved April 24, 2019, from https://www.st.com/en/mems-and-sensors/proximity-sensors.html
36. (2016, November 28). Adafruit VL53L0X Time of Flight Distance Sensor - ~30 to 1000mm ID .... Retrieved April 24, 2019, from https://www.adafruit.com/product/3317
37. (2018, September 20). SparkFun IR Array Breakout - 55 Degree FOV, MLX90640 (Qwiic .... Retrieved April 24, 2019, from https://www.sparkfun.com/products/14844
38. (2018, September 20). SparkFun IR Array Breakout - 110 Degree FOV, MLX90640 (Qwiic .... Retrieved April 24, 2019, from https://www.sparkfun.com/products/14843
39. (n.d.). Bullet HD Pro 2 3 4 Fireproof Glass Lens - BU-GL - Bullet ... - StuntCams. Retrieved April 24, 2019, from http://stuntcams.com/shop/bullet-hd-pro-fireproof-glass-lens-p-662.html
40. (n.d.). The Correct Material for Infrared (IR) Applications - Edmund Optics. Retrieved April 24, 2019, from

https://www.edmundoptics.com/resources/application-notes/optics/the-correct-material-for-infrared-applications/
41. (n.d.). ZnSe Zinc Selenide Technical Data Sheet - Spectral Systems, LLC. Retrieved April 24, 2019, from https://www.spectral-systems.com/wp-content/uploads/2014/04/ZnSe-TDS-6-13-14.pdf
42. (n.d.). ZnSe Zinc Selenide Technical Data Sheet - Spectral Systems, LLC. Retrieved April 24, 2019, from https://www.spectral-systems.com/wp-content/uploads/2014/04/ZnSe-TDS-6-13-14.pdf
43. (n.d.). High-Efficiency Broadband Anti-Reflective (BBAR ... - II-VI Infrared. Retrieved April 24, 2019, from http://www.iiviinfrared.com/pdfs/irim_datasheets/BBAR_Coating_on_ZnSe_8-12.pdf
44. (n.d.). (ZnSe) .Zinc Sulfide (ZnS) - II-VI Infrared. Retrieved April 24, 2019, from http://www.iiviinfrared.com/pdfs/II-VI_InfraredMaterials2009-04a.pdf
45. (2015, September 16). What is an IMU? - Sparton. Retrieved April 24, 2019, from https://www.spartonnavex.com/imu/
46. (n.d.). A Buyer's Guide to IMU Sport Sensor Devices for ... - SimpliFaster. Retrieved April 24, 2019, from https://simplifaster.com/articles/buyers-guide-imu-sensor-devices/
47. (2015, April 22). Adafruit 9-DOF Absolute Orientation IMU Fusion Breakout - BNO055 .... Retrieved April 24, 2019, from https://www.adafruit.com/product/2472
48. (2018, August 21). What is a thermocouple and how does it work? | Omega Engineering .... Retrieved April 24, 2019, from https://www.omega.com/en-us/resources/thermocouples
49. (n.d.). Thermocouple Type-K Glass Braid Insulated [K] ID: 270 - $9.95 .... Retrieved April 24, 2019, from https://www.adafruit.com/product/270
50. (n.d.). Thermocouple Amplifier MAX31855 .... Retrieved April 24, 2019, from https://www.adafruit.com/product/269
51. (n.d.). Adafruit BME680 - Temperature, Humidity, Pressure and Gas Sensor .... Retrieved April 24, 2019, from https://www.adafruit.com/product/3660
52. (2018, April 12). Batteries — choose the right power source for your robot - Medium. Retrieved April 24, 2019, from https://medium.com/husarion-blog/batteries-choose-the-right-power-source-for-your-robot-5417a3ec19ca
53. (n.d.). A Guide to Understanding Battery Specifications - MIT. Retrieved April 24, 2019, from http://mit.edu/evt/summary_battery_specifications.pdf
54. (2018, May 16). What Goes into Building a Robot – MistyRobotics – Medium. Retrieved April 24, 2019, from https://medium.com/mistyrobotics/what-goes-into-building-a-robot-d68426768f56
55. (2018, April 12). Batteries — choose the right power source for your robot - Medium. Retrieved April 24, 2019, from https://medium.com/husarion-blog/batteries-choose-the-right-power-source-for-your-robot-5417a3ec19ca
56. (n.d.). The High-power Lithium-ion - Battery University. Retrieved April 24, 2019, from https://batteryuniversity.com/learn/archive/the_high_power_lithium_ion
57. (n.d.). LiNiMnCo 26650 Battery: 14.4V 5Ah (72Wh, 10A rate, 4S/S). Retrieved April 24, 2019, from

https://www.batteryspace.com/linimnco-26650-battery-14-4v-5ah-72wh-10a-rate-4s-s.aspx
58. (2017, August 14). What are the components of a battery storage system? - Energy .... Retrieved April 24, 2019, from https://www.energystoragenetworks.com/components-battery-storage-system/
59. (n.d.). How The BMS Works | Orion Li-Ion Battery Management ... - Orion BMS. Retrieved April 24, 2019, from https://www.orionbms.com/general/how-it-works/
60. (2015, August 4). Protection Circuit Module (PCM) with Equilibrium Function & Fuel .... Retrieved April 24, 2019, from https://www.batteryspace.com/Protection-Circuit-Module-PCM-with-Equilibrium-Function-and-Fuel-Gauge-for.aspx
61. (n.d.). Power Supply Current Limiter Circuits - Electronics Notes. Retrieved April 24, 2019, from https://www.electronics-notes.com/articles/analogue_circuits/power-supply-electronics/current-limiter-circuit.php
62. (n.d.). Linear vs. Switching Regulators | Renesas Electronics. Retrieved April 24, 2019, from https://www.renesas.com/sg/en/products/power-management/linear-vs-switching-regulators.html
63. (n.d.). Difference Between Linear Regulator and Switching Regulator .... Retrieved April 24, 2019, from https://www.rohm.com/electronics-basics/dc-dc-converters/linear-vs-switching-regulators
64. (2017, July 12). Types of Switching DC to DC Converters | Arrow.com. Retrieved April 24, 2019, from https://www.arrow.com/en/research-and-events/articles/types-of-switching-dc-dc-converters
65. (n.d.). Cytron 10A 5-30V Dual Channel DC Motor Driver - RobotShop. Retrieved April 24, 2019, from https://www.robotshop.com/en/cytron-10a-5-30v-dual-channel-dc-motor-driver.html
66. (n.d.). How it works - Home | Tinkerforge. Retrieved April 24, 2019, from https://www.tinkerforge.com/en/home/how-it-works/
67. (n.d.). Raspberry Pi 3 Model B+ - Raspberry Pi. Retrieved April 24, 2019, from https://www.raspberrypi.org/products/raspberry-pi-3-model-b-plus/
68. (n.d.). Adafruit HUZZAH32 – ESP32 Feather Board ID: 3405 - $19.95 .... Retrieved April 24, 2019, from https://www.adafruit.com/product/3405
69. (n.d.). ROS.org. Retrieved April 24, 2019, from https://www.ros.org/
70. (2016, July 11). Nothing Gets In: Waterproof Enclosure Design 101 (and IP68) - Fictiv. Retrieved April 24, 2019, from https://www.fictiv.com/blog/posts/nothing-gets-in-waterproof-enclosure-design-101-and-ip68
71. (n.d.). Types of Lithium-ion Batteries – Battery University. Retrieved April 24, 2019, from https://batteryuniversity.com/learn/article/types_of_lithium_ion

Appendix A: Thermal Calculations

The amount of energy needed to change the temperature ΔT is calculated using:

$Q_{foam} = (\rho)(A)(d)(C_p)(\Delta T)$

Where ρ is the density, A is the area in square meters, d is the thickness in meters; $(\rho)(A)(d)$ is the volume of the foam, and C_p is the specific heat.

The energy transmitted in Watts through all the materials:

$Q_c = \frac{\Delta T}{R_T}$

Where R_T is equal to the sum of each material's thermal resistance. A material's thermal resistance is equal to:

$R = \frac{d}{k*A}$

Where d is the thickness in meters, A is the area square meters, and k is the thermal conductivity.

Table 10 shows the area and thicknesses of the materials, and Table 11 shows the thermal conductivity used for each material

Table 10. Material thicknesses and areas

Material	Area (in^2)	Area (m^2)	Thickness (in)	Thickness (m)
Foam	479.15	0.3091	0.5	$1.27x10^{-2}$
Air	1133.23	0.7311	0.25	$0.635x10^{-2}$
Teflon	1133.23	0.7311	0.125	$0.3175x10^{-2}$

Table 11. Thermal conductivity for each material

Material	Thermal conductivity(W/m*K)
Teflon	2.9403
Air	0.03
Foam	0.027

The thermal resistances of each layer equal:

$R_o = \frac{1}{30} \cdot \frac{1}{0.0271} = 0.161\ °C/W$

$R_t = \frac{0.3175\times10^{-2}}{2.9403\cdot0.7311} = 0.001477$

$$R_a = \frac{0.635\times10^{-2}}{0.03\cdot0.7311} = 0.2895$$
$$R_f = \frac{1.27\times10^{-2}}{0.027\cdot0.3091} = 1.522$$

The total thermal resistance equals:

$$R_T = R_o + R_t + R_a + R_f = 0.161 + 0.001477 + 0.2895 + 1.522 = 1.974$$

The total energy transmitted through all the materials when the robot starts at 20°C and is subjected to 150°C equals:

$$Q_c = \frac{\Delta T}{R_T} = \frac{150-20}{1.974} = 65.87\ W$$

The amount of energy it takes to change the temperature of the foam ΔT equals:

$$Q_{foam} = (\rho)(A)(d)(C_p)(\Delta T) = 110.71962 \cdot 0.3091 \cdot 1.27 \times 10^{-2} 1120 \cdot \Delta T = 486.794\Delta T\ J$$

For the temperature to change from 20°C to 70°C, the amount of energy equals:

$$Q_{foam} = 486.794\Delta T = 486.794(70-20) = 24339.70665\ J$$

The amount of time it will take for the foam to heat up to 70°C equals:

$$t = \frac{Q_f}{Q_c} = \frac{24339.70665}{65.87} = 369.53\ seconds = 6.16\ min$$

Appendix B: Component Comparison Charts

When researching sensors, the main requirements in choosing the sensors for the robot were operating temperature, current consumption, accuracy, overall functionality and cost. First, since the interior temperature is limited by the temperature at which a battery can discharge (60 °C), it was necessary to check that all electronic components could function above 60 °C. Second, as mentioned in the requirement metrics, the robot must be energy efficient. Therefore in order to have low power consumption the component needs to consume less current. Third, because the robot will be used in a fireground, the sensors need to be as accurate as possible to give the best understanding of the environment and the health of the robot to firefighters. Fourth, since there was a budget in creating the robot, the cost was heavily considered. Finally, overall functionality is significant in the decision making process as sensors with more capabilities may be deemed more beneficial. By combining all these requirements, some sensors were determined:

Infrared Arrays

Prior to choosing infrared (IR) arrays, both thermal cameras and thermopiles were considered. Infrared arrays were chosen since they're made up of thermopiles and because they are basically low- resolution thermal cameras. They are roughly five times less than a cheap thermal camera such as the Lepton 3.5.

Table 12. Infrared Array Sensor Comparison

Requirements	**MLX90640**	**Grid-Eye AMG88**
Manufacturer	Melexis	Panasonic
Operating Temperature	-40 °C to 85 °C	-20 °C to 80 °C
Current Consumption	20 mA	4.5 mA
Cost	$45	$32.5
Resolution	32x24	8x8
Measured Temperature Range	-40 °C to 300 °C	-20 °C to 100 °C
Accuracy	1 °C	3 °C

Temperature, Humidity, and Gas

Measuring ambient temperature and humidity in the interior of the robot keeps track of its health. The following table outlines the temperature, humidity and gas sensors considered and compares it to the BME680. The BME680 was chosen due to its 4-in-1 sensor capabilities with temperature, humidity, gas and pressure.

Table 13. Temperature Sensor Comparison

Requirements	**STS3x-DIS**	**Si7051**	**BME680**
Manufacturer	Sensiron	Silicon Labs	Bosch
Operating Temperature	-40 °C to 125 °C	-40 °C to 125 °C	-40 °C to 85 °C
Current Consumption	1.7uA	195nA	2.1uA
Accuracy	0.2 °C	0.1 °C	1 °C
Cost	$2.2	$1.95	$13.20
Response Time	2s	5.1s	x
Measured Temperature Range	0 °C to 65 °C	-40 °C to 125 °C	0 °C to 65 °C

Table 14. Humidity Sensor Comparison

Requirements	**HDC1080**	**SHT31**	**BME680**
Manufacturer	Texas Instruments	Sensiron	Bosch
Operating Temperature	-20 °C to 85 °C	-40 °C to 125 °C	-40 °C to 85 °C
Current Consumption	1.3uA	2uA	2.1 uA
Accuracy	2%	2%	3%
Cost	$4.3	$8.00	$13.20
Response Time	15s	8s	8s

Measured Humidity Range	0% to 100% RH	0% to 100% RH	10% to 90% RH

Both humidity sensors also have temperature sensing capabilities with an accuracy of 0.2 C.

Table 15. Gas Sensor Comparison

Requirements	**SGP30**	**BME680**
Manufacturer	Sensiron	Bosch
Operating Temperature	-40 °C to 85 °C	-40 °C to 85 °C
Current Consumption	48 mA	12mA
Accuracy	15%	15%
Cost	$13.57	$13.20
Response Time	1s	<1s

Appendix C: Battery Materials [71]

The figure below references a table of different battery materials and their most common uses. The two batteries considered for this robot system were the Lithium Manganese Oxide (LMO) and the Lithium Nickel Manganese Cobalt Oxide (NMC). They are both considered safe, and both have a high specific power and longer life span.

Chemical name	Material	Abbreviation	Short form	Notes
Lithium Cobalt Oxide[1] AlsoLithium Cobalate or lithium-ion-cobalt)	$LiCoO_2$ (60% Co)	LCO	Li-cobalt	High capacity; for cell phone laptop, camera
Lithium Manganese Oxide[1] Also Lithium Manganate or lithium-ion-manganese	$LiMn_2O_4$	LMO	Li-manganese, or spinel	Most safe; lower capacity than Li-cobalt but high specific power and long life. Power tools, e-bikes, EV, medical, hobbyist.
Lithium Iron Phosphate[1]	$LiFePO_4$	LFP	Li-phosphate	
Lithium Nickel Manganese Cobalt Oxide[1], also lithium-manganese-cobalt-oxide	$LiNiMnCoO_2$ (10–20% Co)	NMC	NMC	
Lithium Nickel Cobalt Aluminum Oxide[1]	$LiNiCoAlO_2$ 9% Co)	NCA	NCA	Gaining importance in electric powertrain and grid storage
Lithium Titanate[2]	$Li_4Ti_5O_{12}$	LTO	Li-titanate	

Table 1: Reference names for Li-ion batteries. We willuse the short form when appropriate.

[1] Cathode material

[2] Anode material

Figure 75. Battery Material Comparisons

Lithium Manganese Oxide

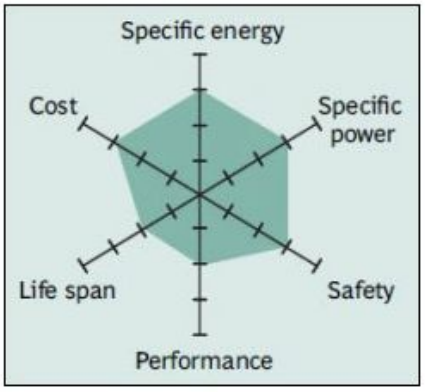

Figure 5: Snapshot of a pure Li-manganese battery.
Although moderate in overall performance, newer designs of Li-manganese offer improvements in specific power, safety and life span.

Figure 76. LMO Snapshot [71]

Summary Table

Lithium Manganese Oxide: $LiMn_2O_4$ cathode. graphite anode Short form: LMO or Li-manganese (spinel structure) Since 1996	
Voltages	3.70V (3.80V) nominal; typical operating range 3.0–4.2V/cell
Specific energy (capacity)	100–150Wh/kg
Charge (C-rate)	0.7–1C typical, 3C maximum, charges to 4.20V (most cells)
Discharge (C-rate)	1C; 10C possible with some cells, 30C pulse (5s), 2.50V cut-off
Cycle life	300–700 (related to depth of discharge, temperature)
Thermal runaway	250°C (482°F) typical. High charge promotes thermal runaway
Applications	Power tools, medical devices, electric powertrains
Comments	High power but less capacity; safer than Li-cobalt; commonly mixed with NMC to improve performance.

Table 6: Characteristics of Lithium Manganese Oxide.

Figure 77. Characteristic of LMOs [71]

Lithium Nickel Manganese Cobalt Oxide

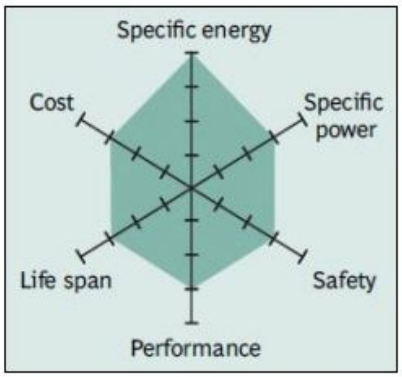

Figure 7: Snapshot of NMC.
NMC has good overall performance and excels on specific energy. This battery is the preferred candidate for the electric vehicle and has the lowest self-heating rate.

Figure 78. NMC Snapshot [71]

Summary Table

Lithium Nickel Manganese Cobalt Oxide: $LiNiMnCoO_2$. cathode, graphite anode Short form: NMC (NCM, CMN, CNM, MNC, MCN similar with different metal combinations) Since 2008	
Voltages	3.60V, 3.70V nominal; typical operating range 3.0–4.2V/cell, or higher
Specific energy (capacity)	150–220Wh/kg
Charge (C-rate)	0.7–1C, charges to 4.20V, some go to 4.30V; 3h charge typical. Charge current above 1C shortens battery life.
Discharge (C-rate)	1C; 2C possible on some cells; 2.50V cut-off
Cycle life	1000–2000 (related to depth of discharge, temperature)
Thermal runaway	210°C (410°F) typical. High charge promotes thermal runaway
Cost	~$420 per kWh (Source: RWTH, Aachen)
Applications	E-bikes, medical devices, EVs, industrial
Comments	Provides high capacity and high power. Serves as Hybrid Cell. Favorite chemistry for many uses; market share is increasing.

Table 8: Characteristics of lithium nickel manganese cobalt oxide (NMC).

Figure 79. Characteristics of NMC [71]

Appendix D: Thermal Test Protocol

Test Procedure

Thermal Testing Firefighting Robot

Firefighting Robot MQP 2019

Objective: Determine thermal integrity of the Firefighting Robot Chassis by measuring and comparing external temperature, and internal robot temperature.

Materials:

- 1 x Firefighting Robot Chassis
    - Foam Layer (sealed with thermal paste)
    - Teflon Layer (sealed with silicone adhesive, thermal paste, and Reflect-A-Cool foil)
    - Aluminum Top Shell
    - Ceramic Standoffs (forming air layer between Teflon and Foam)
    - Axles and bearings (chrome steel)
    - Omni Wheel and Axle (stainless steel)
- 1 x Furnace with 500°F capability and larger than 132 in^3
- 1 x Thermocouple for External Measurement
- 1 x Temperature Sensing Unit
    - 1 x ESP8266 Microcontroller
    - 1 x micro USB to USB 2.0
    - 3 x Thermocouple for internal measurement
- 1 x Computer with Temperature Sensing Unit program

Robot Testing Preparation:

Prior to the procedure, the thermocouples from the temperature sensing unit will be placed within the firefighting robot chassis. The robot should be sealed. This combined element will be described as the “robot.” Depending on the connection, it should record data every second.

Procedure:

1. Preheat furnace to 300°F.
2. Verify that the thermocouples within the robot are accurately transmitting data as shown in the Data Collected Template in the table below. Observe internal base temperature (room temperature).

3. Once furnace reaches 300°F, open furnace, place Robot in the furnace and close furnace shut.
4. Begin automatic data collection by measuring external and internal data simultaneously. Run furnace at 300°F for 15 minutes.
5. Turn off furnace, open it and remove the robot.Allow robot to cool. Observe the time when cooling began, and continue measuring external and internal temperature.
6. Once the internal temperature of the robot reaches base temperature (room temperature), stop collecting data.
7. Repeats steps procedure at a furnace temperature of 500°F for 3 minutes.

Data Collected Template:

The data will be automatically collected and sent to an Excel document. Every data set collected will output the time in which it was collected. The data set will include:

1. External Temperature (°F)
2. Internal Teflon Layer Temperature (°F)
3. Internal Foam Layer Temperature (°F)

The data collected should be monitored while the experiment is ongoing. The time when the furnace turns on (heating phase) and when it turns off (cooling phase) should be observed and noted. The results for the 300°F and 500°F experiments will be collected on two different tables.

Data Table Example:

Time (s)	External Temperature (°F)	Internal Teflon Layer Temperature (°F)	Internal Foam Layer Temperature (°F)

Data collection program

https://gist.github.com/yilverdeja/0c22828b93c2947b7fa5992de3f84f86

Data Acquisition Tool

PLX-DAQ: https://www.parallax.com/downloads/plx-daq

PLX-DAQ version 2 NetDevil Modification: http://forum.arduino.cc/index.php?topic=437398.0

Appendix E: Github Repository

https://github.com/gkmacneal/firefighting_robot_MQP